Probing strong-field gravity with electromagnetic radiation

F Vincent

Observatoire de Paris

Mémoire d'Habilitation à diriger des recherches

Probing strong-field gravity with electromagnetic radiation

by
Frédéric Vincent

Publicly defended
on June 21st 2022
at Observatoire de Paris/Meudon
before the jury consisting of :

Marie-Christine Angonin
Vitor Cardoso
Frédéric Daigne
Frank Eisenhauer
Karine Perraut
Peggy Varnière
Marta Volonteri

Observatoire de Paris - Laboratoire d'Étude Spatiale et d'Instrumentation en Astrophysique

Contents

Acknowledgments

I would like to first thank my habilitation jury for accepting to take the time to read my dissertation and take part in the defense. I know that it is difficult to find time in already very dense agendas, so I appreciate very much the effort.

I would like then to thank very warmly my scientific team here in Meudon. I am very indebted towards my PhD advisers who have become my very close collaborators, E. Gourgoulhon, T. Paumard, G. Perrin. Their continuous support has been central in my ability to make a carreer in astronomy.

Of central importance also has always been my collaborations with younger researchers, in chronological order M. Grould, G. Rodriguez-Coira, G. Heissel, N. Aimar, A. Dmytriiev, to cite those with whom I collaborated over the long term, as well as the Licence and Master students that I supervised typically over few months, also in chronological order R. Danain, W. Kiendrebeogo, N. Aimar, H. Paugnat, S. Aoulad-Lafkih and K. Abd El Dayem. I would also like to thank warmly my HRA pole at LESIA, and in particular the Centers of GalaxieS team with whom it is a pleasure to share everyday scientific life, as well as the ITA staff at LESIA who are all key for making science possible.

Collaboration is the key in my opinion to generate good results, so I would like to thank my main collaborators outside LESIA. In France: P. Grandclément, A. Le Tiec, J. Novak, and the full LUTH/ROC team, as well as Z. Meliani and A. Zech also at LUTH, A. Hees at SYRTE with whom a hopefully long-term collaboration is just starting, F. Casse and P. Varniere at APC; J.-B. Fouvry, J.-P. Lasota, C. Pichon at IAP. In the world: the MPE (F. Eisenhauer, S. Gillessen, and colleagues) and Portugese (V. Cardoso, P. Garcia, and

colleagues) colleagues of the GRAVITY collaboration are my privileged collaborators; my EHT-related-science collaborators, in particular M. Wielgus with whom I collaborate since a decade, and more recently A. Cardenas, S. Gralla, and A. Lupsasca; my postdoc team at the Copernicus Center in Warsaw (M. Abramowicz, M. Bejger, W. Kluzniak, A. Rozanska, O. Straub – in Warsaw and other places! – A. Zdziarski, and my fellow postdocs and PhDs, A. Manousakis, B. Mishra) has been crucial in this important time of my carreer; C. Herdeiro and his collaborators in Aveiro for exotic compact objects science.

I would also like to thank here my colleagues with whom I collaborate for administrative tasks. I would like to cite the IT commission of Paris Observatory and in particular F. Roy with whom I spent endless hours of collaborative work, as well as the members of CNRS section 17.

Let me finish by thanking my university students at all levels, from L1 to M1.

1

General context : probing strong-field gravity

Contents

1.1 Why probing gravity matters?

This section is devoted to discussing the interest of studying strong-field gravity, and in particular black holes. I will consider the question from two different perspectives: I will first discuss the role of gravitation and black holes in the quest for unity that underlines the history of physics (section 1.1.1); I will then focus on the importance of black holes and mainly supermassive black holes (SMBH) in the astrophysics big picture (section 1.1.2).

1.1.1 The quest for unity

Modern science was born in Greece in the VIth century BC, with the advent of the Milesian school. These pioneering thinkers were interested in understanding the *phusis*, i.e. Nature, and can thus be considered the first physicists. The Milesian physicists were immediately interested by the question of the origin of elements of our world, which was related to the problem of unity versus diversity: is it possible to explain the diversity and complexity of our world by considering that all intricate aspects of Nature would be avatars of a simple underlying principle? For Thales (625-545), this principle was water. Other philosophers advocated other elements. Anaximander (610-545) went one step further in abstraction by considering that the baseline principle is none of the elements of our world, but rather an abstract notion called *apeiron* in Greek, which more or less means "something that has not yet been determined". Elements of our world (a drop of water, a fragment of stone...) are declinations of this primitive notion that have thus lost their unity with the underlying principle. The effort of philosophy is precisely to reveal this underlying principle which is not immediately apparent in the diversity of everyday world.

This effort of the infant Greek philosophy to explain the world of our experience makes it very close to what we call now science. It is thus tempting, althoug certainly too general and too quickly said, to put the search for unity, which is at the basis of the effort of the Greek philosophers, as a founding notion of modern occidental science since its birth in the VIth century BC[1].

[1]Determining the "date of birth" of modern science might be considered very naive. Why the VIth century, although people had not waited this time to think on natural problems? For instance, the Egyptian science is much older than that and the great pyramid of Giza, to give but one overwhelming example, dates back to around 2600 BC. However, this science was closer to what we would call a *technique* nowadays, i.e. a *practical* set of knowledge allowing to reach fantastic practical achievments, but without any abstract background (there is no such thing as an Egyptian abstract geometry, for instance). This difference can be highlighted by one well-known example: Pythagora's theorem (dating back to the VIth century as well). Pythagora (if he ever existed as an individual) stated that *any* right-angled triangle satisfies his famous relation. Egyptians knew very well this result *in practice* for this or that particular triangle, but they never expressed the abstract, general theorem of Pythagora. Here, I define "modern science" as precisely this

It goes well beyond the scope of this document to trace this concept of quest of unity in science from the Greek origins to now [more details can be found e.g. in Klein and Lachieze-Rey, 1999]. I will simply highlight a few important steps (definitely without trying to be exhaustive!), starting from Galileo in the XVIIth century[2]:

- the unification of all Galilean frames of reference by Galileo (≈ 1630), forming a class of equivalent viewpoints for describing the laws of mecanics;
- the unification of the motions of falling bodies on Earth, and moving bodies in the sky, by Newton (≈ 1680), within the universal law of gravitation;
- the unification of light, electricity and magnetism within Maxwell's electromagnetism (≈ 1860);
- the unification of space and time within Einstein's special relativity (1905), and the unification of all laws of physics as described in Galilean frames;
- the unification of gravitation and geometry in Einstein's general theory of relativity (1915);
- the unification of electromagnetism, weak, and strong interactions into the common quantum-field-theory framework of the Standard Model (≈ 1960).

The unitary development of physics has thus culminated half a century ago with the development of the Standard Model, which combines special relativity and quantum mecanics to give a consistent description of three of the four fundamental interactions. However, the fourth interaction, gravity, and its theory, general relativity, are not included in this unified picture. It is very tempting to consider that a fully unified scheme should exist. The discussion above shows that this temptation is not only supported by a simple aesthetic consideration. It is also backed by two and a half millenia of history of science that shows that the quest of unity has been at the root of immense successes for modern physics.

It is important to stress that general relativity demands its own demise in the sense that it predicts the existence of singularities inside black holes where its predictive power collapses. It is thus a very reasonable guess to consider that scrutinizing the properties of strong gravity field in the vicinity of black holes might be a promising avenue for challenging the predictions of general relativity, with the ultimate goal of touching its limit from an observational point of view. Moreover, any quantum description of gravitation should be able to explain the expression of black holes entropy as a function of the horizon area,

particular kind of abstract, general reasoning on natural phenomena, developed in the Greece of the VIth century, with the quest for unity as a fundamental question that immediately dominated the field.

[2]Which I would be tempted to call the "second birth" of modern physics!

$S = A/4$, in terms of microstates counting, which is another argument in favor of the central role that black holes should play in the quest for a unified description of gravity. This is one profound motivation for studying strong-field gravity in the vicinity of black holes.

To conclude this section, let us briefly mention one last recent crucial finding that highlights once again the possible existence of deep unifying links, in relation with black holes. The *anti-de Sitter / conformal field theory (AdS/CFT) correspondence*, as conjectured by Juan Maldacena in a pioneering 1997 paper, allows to map results obtained in the framework of a quantum field theory expressed in a 4-dimensional spacetime, to results obtained in the framework of a gravity theory in a 5-dimensional spacetime. More specifically, and to give but one example, the properties of e.g. a quark-gluon plasma (quantum-field-theory sector) can be related to that of black holes in 5 dimensions [gravity sector, see e.g. Golubtsova et al., 2021, for more details]. This correspondence, although of no astrophysical interest, is one more argument in favor of the study of black holes in the aim of progressing towards a more unitary description of physics.

1.1.2 Black holes within the astrophysics big picture

Strong-field gravity and the detailed understanding of physics in the surroundings of supermassive black holes (SMBH) in particular are key problems of astrophysics in general. Indeed, supermassive black holes are crucial pieces of the galactic puzzle, and of the cosmology big picture, at the front of a complicated multi-scale, multi-physics scene.

Regarding the galactic scale, it is well known that there is a correlation between the mass of supermassive black holes and the velocity dispersion of the galactic bulges ($M - \sigma$ correlation; there is no such correlation with the galaxy disk or dark matter halo). This correlation likely is a consequence of an intimate link between the very small scales of the SMBH surroundings and the galactic scales (spanning up to 10 orders of magnitude). This link is certainly partly due to the feedback provided by the SMBH to the bigger-scale galactic environment, through the emission of intense radiation and the ejection of matter likely powered by the rotation of the black hole [see e.g. Fabian, 2012]. The energy delivered from the small to the big scales heats the galactic gas and might thus quench stellar formation by preventing cooling. The link also works in the other direction, with the close-by gas and stellar winds feeding the SMBH, as is the case for Sagittarius A* (see section 3.1).

At the cosmological scale, the evolutionary track of SMBH from the initial black hole seeds to the present-day massive objects is a key question [Volonteri et al., 2021], particularly when considering that most galaxies harbor a massive black hole at their center. The mass

growth from the initial seeds to the present-day universe is a very complex question that is deeply anchored in our understanding of the physics of accretion and ejection in the strong-field regions surrounding the SMBH. Moreover, massive black holes might have formed from overdensities in the early universe, in which case they would have built the potential well in which galaxies would later have grown. SMBH would thus have a very crucial cosmological role if this (accordingly somewhat exotic) scenario is valid.

Last but not least, SMBH are key gravitational-wave sources that will be scrutinized by the future space-based interferometer LISA. Understanding in more and more details the physics of their surroundings is crucial for maximizing the scientific return of this experiment and maybe highlighting new kind of probes. Multi-messenger electromagnetic-gravitational astronomy will obviously be a crucial block of XXIst century astrophysics. The study of strong-field gravity takes a very natural place in this long-term endeavour.

I have focused this section on SMBH because this is my main topic, but studying strong-field gravity in the vicinity of stellar compact objects is also very directly linked to deep astrophysical questions. Let us briefly evoke stellar black holes and their link with massive star evolution and binary evolution; supernova explosion; gravitational wave emission... Neutron stars will be briefly evoked in section 5.2 and I will explain there one reason why they matter for fundamental physics.

1.2 What do I mean by probing

The bottom line of my research, as the title goes, is *probing strong-field gravity*. This program should be restricted to the *electromagnetic counterparts* of strong-field gravity phenomena, emitted in the vicinity of (mostly) *black-hole candidates*. In my current understanding of this problem, this incorporates four main directions of research in order of increasing difficulty:

- studying the **behavior of radiation** from its emission in the close surroundings of black-hole candidates to its observation on Earth ("what are we supposed to see when light is emitted close to a black hole?"). The underlying question is: how precisely should we model the black hole and its surroundings in order to obtain a complete enough prediction of the observables? There are two dimensions in this question: the modeling of the black hole itself (full Kerr metric? Post-Newtonian approximation?), and that of the astrophysical surroundings (geometry of the emitting region, emitter's motion, radiative transfer...). The second part is obviously vital, and often tends to be neglected when people attack the two following objectives. This first objective is essentially always discussed, to some extent, in all my works.

- Assessing the **Kerr consistency** of the object ("is what we see consistent with the Kerr metric?"). The aim here might be to determine the spin parameter of the compact object, then the quadrupole moment, and check that the known Kerr relation between these two quantities holds ("no-hair theorem test"). Another Kerr consistency check has been recently put forward, which aims at evaluating the shape of the photon ring cast by the object on sky (see section 4.4.2). This second objective is discussed in some of my works.

- Studying the **nature of compact objects** (is it more consistent with Kerr than with an alternative object?). Here, a variety of alternative compact objects can be considered (hairy black holes, wormholes...), and we should study how the variation of the spacetime geometry translates into the observables. The big difficulty of this task is to be able to clearly discriminate between the spacetime and the astrophysics impact on the observable, and not mix them. It is easy, but not relevant, to distinguish various compact objects when all "astrophysical pollution" is ignored. This third objective is discussed in some of my works.

- Studying the **underlying theory of gravitation** (is it a black hole as described by general relativity that we see?). This is the most advanced question obviously: we not only are agnostic about the kind of object that we see, but we are also agnostic regarding the underlying theory of gravitation. So we give ourselves a lot of freedom, and should make sure that this freedom does not hide our ignorance regarding the astrophysics of the source. This fourth objective will never be discussed in the following of this dissertation, because I consider that it is very much further than what we can test today and in the forseeable future.

1.3 How to probe gravity: interferometry (GRAVITY, EHT)

Most of my work aims at studying strong gravity as observed by interferometers. I will also briefly discuss activity dedicated at studying X-ray observables (see chapter 5), but I have never dug very far into the data analysis of this topic, and I will thus not dicuss it here. It is of course not the aim of this document to give a complete introduction to interferometry, nor to any particular interferometer. I simply want to introduce as briefly as possible the main interferometric observable (the complex visibility), and quickly introduce the two instruments that drive most of my work, GRAVITY and the EHT.

1.3.1 The world's shortest interferometry primer

The basic idea of interferometry is to measure correlations between values of the electric field emitted by a source sampled at some particular locations. The interest of this is given by the Zernike-van Cittert theorem that basically says that the spatial correlation of the electric field of a source is directly related to the image of the source.

Let us consider an extended source on sky located around some angular coordinates (α, δ). This source emits an electric field that is measured in the aperture plane of a telescope array at points $\mathbf{r}_1$ and $\mathbf{r}_2$ and times t_1 and t_2. The geometry is represented on Figure 1.1. These two waves are then recombined and the recombined flux reads

$$\begin{aligned} F &= \iint_{\text{fov}} |E(\alpha,\delta,\mathbf{r}_1,t_1) + E(\alpha,\delta,\mathbf{r}_2,t_2)|^2 \,\mathrm{d}\alpha\mathrm{d}\delta \\ &= \iint_{\text{fov}} I_1 + I_2 + 2\,\mathrm{Re}\left[E(\alpha,\delta,\mathbf{r}_1,t_1)E^*(\alpha,\delta,\mathbf{r}_2,t_2)\right] \,\mathrm{d}\alpha\mathrm{d}\delta \end{aligned} \tag{1.1}$$

where $I_i = |E_i|^2$, the star denotes complex conjugation, the fov is the field of view on sky, and $E(\alpha, \delta, \mathbf{r}_1, t_1)$ labels the electric field coming from the sky direction (α, δ), measured at location $\mathbf{r}_1$ and time t_1. The integral over the fov takes into account the fact that the source is extended. The resulting quantity is indeed a flux, i.e. intensity (squared electric field) integrated over solid angle. The cross product is the correlation term, the term of interest for interferometry. The time average (over a time long wrt the wave period) of the cross product of the electric field is called the mutual coherence function (coherence and correlation are essentially the same notion). It is defined as

$$\Gamma(\mathbf{r}_1,\mathbf{r}_2,\tau) = \iint_{\text{fov}} \langle E(\alpha,\delta,\mathbf{r}_1,t)E^*(\alpha,\delta,\mathbf{r}_2,t+\tau)\rangle \,\mathrm{d}\alpha\mathrm{d}\delta \tag{1.2}$$

where stationarity has been assumed here for simplicity (so the result does not depend on the value of t).

Let us restrict the discussion to the type of correlation that is studied with GRAVITY and the EHT, i.e. spatial correlation, where one combines the light from different locations at the same time. The spatial correlation function, generally referred to as the **complex visibility** is defined as

$$\mathcal{V}(\mathbf{B} = \mathbf{r}_2 - \mathbf{r}_1) = \Gamma(\mathbf{r}_1,\mathbf{r}_2,\tau=0) = \iint_{\text{fov}} \langle E(\alpha,\delta,\mathbf{r}_1,t)E^*(\alpha,\delta,\mathbf{r}_2,t)\rangle \,\mathrm{d}\alpha\mathrm{d}\delta \tag{1.3}$$

where it is assumed that the spatial coherence depends only on the difference between locations and is independent on the time of recombination t. It is customary to use, rather

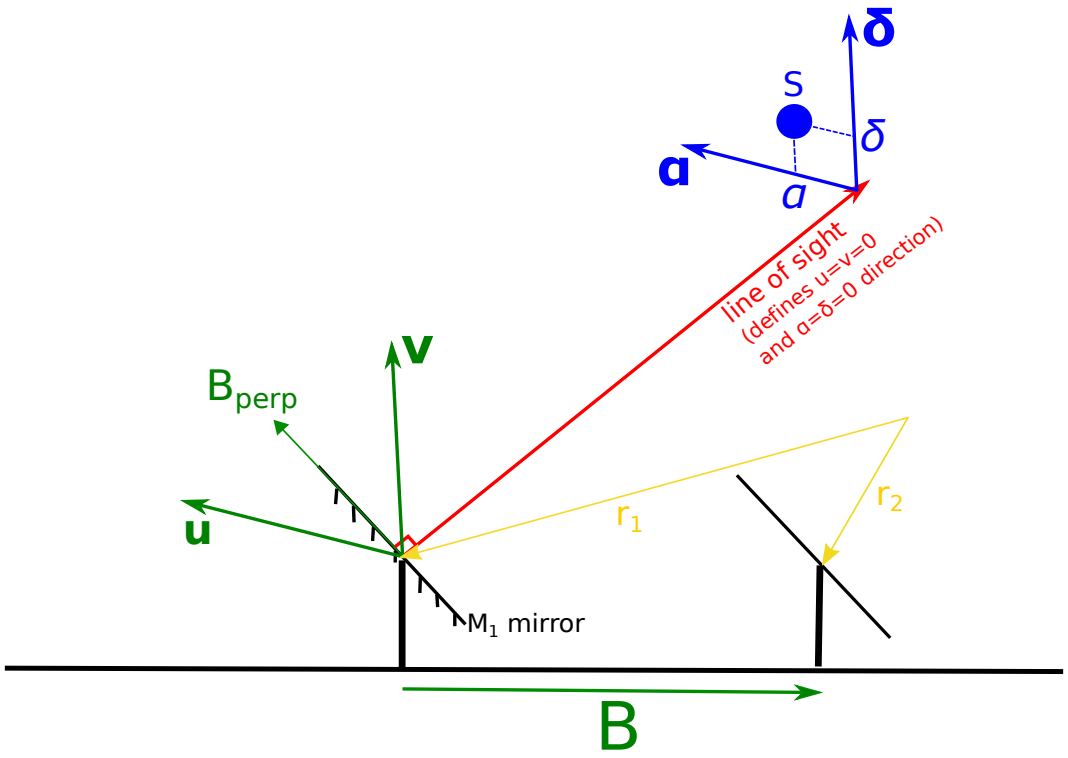

Figure 1.1: *Basic geometry: the line of sight (red arrow) is the direction orthogonal to the M_1 mirror of the telescope (this direction is assumed identical for the two telescopes represented here, as the source is very far). The plane of the sky (in blue) is labeled by angular coordinates (α, δ). The line of sight defines the center of the field of view $(\alpha, \delta) = (0, 0)$. The aperture plane (in green) is labeled by coordinates (u, v) in* rad^{-1}. *The two telescopes are separated by the baseline* $\mathbf{B}$. *The projection of this baseline orthogonal to the line of sight is represented in the (u, v) plane. The electric field emitted by the source S is sampled at the two locations* $\mathbf{r_1}$ *and* $\mathbf{r_2}$ *(in yellow), at times t_1 and t_2. The baseline is* $\mathbf{B} = \mathbf{r_2} - \mathbf{r_1}$.

than the vector $\mathbf{B}$ that lies in the detector plane (i.e. in the plane of the telescopes), the vector $\mathbf{B}_\perp/\lambda$ projected orthogonally to the line of sight (see Fig. 1.1) and normalized by the wavelength. The two orthogonal directions in this plane normal to the line of sight are called (u, v), respectively pointing towards the East and the North. Thus the spatial coherence function becomes

$$\mathcal{V}(\mathbf{B}) \to \mathcal{V}\left(\frac{\mathbf{B}_\perp}{\lambda}\right) = \mathcal{V}(u, v). \tag{1.4}$$

This quantity is the basic observable of interferometers like GRAVITY and the EHT.

At first sight, it is difficult to see what information on an astrophysical source can the complex visibility as defined by Eq. 1.3 bring. This relation becomes trivial if one admits the Zernike - van Cittert theorem which states that

$$\frac{\mathcal{V}(u,v)}{\mathcal{V}(0,0)} = \frac{\iint I(\alpha,\delta)\exp\left(-2i\pi(u\alpha+v\delta)\right)\mathrm{d}\alpha\,\mathrm{d}\delta}{\iint I(\alpha,\delta)\,\mathrm{d}\alpha\,\mathrm{d}\delta} \tag{1.5}$$

so that $\mathcal{V}$ is nothing but the Fourier transform of the intensity distribution on sky, and the coordinates (α,δ) (coordinates on the celestial sphere labeling the physical source) are Fourier conjugates of coordinates (u,v) (coordinates in the telescope plane labeling the complex visiblity). This Fourier link is depicted in Fig. 1.2. An interferometric measurement is thus a sampling of the Fourier transform of the plane of the sky at the few (u,v) points accessible given the baselines of the instruments. From the relation 1.4 it is also clear that the more wavelengths, the more samples. The rotation of the Earth, which leads to gradual change of baseline with time, also helps filling the so-called "u-v plane". Inferring

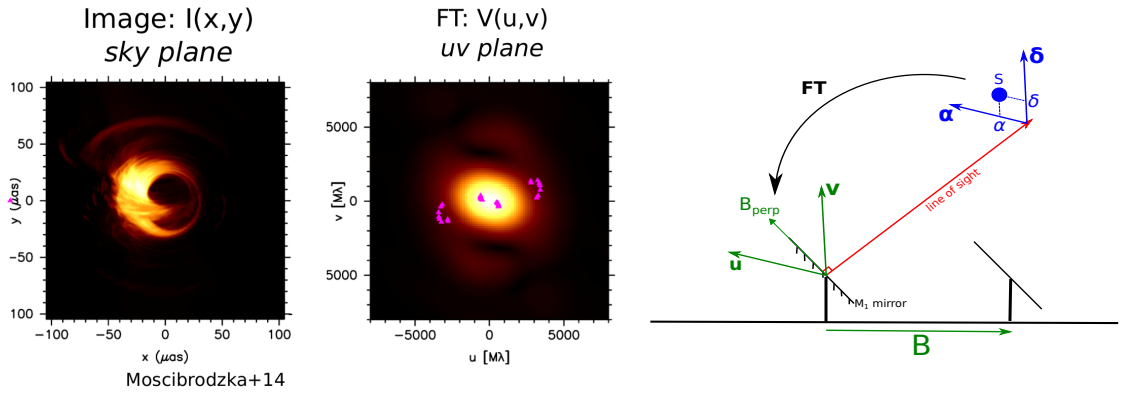

Figure 1.2: The Fourier relation between the plane of the sky and the visibility plane. The Fourier plane is sampled at a few locations corresponding to the (u,v) points accessible given the baselines of the instrument.

constraints on the source given the sparse Fourier data provided by the instrument is then the typically difficult inverse problem that has to be faced in order to link astrophysics with interferometry.

1.3.2 GRAVITY

GRAVITY is a second-generation instrument at the Very Large Telescope Interferometer (VLTI), located in Paranal, Chile. It is an infrared beam combiner that aims at combining the 2.2 μm light received by the four 8-meter telescope of the VLT. One of the central

science goals of GRAVITY is to study the close surroundings of the supermassive black hole at the center of the Milky Way, Sagittarius A* (Sgr A*). GRAVITY continuously observes three sources

- a bright adaptive-optics reference star that is used to correct for the distorsion of the wave front and make it planar at the level of each of the four telescopes;
- a relatively bright fringe-tracker reference star that is used to stabilize the fringes that are constantly jittering because of the atmospheric perturbation;
- a faint science source (typically Sgr A* or the S2 star, the closest to the supermassive black hole), close enough to the two reference sources above to be affected by the same distorsion effects.

The driving achievment of GRAVITY is its ability to secure an astrometric precision (i.e. an error bar on the motion in time in the (α, δ) plane of a source) of a few tens of microarcseconds (μas) within 5 minutes on a source as faint as $m_K = 15$. This requirement was designed to enable GRAVITY to precisely follow the track on sky of the bright infrared outbursts of the Galactic center black hole, and of its closest orbiting star S2. More details on the instrument can be found in the first-light paper [Gravity Collaboration et al., 2017]. The instrument is illustrated in Fig. 1.3.

1.3.3 Event Horizon Telescope

The Event Horizon Telescope (EHT) is a set of millimeter antennas located around the world that observe two main targets, the supermassive black hole at the center of Messier 87 (M87*), and that at the center of the Milky Way (Sgr A*). The driving achievment of the EHT is to ensure an imaging precision[3] of the order of 25 μas, allowing to obtain an image[4] of the surroundings of the two supermassive black holes. More details can be found in Event Horizon Telescope Collaboration et al. [2019], and references therein. The instrument is illustrated in Fig. 1.4.

[3] GRAVITY and the EHT have the same basic observable, the complex visibility, but their final science products are very different. GRAVITY provides astrometry, i.e. the $(\alpha(t), \delta(t))$ on-sky track of the centroid (flux-weighted barycenter) associated to the source, while the EHT provides an image, i.e. a time-averaged intensity map of the source. The relevant instrumental errors are thus called *astrometric precision* for GRAVITY, and *imaging resolution* for the EHT.

[4] This image is the result of a complex inverse problem resolution, it is of course not the direct observable but a derived quantity anchored in the sparse visibility sampling. Calling the EHT a "black hole imager" is a very simplifying and probably misleading formulation. Both GRAVITY and the EHT are samplers of the Fourier plane associated to the on-sky source.

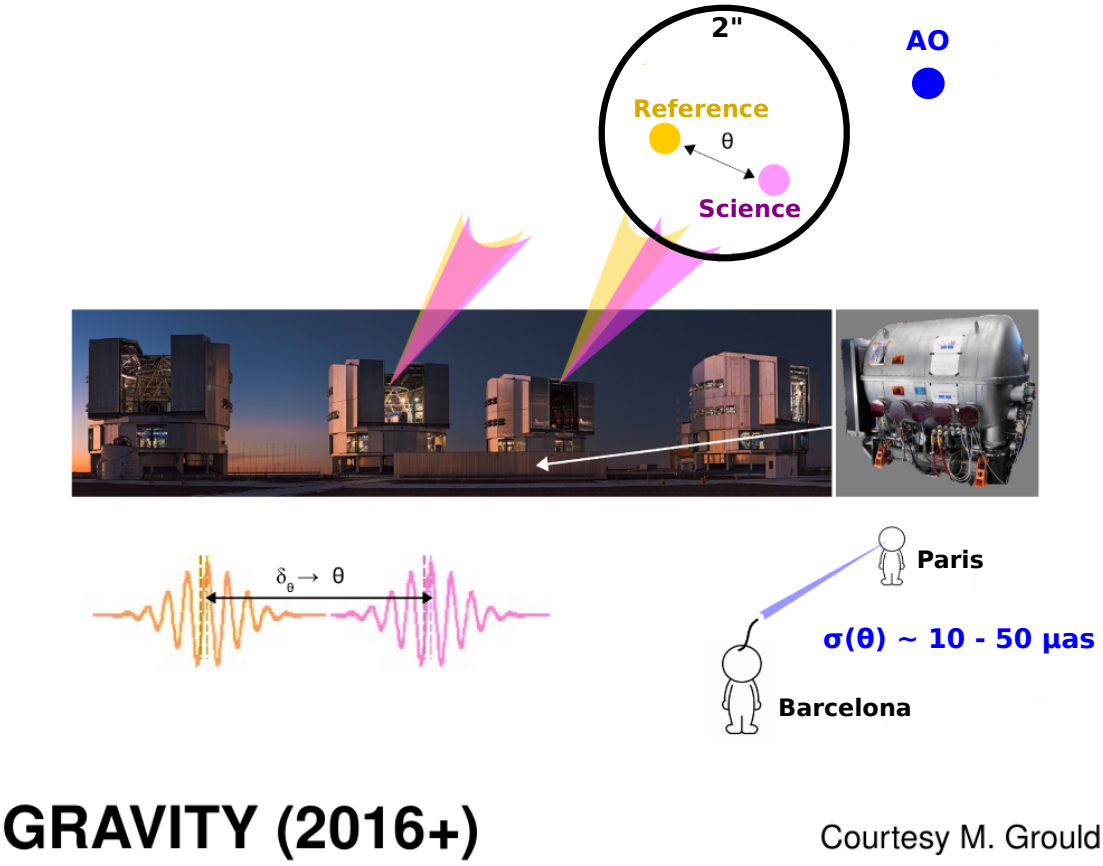

Figure 1.3: The GRAVITY instrument (cryostat in the right panel) combines the light from the four 8m telescopes of the VLT (central panel). The three sources continuously observed (see text for details) are shown in pink (science source), yellow (phase-reference source), and blue (adaptive-optics source). The astrometric precision of few tens of microarcseconds corresponds to the size of one hair in Barcelona as seen from Paris...

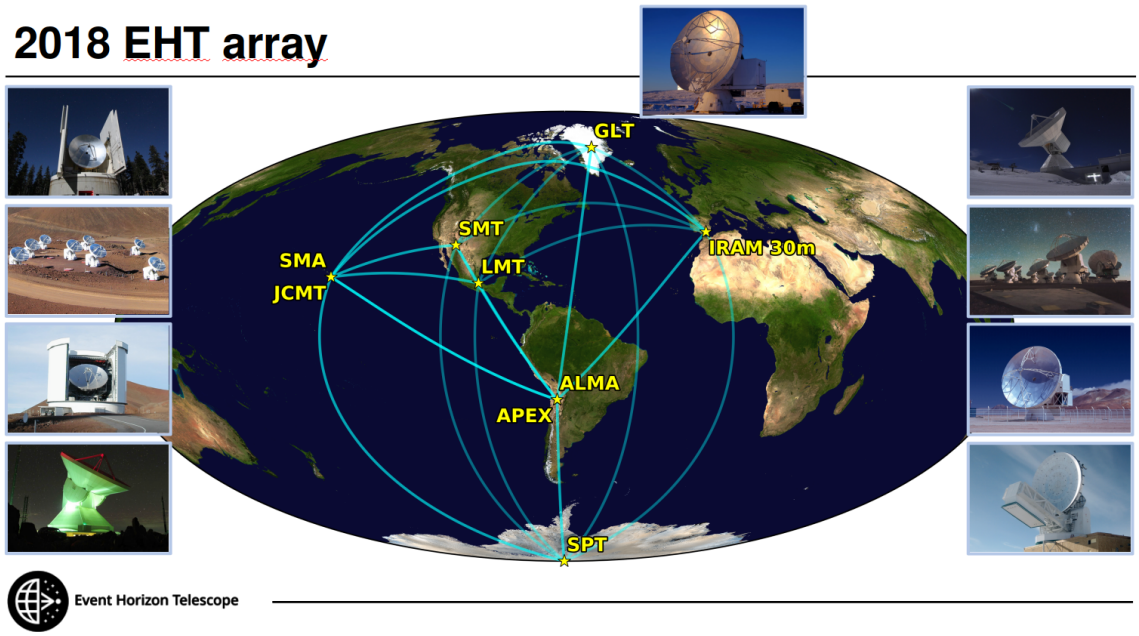

Figure 1.4: The EHT instrument is a worldwide array of millimetric antennas.

1.3.4 The scale of tens of microarcseconds

Tens of microarcseconds is the size of a euro coin on the Moon, or that of one hair in Barcelona as seen from Paris. It is obviously a fantastic technical achievment to reach such fantastically minute scales. These scales are not chosen by chance: they correspond to the angular size on sky of the photon rings or black hole shadow (see section 4.4.1 for a detailed definition of these notions) of M87* and Sgr A*. Accessing this scale means touching the immediate vicinity of the event horizon of a supermassive black hole.

1.4 Electromagnetic probes of strong-field gravity

This section focuses mostly on the probes that will be studied in more detail in the rest of the document (mostly, the observables of GRAVITY and the EHT). It also briefly mentions the X-ray probes, one of which is briefly discussed at the end of the document.

I focus here only on black hole observation and do not discuss the very important tests performed on pulsars [see Kramer, 2016, for a review].

1.4.1 Emission by hot flows (Sgr A*, M87*)

The main source of emission of strong-gravity electromagnetic signal discussed in this document is the inner accretion flow surrounding low-luminosity galactic nuclei like the environment of Sgr A* at the center of our Milky Way, and that of M87* at the center of Messier 87. Let us very briefly review here the main features of accretion flows on such galactic nuclei, which are generically called *radiatively inefficient accretion flows* (RIAF), or *hot flows* Yuan and Narayan [2014].

The arguably most famous accretion model is the thin-disk model of Shakura and Sunyaev [1973] which is likely one of the most cited papers of the astrophysics literature[5]. This model describes a geometrically-thin, optically-thick accretion disk surrounding a black hole. It is very efficient at radiating away the viscous energy dissipated by the orbiting motion of the fluid, and thus reaches typical temperature far below the virial temperature. This model is well adapted for modeling the core of active galactic nuclei and certain states of X-ray binaries. However, it is not able to reproduce the very low radiative efficiency of low-luminosity galactic nuclei like Sgr A* and M87*. RIAF are geometrically-thick, optically-thin accretion models that store part of the viscously dissipated energy as heat kept by the flow, and not radiated away. These flows are thus much hotter (with temperature approaching the virial temperature) and radiatively much less efficient than the thin-disk model. We will describe two implementations of RIAF below, for Sgr A* and M87*, see sections 3.3 and 4.2.

It is possible to use these hot flows for studying strong gravity in particular by means of direct **polarimetric imaging** of the surroundings of the black hole event horizon (EHT for M87*, soon for Sgr A*), or by following the **motion of transient outbursts** in the vicinity of the black hole (GRAVITY for Sgr A* flares).

1.4.2 Stellar orbits around Sgr A*

The accurate **follow up of stellar orbits** is another means of probing the gravitational potential of the central compact object. This represents one of the major goal of GRAVITY, in particular regarding the orbit of the closest star to Sgr A*, called S2.

Stellar orbits evolving around a black hole are affected by a number of relativistic effects. The frequency of a photon emitted by such a star will be subject to gravitational redshift when traveling in the strong gravitational field of the compact object. The orbit itself will rotate in its own plane and no longer remain a time-independent Keplerian ellipse due to

[5] More than 10^4 citations.

the Schwarzschild precession. Higher-order and thus more subtle effects are linked to the spin of the black hole.

1.4.3 Stellar orbits vs. hot flow

There are thus two main kinds of probes for GRAVITY and the EHT: the inner accretion flow and the more distant orbiting stars. They both have pros and cons:

- The inner flow has the obvious advantage of being closer to the black hole, which is a key argument when probing strong gravity is at stake. However, these inner regions are rather poorly constrained as of today and are plagued with big astrophysical uncertainties.
- The close-by stars are obviously further away, which is a drawback for testing the finest strong-gravity effect (like that of the black hole spin), but they are much better understood physical objects as compared to the inner flow and can thus be considered as good realizations of a test particle.

It is certainly very important to study these two categories of probes at the same time and try to retrieve the best from each of them. This discussion also naturally highlights the crucial importance of looking for closer-in faint stellar objects within the orbit of S2, which is a key science driver of the upgrade of GRAVITY, GRAVITY+.

1.4.4 X-ray probes of strong gravity

X-ray binaries are another very interesting arena for testing strong-field physics. Various methods are used: continuum fitting, iron line, quasi-periodic oscillations, polarimetry, most of which are not discussed in this document [see Bambi, 2017, for a review]. Only quasi-periodic oscillations are discussed in section 5.1.

1.5 Conclusion: my science questions

This chapter has hopefully allowed to clearly define the general context within which my science takes place. This context being given, the following paragraphs present five science questions that are driving all my research.

1. What properties of accretion flows are key to reproduce electromagnetic strong-field observables? By "strong-field observable" here I mean radiation emanating from the inner few tens of gravitational radii surrounding the compact object, which will typically be a stellar or supermassive black holes, or an exotic alternative. The goal here is to be able to pick the few properties of accretion flows that drive the observables. These properties are typically: the geometry of the flow, the dynamics of the emitting fluid, the absorption/emission properties of the fluid. Electromagnetic observables from the surroundings of black holes can be predicted by means of sophisticated numerical techniques (GR(R)MHD[6] codes, GRPIC[7] codes with radiative transfer). My point is not to use such advanced techniques, but rather, educated by the output of these studies, to determine simple analytical prescriptions regarding the properties of the flow that drive the observables. To put it as simply as possible, my aim is to determine the *simplest reasonable* model, educated by more sophisticated descriptions, that allows to account for the observables. What is the interest of such a simple modeling? Is it not preferable to rather use the most advanced available techniques? My conviction is *no, it is not*. Simple analytical models are crucial to be able to scan a broader parameter space than what is covered by simulations. Sophisticated simulations are indeed limited by the facts that

- they need to make simplifying assumptions, like the sub-grid electron heating prescription of GRMHD models, which selects a part of the parameter space;
- they are expensive in terms of computing time, so that it is important to use simpler and cheaper descriptions for investigating more easily the parameter space;
- they are dependent on initial conditions that are typically very badly constrained, so that it is very useful to scan a broader parameter space with simple analytical models.

Moreover, analytical models are very well suited to separate various effects that superimpose in the final observable. It is easy to switch on and off whatever physical effect of interest (emission, absorption, dynamics, relativistic effects...) which is key to provide a clear understanding of the complictated final observables.

2. How much can we constrain the properties of the accretion/ejection flows close to supermassive black holes? The aim here is to use the output of question 1. above to try to build robust conclusions regarding the physical properties of the accretion/ejection flows surrounding supermassive black holes. In particular, we will be interested in determining whether the flow is rather disk-dominated or jet-dominated, constraining the dynamics of the emitting matter, determining whether the flow is strongly

[6] GR(R)MHD=General-relativistic (radiation) magneto-hydrodynamics
[7] GRPIC=General-relativistic particle-in-cell

or weakly magnetized, or whether we can constrain the putative non-alignment between the black-hole and accretion-flow angular momenta ("tilted disk models"). Using simple, few-parameter, analytical models to answer such questions is important because it allows to draw conclusions that are not affected by the choice of initial or boundary conditions that numerical simulations have to make.

3. How do relativistic effects shape strong-field observables? Relativistic effects distort electromagnetic observables in many respects, that are often intricate and difficult to disentangle. Fig. 1.5 illustrates one particular family of relativistic effects: the timing effects at play on radiation that modulate the observation time of a photon emitted close to a black hole[8]. It is an important part of my activity to understand and discuss these effects, and determine to what extent they might lead to probe the compact object's properties.

4. What spacetimes should be considered for studying strong-field effects? The question here is to determine what is the most relevant spacetime description that should be used in the prospect of probing strong-field gravity. The Kerr spacetime is an obvious choice. Post-Newtonian expansions of this spacetime are natural alternatives. Spacetimes of other non-black-hole objects are also key when challenging the black hole paradigm is at stake.

5. How to use electromagnetic strong-field observables in the perspective of probing gravity? Here I use the notion of "probing" in the sense defined in section 1.2. Based on the knowledge developed when studying the four first questions above, the final aim is to develop methodologies for challenging the black hole paradigm, test the nature of compact objects, and ultimately test the theory of gravity in the strong-field limit.

Considering these science questions, and in particular the most advanced fifth one, implies obtaining exquisite precision data. This is allowed by the latest generation of instruments, GRAVITY and the EHT, but is restricted to very few astronomical sources. Only Sgr A* and M87* are close and big enough that we can scrutinize their surroundings with precisions of the order of the size of their event horizon. However, the questions above are very general, and do not depend on the particular source that is observed. This is the reason why it is of the utmost importance to put so much effort on so few objects, because they are so special in terms of their apparent size from Earth.

[8]Note that separating the Shapiro delay into two sub-effects in Fig. 1.5 is justified only by pedagogical reasons. This splitting is coordinate-dependent, so there is only one, global, physical effect, which is separated here into two to highlight the various underlying causes of this one and only effect.

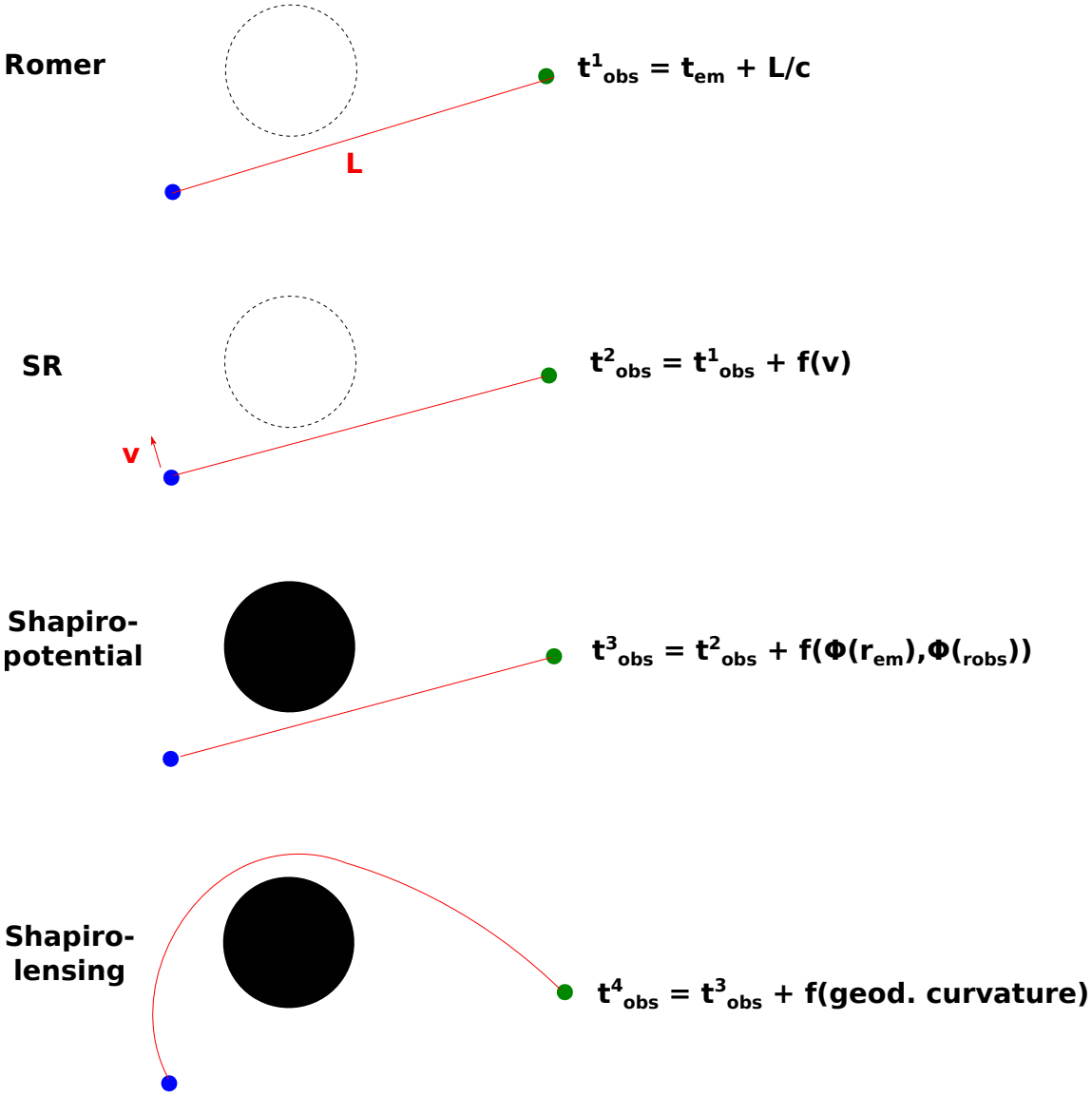

Figure 1.5: Romer and relativistic timing effects affecting radiation. The black disk represents a black hole event horizon while the dotted circle highlights that there is no compact object and the spacetime is flat. A photon is emitted in all cases at the blue dot and received at the green dot. It follows the red trajectory. The observation time of the photon is expressed as a function of the emission time. In the top row, only the finite velocity of light in flat spacetime is considered (Romer effect). In the second row, the special-relativistic (SR) effect linked with the relative motion of the observer and emitter is considered. In the third row, the delay due to the varying gravitational potential Φ between emission and reception is considered, while the photon is supposed to still follow a flat-spacetime trajectory (Shapiro delay due only to the varying potential, "Shapiro-potential"). In the bottom row, the full general-relativisitic null geodesic followed by the photon is considered, which adds an extra delay (Shapiro delay due to the curvature of the geodesic, "Shapiro-lensing"). Note that the curvature of null geodesics illustrated in the bottom row does not only change the observation time, but also the apparent direction of incidence, leading to strong lensing effects, the analysis of which is a key part of my activity. This figure illustrates only *timing* relativistic effects (delay on the observation time) affecting the *radiation*. There are also *spectral* relativistic effects on the radiation (Doppler shift), and relativistic effects that affect the emitter's dynamics in the strong-field region (e.g. relativistic precession).

2

Main methodology : Gyoto code

The main motivation of my PhD thesis was to develop a ray-tracing code, with the aim of applying it to the modeling of stellar orbits and flares surrounding Sgr A* in the context of the GRAVITY instrument development. This effort lead to the birth of Gyoto (General relativitY Orbit Tracer of the Observatory of Paris), a project developed in collaboration with Thibaut Paumard, Eric Gourgoulhon and Guy Perrin [Vincent et al., 2011].

Gyoto is a very modular public C++ code[1] which is able to compute null and time-like geodesics (i.e. trajectories of photons and massive particles) in any spacetime. The underlying spacetime metric might be specified either analytically or numerically. It is also capable of integrating the radiative transfer equation along the null geodesics of photons, making it much more than a simple ray-tracing algorithm, but really a machinery dedicated at producing accurate strong-gravitaional-field observation simulations.

Since my PhD, the Gyoto code has evolved a lot and has in particular gained a carefully designed architecture lead by Thibaut Paumard, who has been in charge in particular of making the general choices of the code architecture, defining the input/output formats, developing the parallelization of the code (multithreading, MPI), the development of a python interface, and the compilation machinery for Mac and Linux. My task was focused on adding specific C++ classes in the code in order to apply Gyoto to a variety of astrophysical problems that will be presented in the chapters below.

I would define my profile as that of a relativistic astrophysicist. As such, my main interest is in the modeling of physical phenomena in the vicinity of compact objects with always

[1] gyoto.obspm.fr

a strong emphasis on the link with observational tests. The pure numerical developments are not a major part of my activity and I will thus not devote more space on the technical details of the GYOTO code (Figure 2.1 illustrates the general structure of the code and will be enough for our future needs), and focus on the astrophysical applications. All the next chapters are strongly dependent on the use of GYOTO which really appears as the unifying technical theme of my activities.

I will conclude this short chapter by mentionning that GYOTO is obviously not the only ray-tracing tool in the literature. A complete review would be a difficult exercise given the impressive number of such codes that have been published in the last decade. Let us cite few important codes (non-exhaustive list): geokerr [Dexter and Agol, 2009, optimized for Kerr spacetime, with polarization, does not allow non-Kerr spacetimes], GRay [Chan et al., 2013, massively parallel, arbitrary spacetime], pyhole [Cunha et al., 2015, arbitrary spacetime, no astrophysical radiative transfer], ipole [Mościbrodzka and Gammie, 2018, with polarization, arbitrary spacetime], and the BHOSS code (of Z. Younsi, I am not aware of specific publication describing the code, which is used in many publications). Compared to this impressive list, the specificity of GYOTO is the fact that it contains a lot of built-in astronomical sources (stars, various disks, jets...) which allow to simply tackle a broad range of astrophysical questions. The main shortcoming of GYOTO is that it does not yet allow polarized radiative transfer, but this is under construction (see the perspectives in chapter 7).

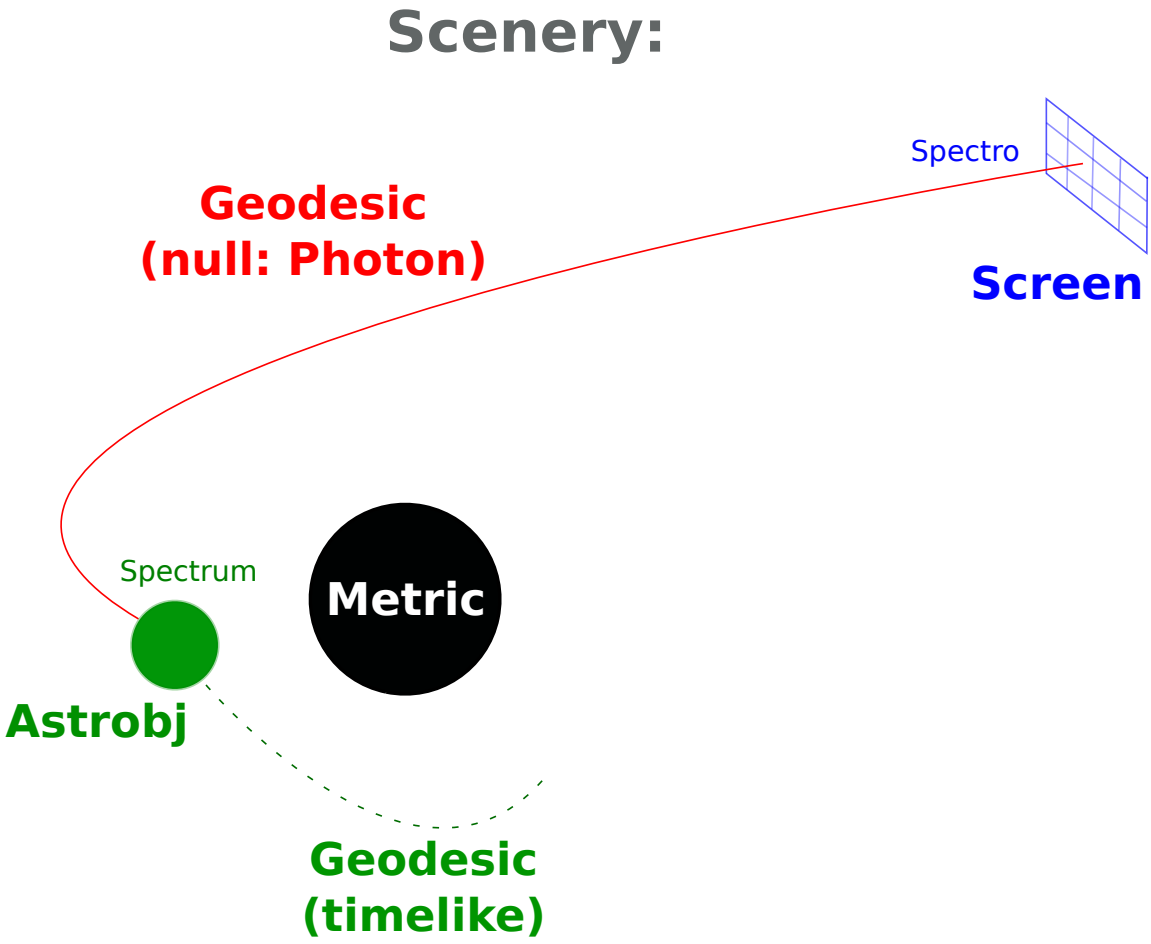

Figure 2.1: Sketch of the main C++ classes of GYOTO. A Scenery is made of some particular Metric, with some astronomical object (Astrobj) evolving in it (for instance, a star following a timelike geodesic). This Astrobj will emit some radiation that will follow null geodesics (Photon path) until it reaches a distant observer's Screen. Inside the Astrobj, the Photon path is integrated in parallel with the integration of the radiative transfer equation, allowing to obtain a realistic map of specific intensity on the observer's Screen.

3

Science field 1: Sgr A* close environment

Contents

3.1 Sgr A* environment

The region of interest for my science is the very vicinity of the central supermassive black hole of the Galaxy, Sgr A*. However, in order to set the scene, let us briefly introduce the

main components of the Galactic center at the parsec scale. They are illustrated in Fig. 3.1.

This section is inspired by Genzel et al. [2010], and all references can be found there.

Sgr A* is located close to the geometrical center of spiraling streamers of ionized gaz forming the HII region known as the *minispiral*. It is surrounded on sky by the set of dense molecular clouds forming the *circum-nuclear disk*. The inner few parsecs of our Galaxy also harbor a dense and luminous *Nuclear Star Cluster*. It is mainly (96% in number) composed of old (>1Gyr), cool (3500K), low-mass (1 $M_\odot$) *late-type stars*. This population has a randomized, isotropic orientation of orbits. A big surprise was the discovery of increasingly many young (few Myr), hot (20 000K), high-mass (tens to 100 $M_\odot$) *early-type O/WR/B stars* that are rotating clockwise in a *warped disk* within the inner central 0.5pc ($\approx 10''$). Still closer in, the so-called *S-star cluster* harbors a population of mainly B stars occupying the central arcsecond (0.04pc, $200\,000\,GM/c^2$, where M is the central black hole mass), with an isotropic distribution of orbits. The closest S star to Sgr A*, called *S2*, will be one of the important topics of this chapter. With these two populations of massive stars (clockwise disk + S stars), the Galactic center appears as one of the richest massive-star formation regions of the Milky Way. The formation history of these young stars that were formed or transported so close to a supermassive black hole is puzzling and known as the paradox of youth. We will not discuss this important question any further here.

The population of parsec-scale young stars orbiting in the clockwise disk is of fundamental importance for the smallest scales of the Galactic center. Indeed, the winds expelled by this population, and in particular the few tens of Wolf-Rayet stars that launch winds at speeds of $\approx 10^{-5}\,M_\odot\,\mathrm{yr}^{-1}$, are the reservoir of fresh gas that is accreted onto the supermassive black hole (see bottom right panel of Fig. 3.1). In comparison, the mass-loss rates of the B stars forming the S-star cluster are much weaker (e.g. $\approx 10^{-8}\,M_\odot\,\mathrm{yr}^{-1}$ for the star S2). A small fraction of all this expelled gas will make it to the central black hole and build a geometrically thick accretion disk with an accretion rate predicted by recent simulations at the level of $\approx 10^{-8}\,M_\odot\,\mathrm{yr}^{-1}$ [e.g. Ressler et al., 2018] at the scale of the horizon (see top right panel of Fig. 3.1).

Sgr A* is known to be a particular inefficient accreting black hole, our Galactic center being an example of a low-luminosity galactic nucleus. The accretion rate at the parsec scale of the clockwise disk that contains the Wolf-Rayet stars feeding the inner accretion flow is of $\approx 10^{-3}\,M_\odot\,\mathrm{yr}^{-1}$. The accretion rate is constrained in the inner regions (<100M) by the observed Faraday rotation at submillimeter wavelengths: it drops to $10^{-7} - 10^{-9}\,M_\odot\,\mathrm{yr}^{-1}$, the exact value depending on the assumptions on the accretion flow. This value is in good agreement with that provided by numerical simulations at the scale of the horizon above. The drop by 5 orders of magnitude in accretion rate from 1pc to the event horizon is linked to the very small fraction of the total gas ejected by the Wolf-Rayet stars that is bound to

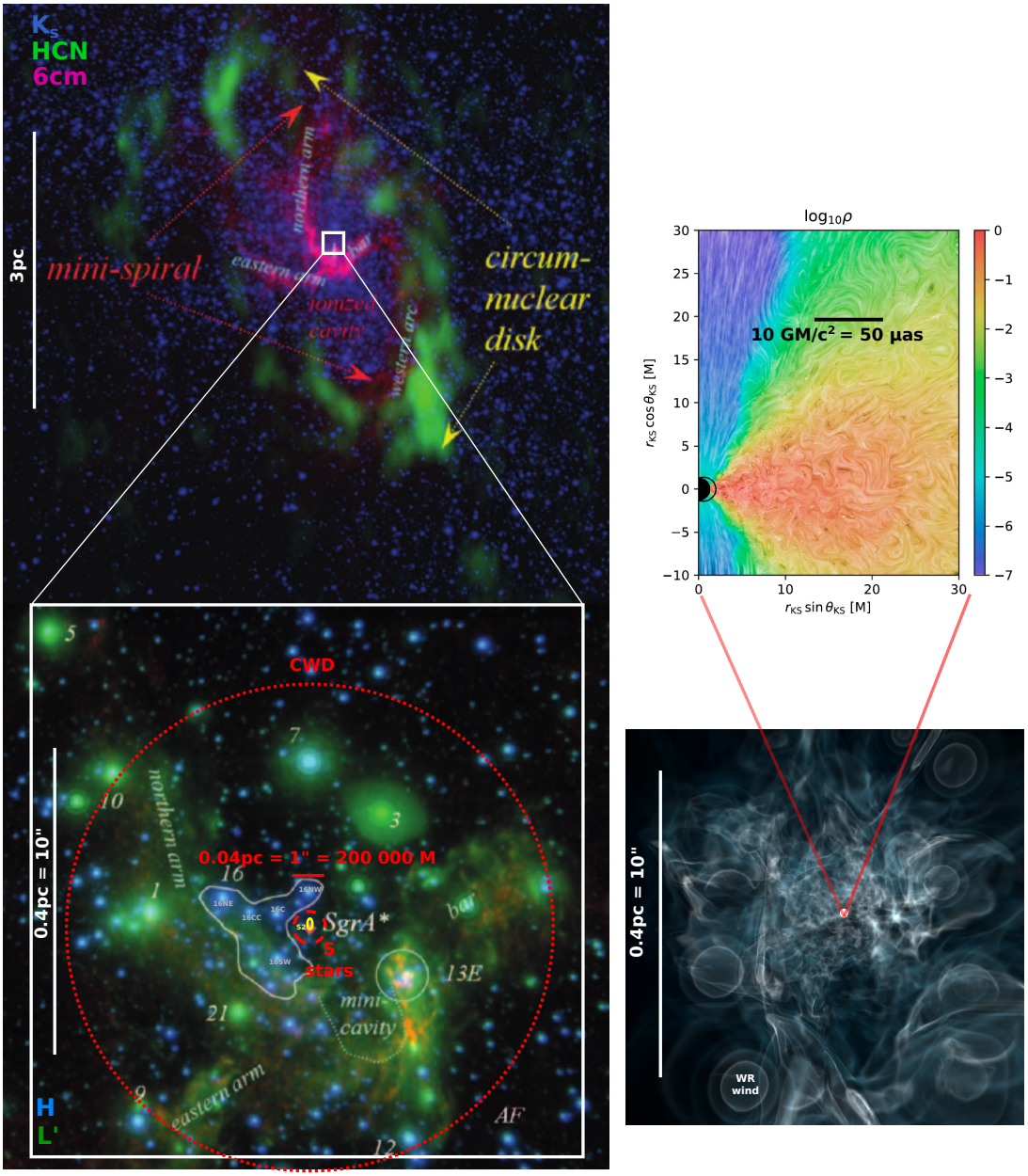

Figure 3.1: **Top left panel:** 10pc-scale multiwavelengths image of the Galactic center with the K_s band (2.2 μm) in blue (stars), HCN(1-0) emission in green (dense molecular clouds, forming the circum-nuclear disk) , and radio emission in pink (ionized HII region, the minispiral). **Bottom left panel:** 1pc-scale image of the surrounding of Sgr A* with H band (1.6 μm) in blue and L' band (3.8 μm) in green. Few of the IRS stars are labelled. The dotted red circle encompasses the clockwise disk (CWD) of young stars (note that not all stars within this circle are part of the disk). The dashed red circle shows the central arcsecond (0.04 pc) occupied by the S-star cluster, which corresponds to 200 000 gravitational radii GM/c^2. The tiny yellow orbit at the center of the image represents approximately to scale the orbit of the closest star to Sgr A*, S2, which approaches Sgr A* at a distance of 3000 GM/c^2 at its pericenter. The flares of Sgr A* likely take place in the inner accretion flow, within the inner few tens of gravitationnal radii from Sgr A*. Both left panels adapted from Genzel et al. [2010]. **Bottom right panel:** hydrodynamical simulation of the stellar winds launched by 30 Wolf-Rayet stars orbiting around Sgr A*. These stellar winds are the reservoir of the gas accreted onto the supermassive black hole at the smallest scales. Figure from Ressler et al. [2018]. **Top right panel:** zoom on the innermost accretion/ejection flow surrounding Sgr A*. Figure from Porth et al. [2019].

the black hole. Most of it is ejected away in outflows [Ressler et al., 2018]. On top of this low-luminosity quiescent state, Sgr A* experiences regularly (few times a day on average) outbursts that can lead to an enhancement of the X-ray flux by as much as more than two orders of magnitude, and as much as more than one order of magnitude in the infrared. These so-called *flares* will be another major topic of this chapter.

3.2 S2

3.2.1 Detecting relativistic effects on the orbit of S2

I took part in the supervision of the last year of the PhD of Marion Grould in 2015-2016, at the level of $\approx 30\%$, together with Guy Perrin and Thibaut Paumard. In this framework I collaborated with Marion on a project devoted to studying the relativistic effects on the orbit of the star S2 and their detectability. Marion was leading the research and my role was that of a supervisor, with frequent discussions and suggestions.

This project lead to the publication of Grould et al. [2017b] (with me as second author). This paper is dedicated to first presenting the astrometric and spectrometric impact of various effects (Roemer effect, Doppler, relativistic redshift, precession, Shapiro...) on the orbit of S2. Then, a statistical study is developed, using mock data with chosen error bars, and taking into account more and more refined models (from Keplerian to fully general relativistic) that incorporate these various effects one by one. The question is to determine, for each effect, the minimum time span needed to detect it with a given astrometric and spectroscopic accuracy. We have taken in this paper a very conservative point of view, considering that an effect is detected when a (simpler) model that does not take this effect into account fails to fit the observables, while a (more sophisticated) model that takes this effect into account does fit the data. This is very conservative in the sense that the more sophisticated model will start to be prefered (in the sense of Bayesian model comparison) much before the simpler model fails to fit the data.

In my opinion, this paper is particularly useful for its pedagogical introduction of the methodology needed to perform fully general-relativistic orbit fitting, and for the presentation of the various relativistic effects at play.

On this topic, Yu et al. [2016] and Waisberg et al. [2018] studied the prospect of constraining the spin parameter of Sgr A* by following putative closer-in stars, while Bozza and Mancini [2012] investigated the lensing effects on S stars and their detectability by GRAVITY. I am currently starting to supervise a Master student (with hope for an associated PhD grant), Karim Abd El Dayem, who is in charge of reviving this topic in our

team.

3.2.2 The extended mass distribution around S2

Gernot Heissel has joined our group at LESIA in February 2020 (at a difficult time for starting a position on a completely new topic!). The goal of his postdoc was to explore the possibility of using S2 astrometric data as observed by GRAVITY. I took part in the supervision of his postdoc at the level of $\approx 30\%$, together with Guy Perrin and Thibaut Paumard.

Let us briefly give the context of this study. As will be presented in section 3.2.3, the GRAVITY collaboration has recently detected the relativistic precession effect on the orbit of the S2 star, i.e. a prograde rotation of the Keplerian ellipse in the orbital plane. However, the black hole is not the only player that can lead to a precession effect. If Sgr A* is surrounded by a distribution of extended matter (e.g. dark matter), this extended matter will also lead to a precession effect, which is retrograde rather than prograde. It is thus of paramount importance to constrain the presence of such an extended mass component, and to try as much as possible to separate the relativistic precession from the extended mass precession. This question was raised as early as in Rubilar and Eckart [2001]. The recent results of Gravity Collaboration et al. [2020] has constrained this extended mass to less than 0.1% of the central mass (i.e. $\approx 4000\,M_\odot$).

The first goal of Gernot was to add a new piece in the numerical tool for analyzing GRAVITY data developed at LESIA (see section 3.6). This piece is a post-Newtonian orbit-fitting code, OOGRE, that allows to take into account not only the gravitational influence of the central supermassive black hole, but also that of a continuous distributed mass. The second goal was to use this new software in order to give prospects of the future capability of GRAVITY to constrain the extended mass distribution around Sgr A*, by using mock S2 astrometric data. A paper was recently published that presents these results, Heißel et al. [2021] (with me as fourth author, and non-first authors in alphabetical order).

The main results of this paper are the following. First, Gernot showed that the relativistic and extended mass precession effects have a very different integrated effect along the orbit: the relativistic precession mainly acts close to the pericenter, while the extended mass precession mostly takes place close to the apocenter (see Fig. 3.2). This is actually very reasonable since more and more extended mass is enclosed within the orbit as the star approaches the apocenter, while the relativistic effect is obviously stronger close to the compact object (and would vanish very far away). Second, Gernot showed that a full orbit of data is needed in order to substantially constrain the extended mass component. Data

only concentrated close to the apocenter are not sufficient to substantially constrain the extended mass profile, even though the extended mass precession only affects the part of the orbit closer to the apocenter.

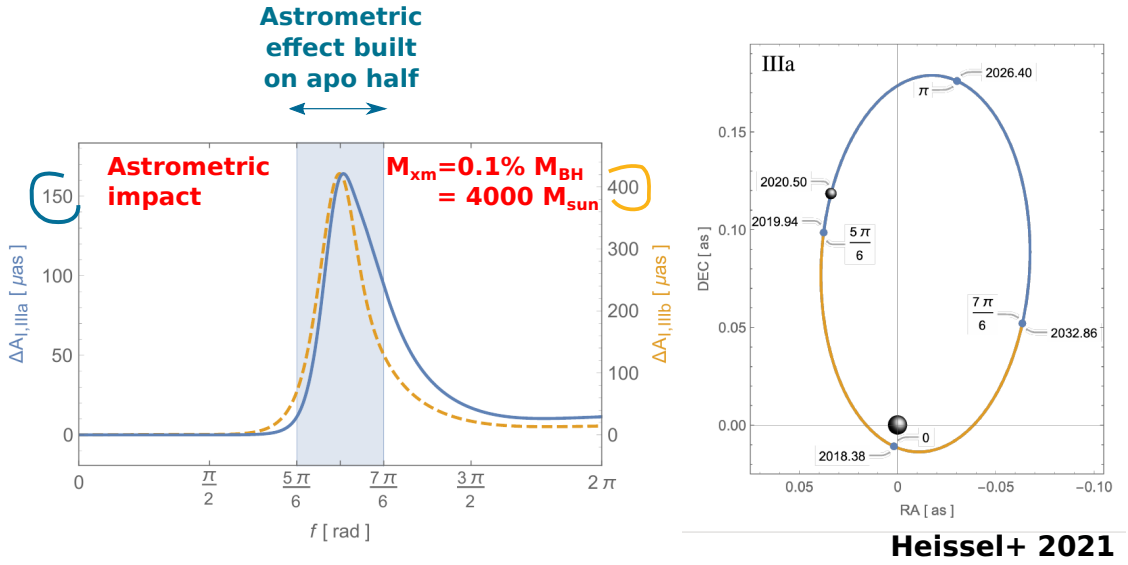

Figure 3.2: **Left:** difference between the astrometric impact of the pericenter precession in a model with and without extended mass (two colors for two different extended-mass models). The extended mass shows its effect only in the apocenter half of the orbit. **Right:** the S2 orbit with the apocenter and pericenter halves shown in blue and yellow. Figure from Heißel et al. [2021].

3.2.3 The GRAVITY collaboration precession detection

Gravity Collaboration et al. [2020] (with me as co-author) has detected the relativistic precession in the orbit of the star S2, in agreement with the general-relativity (GR) prediction, as illustrated in Fig. 3.3. This finding is of course of fundamental importance in the context of testing general relativity. This test is the exact same as the historical first test of general relativity carried out by Einstein in 1915 when he could check that the relativistic precession of Mercury was exactly explaining the disagreement with the Keplerian theory exhibitted by Le Verrier in 1859 (see Fig. 3.4). However, the case of S2 is also very different in the sense that here the test body is orbiting around a black hole rather than a weak-field object like the Sun. The confirmation of the prediction of general relativity for S2 is thus an important result that goes in the direction of scrutinizing the agreement between observation and theory in the strong-field regime.

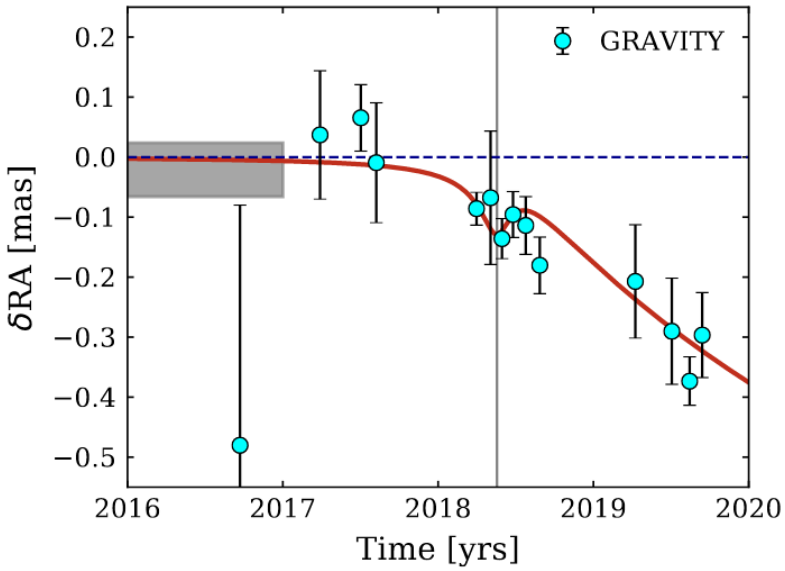

Figure 3.3: Right ascension of the star S2 as measured by GRAVITY. The scaling is such that a Newtonian orbit (without precession) would be consistent with zero. The general-relativistic (1PN) prediction is the red curve. From Gravity Collaboration et al. [2020].

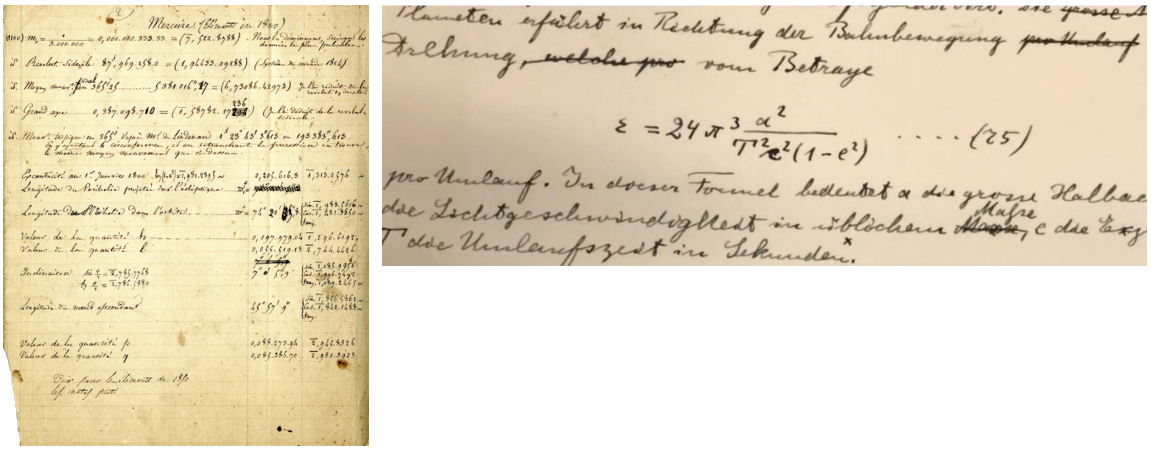

Figure 3.4: **Left:** calculations of Le Verrier in 1856 regarding the orbit of Mercury. **Right:** the relativistic precession effect on the orbit of Mercury as computed by Einstein in 1915.

My own contribution to the GRAVITY Collaboration paper was rather modest, mostly limited to participating to the observation runs and to the orbital data analysis in order to take part in the production of the final "science" data set, used for the paper analysis.

3.3 Simple analytical quiescent modeling of Sgr A*

Besides the stellar orbits, and primarily that of S2, the accretion/ejection flow surrounding Sgr A* is of major interest for studying the properties of matter and radiation in a strong gravitational field. Already during my PhD I devoted significant effort to the development of a model of the quiescent accretion flow surrounding Sgr A*, taking into account an ionized compact torus surrounding the black hole [Straub et al., 2012; Vincent et al., 2015, with me as second author for the first reference]. However, this model was not able to account for the radio data of Sgr A* which is emitted far from the object and cannot be captured by the compact torus model.

Vincent et al. [2019] present an extension of this early model, which takes into account both an ionized torus and a jet (see the blue structures of Fig. 3.6). The torus emits thermal synchrotron radiation, while the jet emits κ-distribution synchrotron. The κ distribution essentially bridges a thermal distribution for low values of the electrons velocity, to a power-law distribution for high values of the velocity. Both the torus and the jet are described completely analytically.

This torus+jet model allows to nicely fit the radio to infrared spectrum of Sgr A* whatever the inclination under which Sgr A* is seen. The constraints on the radio size of Sgr A* are in reasonable agreement with the prediction of the torus+jet model, while the constraints on the quiescent infrared spectral index are perfectly satisfied by our model. We also modeled EHT-reconstructed data and showed that the torus and jet structures are present in the reconstructed images, which highlights the importance that Sgr A* EHT data might have for constraining the accretion/ejection model. Another interesting feature of our model is that its best-fit parameters are very close to that obtained by Davelaar et al. [2018] when fitting sophisticated GRMHD simulations to the same observations. This shows that the important physics is captured in the framework of our very simple model.

This quiescent model of Sgr A* will be at the basis of the flare analysis presented in section 3.4.2.

The literature on the topic of modeling Sgr A* spectral properties is so vast that it goes far beyond the scope of this document to make a complete review. These studies can be divided into three areas:

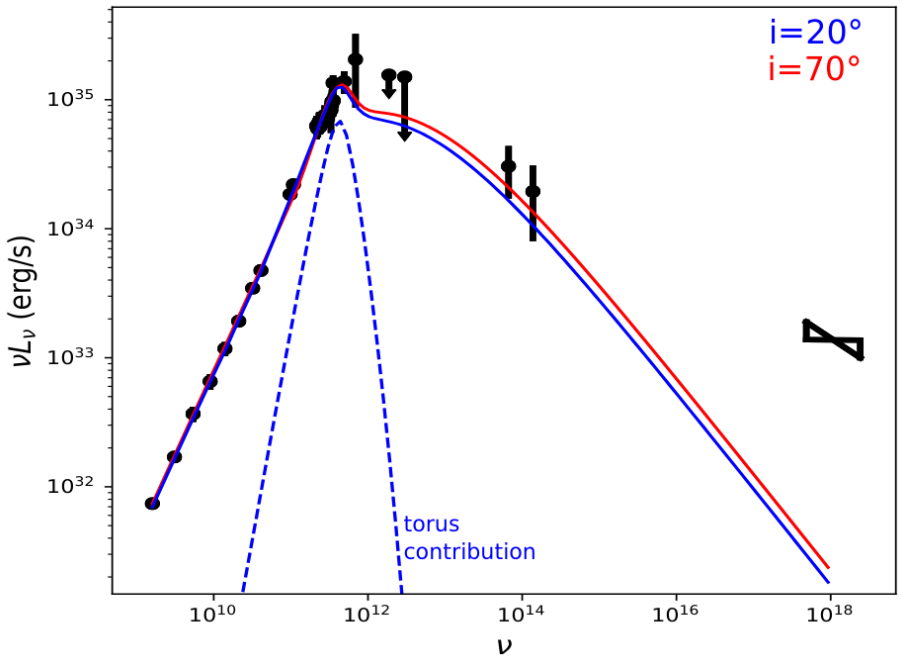

Figure 3.5: Best-fit spectrum of the quiescent Sgr A* torus+jet model. See Vincent et al. [2019] for details and references of the data.

- analytical models, like that of Vincent et al. [2019]. This area is probably the least populated. Let us cite Özel et al. [2000, hybrid thermal/non-thermal disk model], Markoff et al. [2001, jet model], Broderick et al. [2016, RIAF disk model]. The interest of analytical models as compared to numerical simulations was already discussed in section 1.5, the main arguments are reminded below;

- GRMHD simulations. This area is by far the most populated. Let us cite among many others in the recent literature Dexter et al. [2020, with electron heating prescription from PIC simulations], Ressler et al. [2020, initial conditions anchored in realistic stellar winds], Yoon et al. [2020, discussion of the importance of radiative cooling]. GRMHD simulations are key to study the global properties of accretion/ejection flows onto Sgr A*. Their main drawbacks is that they do not model self-consistently electron heating, and rely in the best cases [e.g. Dexter et al., 2020] on prescriptions from PIC simulations, and cannot capture pair-creation processes;

- GRPIC simulations, which, compared to GRMHD, are able to capture the physics of particles from first principles, thus getting rid of the drawbacks cited above. In my view, this is really the most promising avenue that might revolutionize our understanding of the accretion/ejection flows around black holes in the close future. GRPIC simulations are very new, the first such code being Parfrey et al. [2019, 2D simulations]. It is too early to have already reached a "steady-state" of publications and major results, contrary to GRMHD simulations. Let us cite the very promising pioneering results of the first 3D global GRPIC simulation of black holes environment by Crinquand et al. [2022].

To conclude this part, let us remind the arguments in favor of developing simple analytical models of accretion/ejection flows, in the present context of flourishing sophisticated GRMHD and GRPIC simulations. The interest of simplicity is to be able to determine what observables are robust against changes in the initial conditions or in the numerous technical choices that have to be made by simulations. It is thus very reassuring when a simple analytical model, that focuses only on the main characteristics of the flow, produces very similar predictions as that of much more complex models. Moreover, analytical models are perfect testbeds for investigating the impact of individual parameters or specific physical effects (e.g. relativistic effects), because they allow to easily switch on and off various parts of the physical model. One particularly important point allowed by analytical models is to discriminate between observables that are gravity-driven, or astrophysics-driven, which is of course key in the prospect of probing strong gravity (I will come back to this in section 4.4.1). Finally, analytical models allow very fast computations and are thus important for investigating large regions of parameter space, which is not doable with costly sophisticated simulations.

3.4 Flares

3.4.1 Early studies

I will focus on my most recent activity on flares and just remind quickly earlier results.

Vincent et al. [2014b] present an early prospective study of the then-future ability of GRAVITY to make a difference between the astrometric signature of an orbiting "hotspot" and that of an ejected blob. The paper develops three models of flares: a hotspot triggered by the onset of a "Rossby wave" (see section 5.1.1 for details) instability in the accretion disk, statistical fluctuations of the physical properties of the accretion disk, ejected blob of plasma. It concludes that GRAVITY can make a difference between an orbiting hotspot and an ejected blob provided the inclination is $\gtrsim 45°$ and the flare is bright enough (brighter than $m_K = 15$). This result will be quickly rediscussed in the light of the recent GRAVITY Collaboration detection in section 3.4.3.

Mossoux et al. [2015] (with me as third author) study an X-ray flare of Sgr A* observed by XMM in 2011, which shows a remarkable double peak structure. It is tempting to attribute this double peak to a hotspot seen edge-on, with the second peak being due to the Einstein ring generated by the hotspot when seen behind the black hole. Our study demonstrates that a hotspot model cannot account for the observed data: the observed variation of the light curve, which comes back at the quiescent level between the two successive peaks, is not in agreement with the hotspot prediction.

3.4.2 Magnetic reconnection model

I am supervising (at $\approx 85\%$) the PhD of Nicolas Aimar since 2020. Nicolas focuses mainly on the study of Sgr A* flares. During his Master internship he has considered a simple hotspot model and has focused on the impact of the quiescent radiation of Sgr A* on the flare observables (astrometry and light curve). Since 2021 his major interest is to develop a semi-analytical flare model dedicated at capturing the core physics of magnetic reconnection close to a black hole.

The basic idea of magnetic reconnection as a flare model for Sgr A* is that the magnetic field lines in the close environment surrounding Sgr A* is very turbulent and can lead to the formation of magnetic zero points where the geometry of the field lines can suddenly rearrange, leading to efficient acceleration of the local electrons. The accelerated electrons are concentrated in a compact region known as a plasmoid, which is a natural candidate for

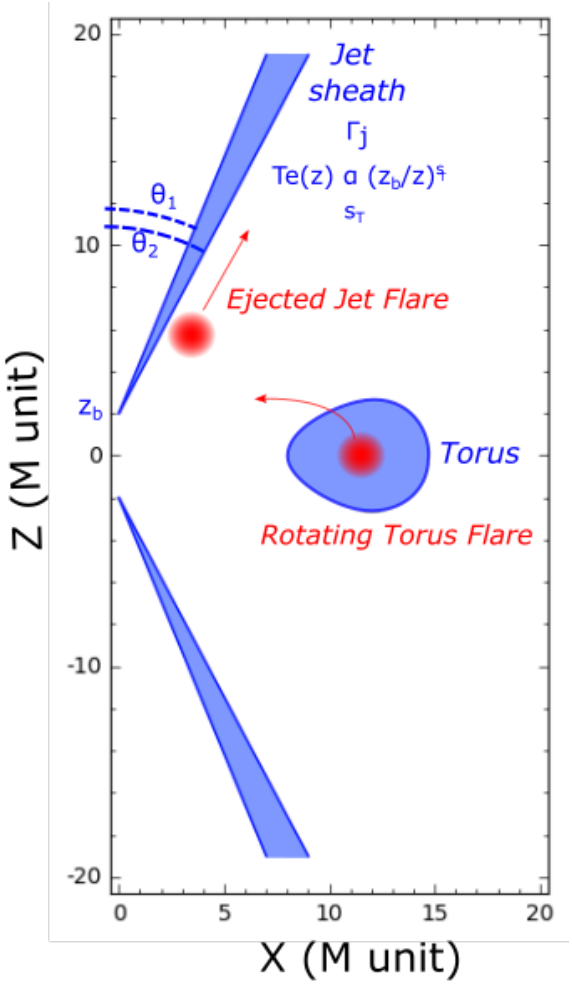

Figure 3.6: Scheme of the torus-jet model for the quiescent state in blue and flares in red. Two trajectories are considered for the flare, which can either be ejected along the jet sheath, or rotate in the torus. The jet is parametrized by the angles θ_1 and θ_2 that describe the angular opening of the radiation-emitting sheath, by the base height z_b, the constant Lorentz factor Γ_j , and the temperature power-law index s_T. The jet is symmetrical with respect to the equatorial plane, and axisymmetric. Figure from Aimar et al. (2022, in prep.).

the observed hotspots close to Sgr A*. Magnetic reconnection is a complicated phenomenon that starts only recently to be studied in a black hole environment through 3D GRMHD and 2D GRPIC simulations [Ripperda et al., 2022; El Mellah et al., 2021]. Our goal is not to use such very elaborate simulations, but rather to keep the same point of view as in our study of the quiescent radiation of Sgr A* (see section 3.3) and privilege simpler semi-analytical models that allow to capture the main physics while erasing the extremely complex (and little constrained) details.

Nicolas has built his reconnection flare model starting from the quiescent torus+jet model presented in section 3.3, see Fig. 3.6. We consider that a reconnection event can be triggered either in the jet sheath or in the equatorial plane inside the torus. The reconnection itself is not modeled, we rather focus on its consequence which is the appearance and time evolution of the plasmoid discussed above. We consider a compact plasmoid (of typical size GM/c^2) in which accelerated electrons (following a κ distribution) are injected between the initial time $t = 0$ and a chosen injection time $t_{\rm inj}$. We consider a linear increase of the density of the electrons with time inside the plasmoid. For $t > t_{\rm inj}$, the injection stops and the density inside the plasmoid remains constant. An important ingredient of Nicolas' model is the ability to accurately follow the time evolution of the distribution of the electrons inside the plasmoid, that cool by emitting synchrotron radiation. This piece of the model was added by collaborating with Anton Dmytriiev, who was a PhD in Paris Observatory until 2020 and is now a postdoc in North-West University, South Africa. His kinetic code EMBLEM [Dmytriiev et al., 2021] is able to evolve a population of electrons and to self-consistently determine the emission of this population. Nicolas was able to interface EMBLEM with Gyoto in order to accurately follow the emission of the accelerated electrons in the plasmoid, and thus be able to compute the photometric and astrometric observables associated to this plasmoid, on top of the quiescent radiation provided by the torus+jet model of section 3.3.

This project has lead to a paper with Nicolas as first author, Anton as second author, myself as third author, which should be submitted in the summer of 2022. At the time of writing this document, the paper is still in progress, and I will illustrate the results of Nicolas by Fig. 3.7, which compares the astrometric and photometric signatures of a simpler model, a hotspot with a prescribed Gaussian-modulated synchrotron emission, to the July 2018 GRAVITY Collaboration flare data (see section 3.4.3).

The key interest of Nicolas' model is that it allows to generate reasonably realistic observables (certainly one of the most realistic predictions from a semi-analytical model in the literature) within a limited computation time. This will allow us to study the parameter space and try to disentangle between astrophysics-driven and gravity-driven features in the observable, which is key in the prospect of using flares as probes of the spacetime geometry close to the compact object. Let me stress that the self-consistent treatment of the electron

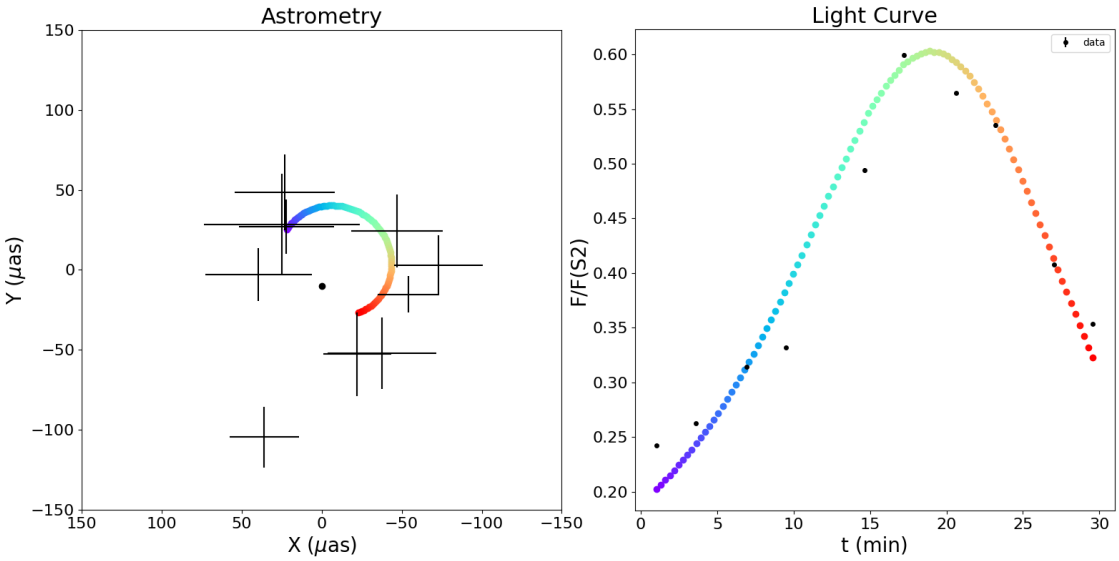

Figure 3.7: Prediction of a Gaussian-modulated, synchrotron-emitting hotspot model for the astrometry (left) and light curve (right) compared to the GRAVITY flare data of 22 July 2018. Colors encode observing time. This result is not a fit but rather a "first guess", the parameters were chosen to match the main features of the observables. Figure from Aimar et al. (2022, in prep.).

cooling within the plasmoid is also a very important ingredient of the model, which, to my knowledge, is not incorporated in GRMHD simulations [e.g. Scepi et al., 2022].

Similarly as for quiescent models, flare models of Sgr A* have given rise to a very rich literature, again separated in the three same areas as for quiescent modeling (see section 3.3). It is thus beyond the scope of this document to make a complete review. As before, I will cite the most relevant recent publications, focusing on magnetic reconnection models by GRMHD simulations [Ripperda et al., 2022; Scepi et al., 2022], and GRPIC simulations [El Mellah et al., 2021]. Let us stress that only PIC simulations are able to self-consistently trace the non-ideal physics of reconnection. Similarly as for quiescent models, my conviction is that GRPIC will be key to strengthen our understanding of the phenomena at play during Sgr A* bursts. Note that El Mellah et al. [2021] obtain a typical time of the flare event that is too short to explain Sgr A* data. It might be that an interplay between the black hole magnetosphere (which is the only part of the flow modeled by the PIC simulation) and the larger-scale disk (not modeled in the simulation) could allow obtaining a better agreement.

3.4.3 The GRAVITY collaboration "hotspot" detection

A breakthrough of the GRAVITY collaboration was to detect circular orbital motion very close (few gravitational radii) to the black hole for three flares of 2018. This result was presented in Gravity Collaboration et al. [2018] and is illustrated in Fig. 3.8. The main conclusions of this paper are that: (i) at least these flares of Sgr A* are compatible with a hotspot model in *circular rotation close to the black hole*, (ii) the *inclination* under which Sgr A* is seen *is rather low* (closer to face-on). This result is of great importance, first because it demonstrates with full confidence that at least some flares are strong-field events that might thus be considered as probes of this very fascinating region; second, because it gives a very convincing argument in favor of hotspot-like models. An interesting point to note is that the simple hotspot model used in Gravity Collaboration et al. [2018] leads to a predicted track that lies always inside the observed orbit. The velocity of the hotspot was assumed to be Keplerian in our model, so this means that the observed hotspot has a slightly super-Keplerian velocity. This is rather puzzling because the latest GRMHD models of hot flows are either approximately Keplerian when they are weakly magnetized (so-called SANE models), or slightly sub-Keplerian when they are strongly magnetized (so-called MAD models). For me this point is an open question that might be an important hint.

My personal contribution to the Gravity Collaboration et al. [2018] paper was devoted to taking part in the observation runs, and redoing independently the astrometric data

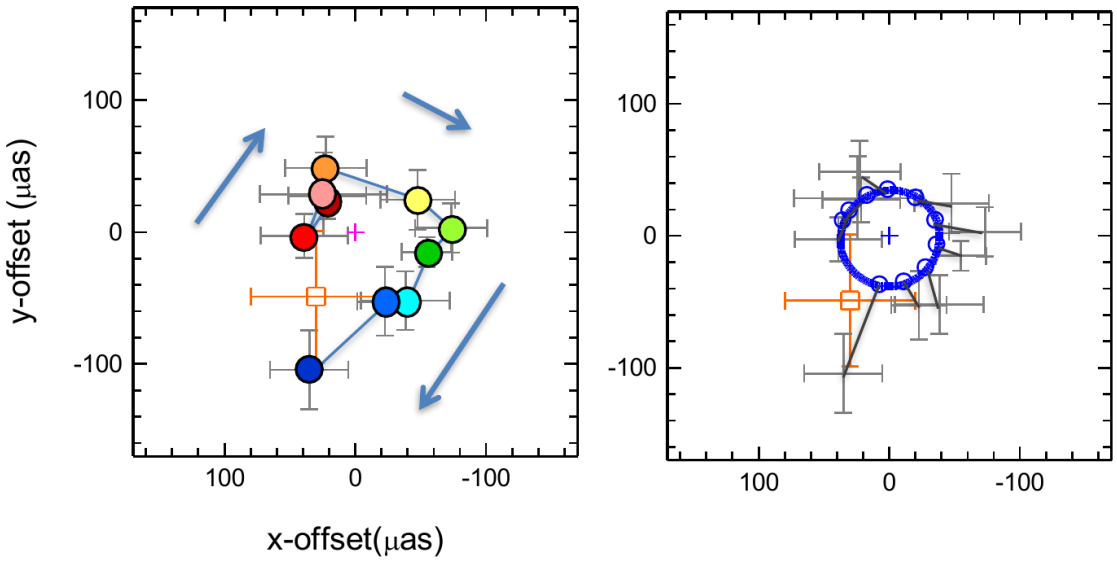

Figure 3.8: Gravity Collaboration et al. [2018] astrometry of the July 2018 event. **Left:** The red cross is the predicted position of the center of mass from the S2 orbit, while the colored data show the time evolution of the flare's infrared centroid. **Right:** same orbit with the best-fit model obtained with a simple hotspot scenario (blue track).

analysis first performed at MPE (a total of four such independent analyses were carried out in total to strenghten the result). Thibaut Paumard then used my reduced data to fit the orbit with a simple hotspot model implemented in the GYOTO code and found constraints on the orbit that are very similar to that found at MPE (a total of three independent ray-tracing codes were used to strengthen the result, all found comparable best-fit results).

Gravity Collaboration et al. [2018] having constrained the inclination of Sgr A* to rather low values, it is not possible to distinguish a hotspot orbiting in the equatorial plane of the black hole with a hotspot ejected along a jet. This is in agreement with the analysis of Vincent et al. [2014b] presented in section 3.4.1.

3.5 Alternative objects

The most advanced realistic objective regarding the probing of strong-field gravity, as listed in section 1.2, is dedicated to studying the nature of compact objects, i.e. making an observational distinction between a black hole and an alternative object. In this context, I have been interested in studying one particular alternative to black holes: boson stars. A

boson star is a compact object made of a self-gravitating assembly of spin-0 bosons (like the Higgs boson for instance), which has no surface[1], no event horizon, and no central singularity. It is a very well defined object and I consider it as a perfect testbed for horizonless objects. Let us make the objective very clear: my aim, by analyzing such exotic objects, is definitely not to try to demonstrate that all black hole candidates are actually rather boson stars[2]. The aim is to strengthen (or put in question!) the black hole paradigm by determining whether observations definitely favor the black hole scenario, as compared to reasonable alternatives. From my point of view, boson stars are thus not interesting *per se*, but only in so far as they constitute a well-defined class of objects that do not share the characteristic feature of black holes, i.e. the existence of an event horizon. Using boson-star spacetimes at Paris Observatory was also a very natural choice because our colleagues at Paris Observatory/LUTH, specialists of numerical relativity, had developed in 2014 a thorough study of the properties of rotating boson stars [Grandclément et al., 2014], and had thus state-of-the-art spacetime metrics available for us, and an advanced knowledge of the properties of these exotic spacetimes.

Constraining the nature of Sgr A* is a challenging task because of the rather limited detailed knowledge that we currently have of the close environment of Sgr A*. It is thus very difficult to say for sure whether some particular observable feature is the definitive proof of the nature of the compact object, or whether this feature is simply due to some particular unconstrained astrophysical phenomenon. Still, it is of the utmost importance to study the observables associated to strong-field phenomena close to Sgr A*, considering alternatives to the standard Kerr black hole.

3.5.1 Boson stars: image of Sgr A*, stellar trajectories, hotspot

My first interest in this context was to compute the image of the accretion flow surrounding Sgr A*. I considered the ion-torus quiescent model of Sgr A* presented in section 3.3 [Vincent et al., 2015], and computed its millimeter image (i.e. the EHT-like observable) when a rotating boson star is considered rather than a Kerr black hole. This lead to the interesting result, presented in Vincent et al. [2016b], that the resulting image, when degraded to the resolution of current instruments, is extremely similar to that of a black hole image (see Fig. 3.9). This result does not demonstrate that it is impossible to make a difference between a black hole and a boson star, because our modeling is extremely simple and does not allow to self-consistently evolve the accreting matter in a black hole spacetime and

[1] The name "star" is thus very misleading, but it has been long accepted; a boson star is a distribution of scalar field that exponentially decreases with radius, so there is no clear notion of a surface.

[2] Stellar black holes are definitely not boson stars. Reasonably realistic formation scenarios are only proposed for supermassive boson stars at the center of galaxies: early inhomogeneities of a putative primordial scalar field could have been the seeds of present-day supermassive boson stars at the center of galaxies.

in a boson star spacetime. It is likely that the astrophysics will be different in these two cases [this was actually recently partially demonstrated by Olivares et al., 2020], which might lead to observable differences. However, the key point demonstrated by our study is that the difference of spacetime geometry *alone* is not able to make a clear difference between the black-hole and the boson-star observables. Only the poorly-constrained astrophysics can make a difference. This result highlights even more the big difficulty of telling the nature of a compact object: it is really a difficult task to disentangle the geometry from the astrophysics. The same point will be made in the context of M87* in section 4.4.1.

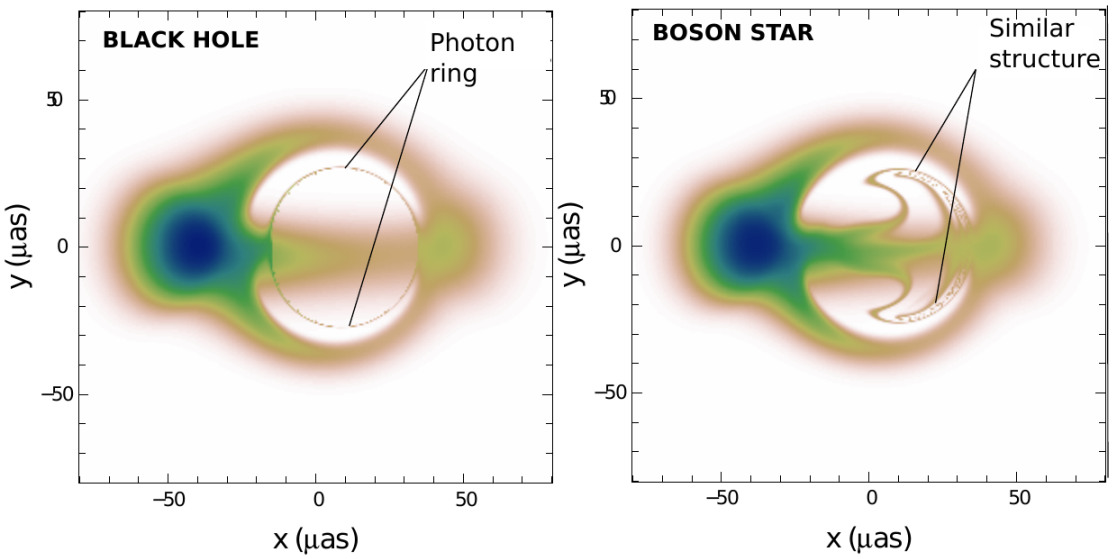

Figure 3.9: Image of an ion torus surrounding Sgr A* when this object is considered to be a rotating black hole (left) or a rotating boson star (right). The image is different, but with the $\approx 25\,\mu$as resolution of the EHT, both objects will lead to similar observables. Image from Vincent et al. [2016b].

Grould et al. [2017a] (with me as third author) then discussed the question of stellar orbits in a boson star spacetime, with the same objective of determining whether particular observable signatures are within reach, as compared to the classical black hole scenario. At the time of writing this paper, Marion Grould was a postdoc at Paris Observatory/LUTH and my contribution to the paper was rather limited because Marion already had a perfect knowledge of GYOTO. I helped a bit with the development of ray-tracing in non-Kerr spacetimes, which was new for Marion. The main result of Marion's study is to highlight boson-star stellar orbits that are very different from Kerr (e.g. orbits that are bound in Kerr, and become unbound around a boson star, or very specific "pointy-petal" orbits in the boson-star spacetime that have no equivalent in Kerr). This study does not go as

far as performing orbit-model fitting in both spacetimes, taking into account the accuracy of GRAVITY, which is a necessary step in order to determine whether an observational difference could be made.

The third obvious observable of interest are Sgr A* flares. This last step was taken only recently by Portuguese colleagues of the GRAVITY Collaboration, Joao Luis Rosa (now postdoc at the University of Tartu in Estonia), Paulo Garcia and Vitor Cardoso. I am participating since 2020 in this project. The main idea of the project was to compute the astrometric and photometric observables associated to a simple hotspot orbiting around a non-rotating black hole and a non-rotating boson star, Joao and Paulo have been leading the research work and have used the GYOTO code for performing these computations. My contribution was devoted to technical guidance for Joao regarding the use of the code, and participating in the discussions and interpretation of the results. This project has lead to a paper with Joao as first author, myself as third author, which should very soon be submitted. The main result is that the horizonless nature of boson stars leads to a particular "plunge-through" image due to photons that travel through the compact object (which is obviously impossible for a black hole). It remains to be determined whether this interesting feature can lead to a clear failure of the boson-star model compared to GRAVITY data.

3.5.2 Other exotic objects: black hole with scalar hairs, wormhole, non-GR black hole

Motivated by the breakthrough discovery of a new solution to the Einstein field equations, the so-called Kerr black holes with scalar hairs [Herdeiro and Radu, 2014, this model can be seen as a black hole inside a surrounding boson star], I collaborated with Carlos Herdeiro to determine the observational appearance of such exotic compact objects surrounded by my standard accretion model [Vincent et al., 2015], in the exact same spirit as the boson-star imaging paper presented in the previous section. Vincent et al. [2016a] discusses potentially observable differences between standard black holes and these hairy black holes. It shows that the high-order very lensed features of the image have a different morphology and angular size in both spacetime, and that the central flux depletion known as the black hole shadow in the standard Kerr spacetime can disappear in the hairy black hole spacetime (see Fig. 3.10). These notions (high-order features, shadow) will be introduced in depth in section 4.4.1.

Such exotic spacetimes imaging studies have been continued through collaborations with young researchers. Lamy et al. [2018] (with me as fourth author, F. Lamy being a thrid-year PhD student at the time) studied a new wormhole spacetime, inspired by regular black hole solutions. From my point of view, the interest of this setup is to consider a different kind of

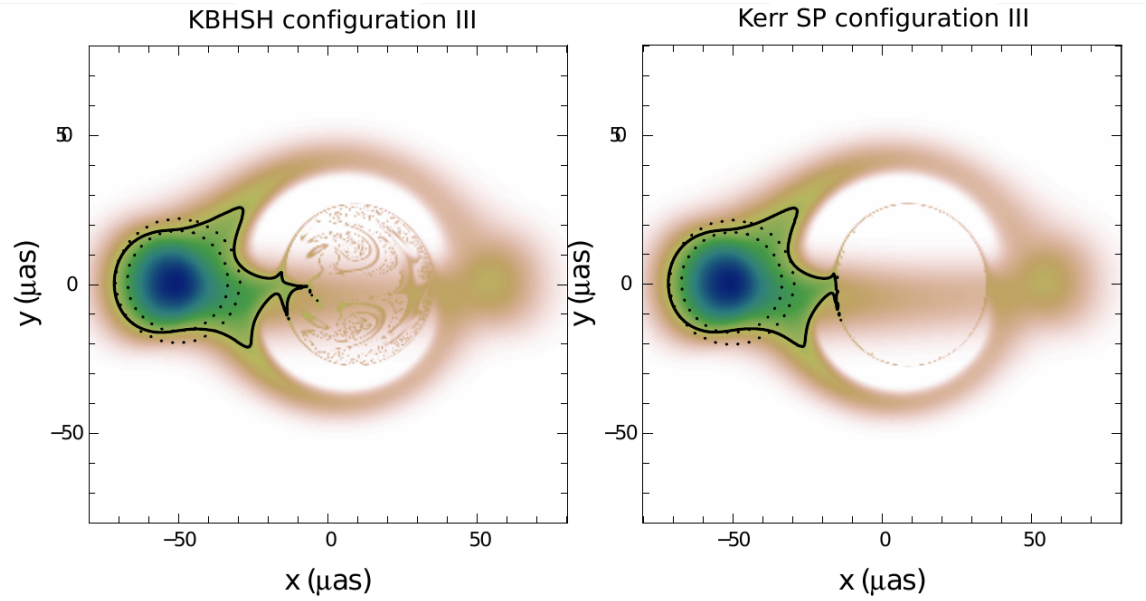

Figure 3.10: Image of an ion torus surrounding Sgr A* when this object is considered to be a black hole with scalar hairs (left) or a standard Kerr black hole (right). The scalar hair completely changes the lensing properties of photon in the central part of the image, leading to the disappearance of the central flux-depleted region of the Kerr case.

horizonless object and compare it to both the standard Kerr spacetime, and the boson star spacetime. F. Lamy comes to the same conclusion as my 2016 boson-star study, i.e. that it is impossible with current facilities to make a difference between a black hole image and a wormhole image. This highlights again the extreme difficulty of telling the presence of an event horizon, and demonstrates that this conclusion is not restricted to the particular choice of the boson star geometry. My contribution to this study was rather limited: I helped F. Lamy mastering the use of GYOTO and participated in the discussion of the results. I have reused this wormhole spacetime in my M87* study presented in section 4.3.

As explained in section 1.2, I do not give a strong priority in studying non-GR theories, because my conviction is that the observational distinction between theories through electromagnetic probes is outside our current reach. I made one recent exception by collaborating to the study of Van Aelst et al. [2021] (with me as third author, K. Van Aelst being a postdoc) who studied black hole solution in a non-GR alternative theory known as cubic Galileon theory. My contribution was similar as in the previously mentionned paper: I guided K. Van Aelst for using GYOTO and participated in the discussion of the results. The conclusion of this study is that the millimeter images in a black hole and cubic Galileon spacetime do differ, but that this difference is very likely strongly degenerate with the astrophysics parameters of the accretion model.

3.6 GRAVITY data analysis

Last but not least, I took part in the development of the LESIA data analysis tool for GRAVITY observations. The main developer of this tool is Thibaut Paumard which explains why I don't put a strong emphasis here. My contribution was to write an early version of the FitGCData software introduced below, that was later enhanced and fully reorganized by Thibaut, in such a way that the tool is now very versatile and easy to use. I still reasonably master the full pipeline and am able to dig into the code when needed. The LESIA data-analysis pipeline contains three main python codes:

- FitGCData allows to fit a one-source, a binary, or a three-source model to the GRAVITY data, and to obtain the coordinates of the observed sources (Sgr A*, S2, other stars) in the field. My contribution to this software was to write an early version in 2017. The later evolutions were due to Thibaut Paumard.
- FitS2 allows to perform relativistic orbit fitting on the S2 star alone or on multiple stars at the same time, considering various methods, from a simple Keplerian fit to a full-GR fit, through the recent inclusion of a post-Newtonian fit added by Gernot Heissel in 2021 (see section 3.2.2). The early development of the tools were done

during the PhD of Marion Grould. The input of this software are the sky positions of the sources (i.e., the output of the previous software), together with radial velocity data. I contributed a bit to this software, with in particular recent additions that aim at allowing an easy comparison between the full-GR and post-Newtonian formalisms.

- FitFlare allows to fit a hotspot model to flare data observed by GRAVITY. It was developed and used by Thibaut Paumard for the collaboration paper of 2018 [Gravity Collaboration et al., 2018]. I am only a user of this software.

I am regularly using in particular FitGCData when analyzing on-the-fly data during GRAVITY observation runs of the Galactic center. This tool helps quickly determine whether we understand what we see, before the more in-depth analysis that takes place after the runs.

Figure 3.11 shows an example of a fit on GRAVITY data using FitGCData on 2018 data taken close to the pericenter of S2, so that both Sgr A* and S2 are well visible in the field.

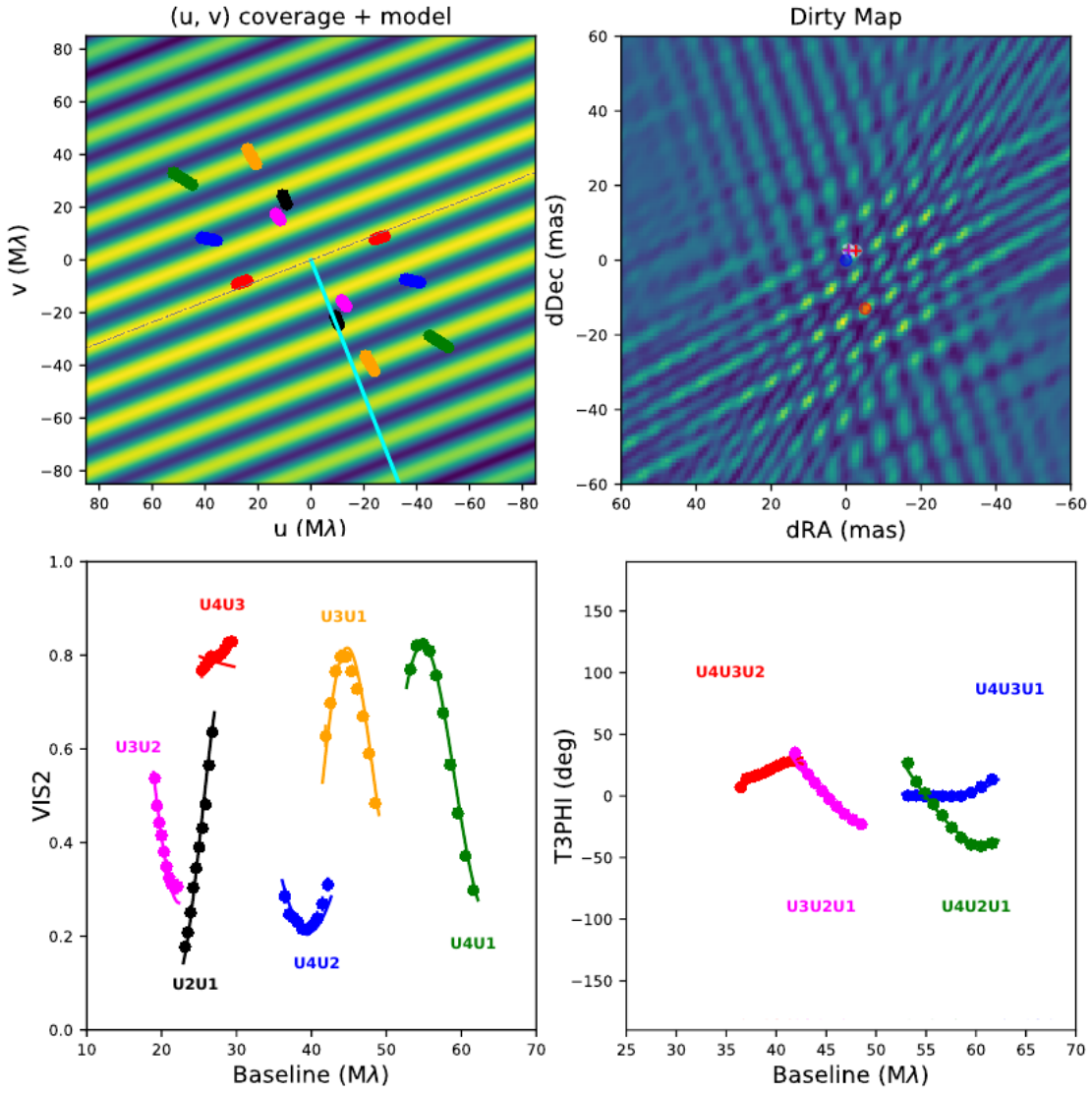

Figure 3.11: Output result from the FitGCData software to GRAVITY data of 2018-05-05 showing the binary Sgr A* (bright state) - S2. The top-left panel shows the uv plane and the observed baselines, the cyan vector showing the binary separation. The top-right panel shows the dirty map, with the position of Sgr A* shown by the blue circle, and that of S2 by the red circle. The bottom panels show the squared visibility modulus and the closure phase, with the best-fit model overplotted. The red baseline is badly fitted because it is orthogonal to the binary separation and thus does not catch any binary signal.

4

Science field 2: Imaging M87*

Contents

4.1 M87* environment

The galaxy Messier 87 (M87) is a giant elliptical galaxy located in the Virgo cluster, first observed by the French astronomer Charles Messier in 1781. Since a century it has been known to give rise to a large-scale ejecta [Curtis, 1918][1]. The central engine of this jet is

[1] Curtis [1918], using Lick Observatory's 0.9m Crossley reflector, wrote: *A curious straight ray lies in a gap in the nebulosity [⋆] in p.a.* 20°*, apparently connected with the nucleus by a thin line of matter.*
[⋆] Before the discovery of Hubble's law in 1924, what we now call galaxies were called nebulosities. The extragalactic nature of some of these nebulosities, our modern galaxies, was only established by Hubble in 1924, few years after the 1920 Shapley-Curtis "Great Debate", with Shapley advocating the statement that there is nothing in the Universe past our Milky Way, while Curtis advocated the statement that distant spiral nebulae (like M87) are extragalactic.

likely a supermassive black hole, M87*. It is, like our Galactic Center, a low-luminosity galactic nucleus, displaying a hot, optically thin and most likely geometrically thick accretion/ejection flow. The distance to M87 is of the order of the mean distance to the Virgo cluster, that is 16.5 Mpc. The mass of M87* has been assessed to be 3.5×10^9 $M_\odot$ by means of gas-dynamics fitting [Walsh et al., 2013] and to 6.6×10^9 $M_\odot$ by means of stellar-dynamics study [Gebhardt et al., 2011].

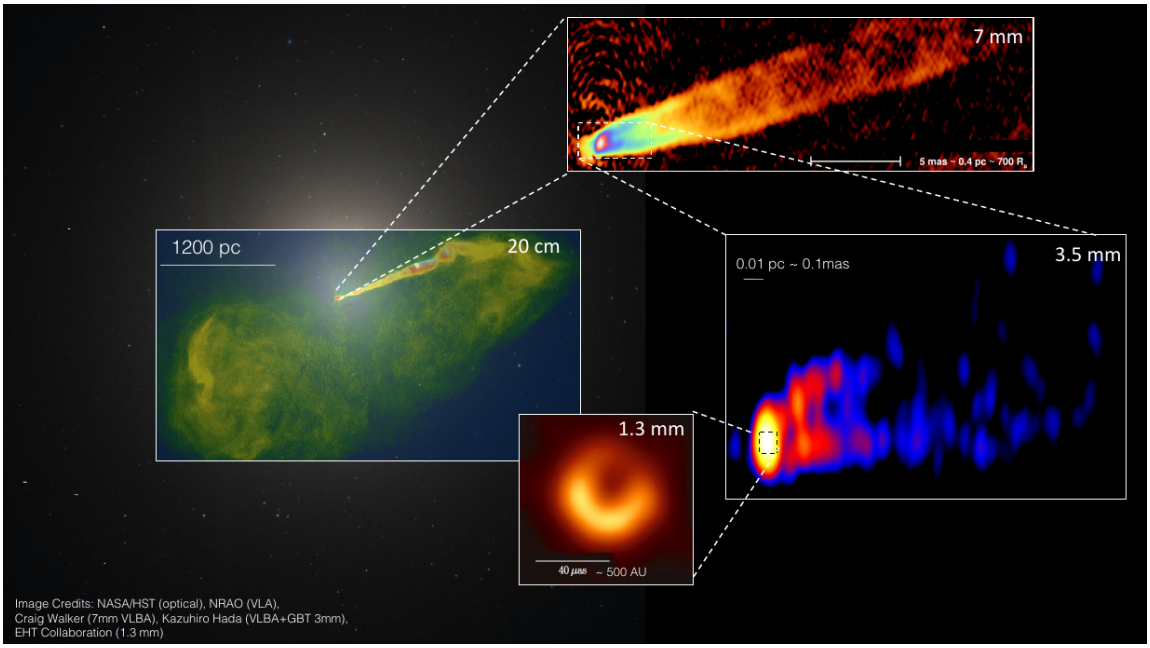

Figure 4.1: Image of the jet of M87 at various scale, culminating with the 2019 horizon-scale image of the EHT collaboration.

4.2 Accretion models for M87*

The study of Vincent et al. [2021] and my latest first-author draft (Vincent et al., 2022, to be soon submitted, see section 4.4.3) present an accretion model designed for M87*. The basic ideas are very close to the kind of accretion flow used for my Sgr A* works (see section 3.3), because Sgr A* and M87* both give rise to a radiatively inefficient flow. However, some differences are worth emphasizing, as well as the differences between the M87* 2021 and 2022 models.

The main difference between my latest Sgr A* quiescent accretion flow model [Vincent et al., 2019] and my earliest M87* accretion model [Vincent et al., 2021] is the fact that

the geometrically thick, optically thin accreting structure is modeled for M87* by a simple "thick disk" parametrized by its inner radius and opening angle (see Fig. 4.2, left panel), implementing simple power-law profiles for the density and temperature, rather than an ion torus as was used for Sgr A* (see section 3.3 and Fig. 3.6). This choice was made for three reasons:

- to consider a simple purely geometric structure that is agnostic on the underlying spacetime (the ion torus is anchored in the spacetime geometry);
- to allow a simpler comparison to numerical simulations that typically obtain thick-disk-like geometries with simple power-law dependencies of the physical quantities (while the ion torus model does not lead to power-law profiles of the physical quantities, the distribution is much more compact and peaked around the central radius of the torus);
- to allow considering an accretion flow that extends down to the event horizon, which has an important impact on the black-hole shadow properties (see section 4.4.1).

Besides this, the astrophysics of the M87* model is the exact equivalent of my Sgr A* models, so it will not be discussed any further here.

The main difference between my 2021 and 2022 models for M87 is related to the fact that the latter model is explicitly dedicated at studying the highly lensed features ("photon rings", see section 4.4.1), which are extremely sensitive to any kind of discontinuity of the accretion flow profile. My 2021 model was discontinuous at the limit between the inside and the outside of the thick disk, and the velocity transition at the innermost stable circular orbit[2] was only continuous but not continuously differentiable. This was not a concern for my 2021 paper, which does not discuss the detailed observable associated with the photon rings, but was a major drawback when their precise study was at stake. Indeed, the very minute non-smoothness of the physical distributions lead to clear spurious signals in the Fourier transform (i.e. the visibility signal), and prevented a precise analysis of the signature of the photon rings (see section 4.4.3). Consequently, my 2022 model is C^1 everywhere outside the horizon and provides a practical scenery for investigating photon rings. See Fig. 4.2 for an illustration of the 2021 vs. 2022 models.

Similarly as for the Sgr A* case, a wealth of accretion/ejection flow models have been recently published for M87*, mostly motivated by the EHT data. Here again I will cite

[2]The innermost stable circular orbit, or ISCO, is the closest circular orbit allowed around a black hole. Contrary to the Newtonian case, not all radii are allowed for circular orbit in GR. For $r < r_{ISCO}$, no stable circular orbit exists. This particular location has importance in accretion disks physics, and will be again discussed in the X-ray binary chapter, see section 5.1.

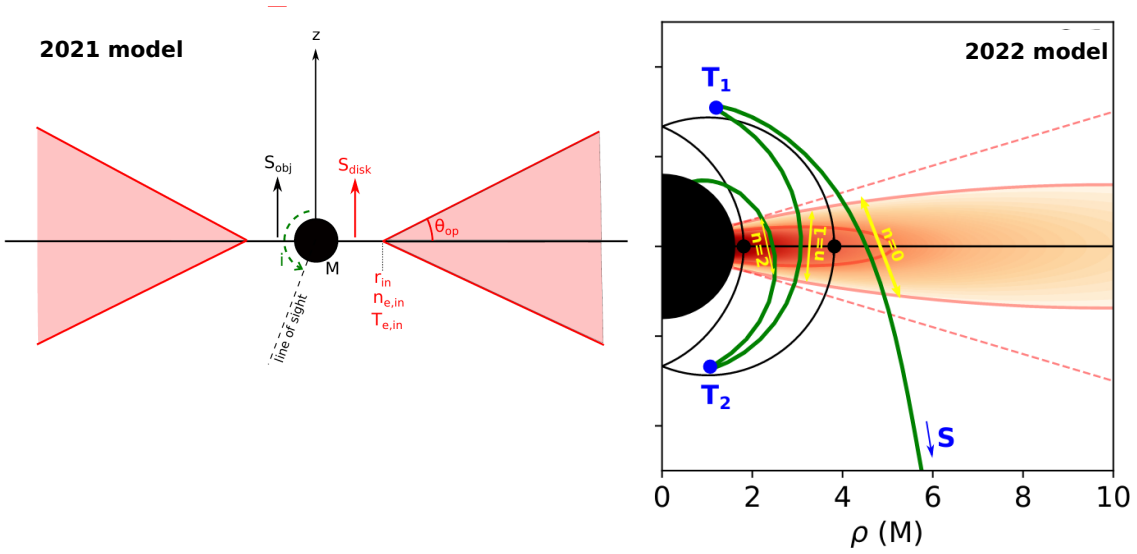

Figure 4.2: The 2021 M87* accretion models is illustrated in the left panel. It has discontinuities at the limit of the disk (in red) and the 4-velocity prescription chosen is not C^1 at the inner edge. The 2022 model (right panel) is everywhere C^1 outside of the event horizon. The green curve is a strongly-lensed photon geodesic.

but a few important recent publications, all based on GRMHD simulations: Davelaar et al. [2019, impact of electron distribution function (thermal/non-thermal)], Chatterjee et al. [2020, tilted jet model], Yao et al. [2021, radiation GRMHD simulation, with Monte-Carlo simulation of the anisotropic radiation field]. The comments on the comparison between analytical models and sophisticated simulations that were made for Sgr A* (see section 3.3) of course apply similarly here and will not be repeated.

4.3 Constraining the nature of M87*

The goal of Vincent et al. [2021] was to compute images of the simple thick-disk accretion model presented in the previous section, tuned to the millimeter properties of the source (i.e. giving rise to a ≈ 0.5 Jy flux at 230 GHz[3]). We first computed images of this model surrounding a standard Kerr black hole and obtained a very good agreement with the recent EHT observations. We then considered alternative compact objects rather than a Kerr black hole, and computed the image of our thick disk surrounding a boson star

[3]Note that I never performed a multi-wavelength spectral fit to M87* flow, contrary to what I did for Sgr A* in Vincent et al. [2019].

(see section 3.5), a non-rotating compact star (i.e. a photosphere located just above the Schwarzschild event horizon), or a rotating wormhole (see section 3.5.2, and Fig. 4.3). Our

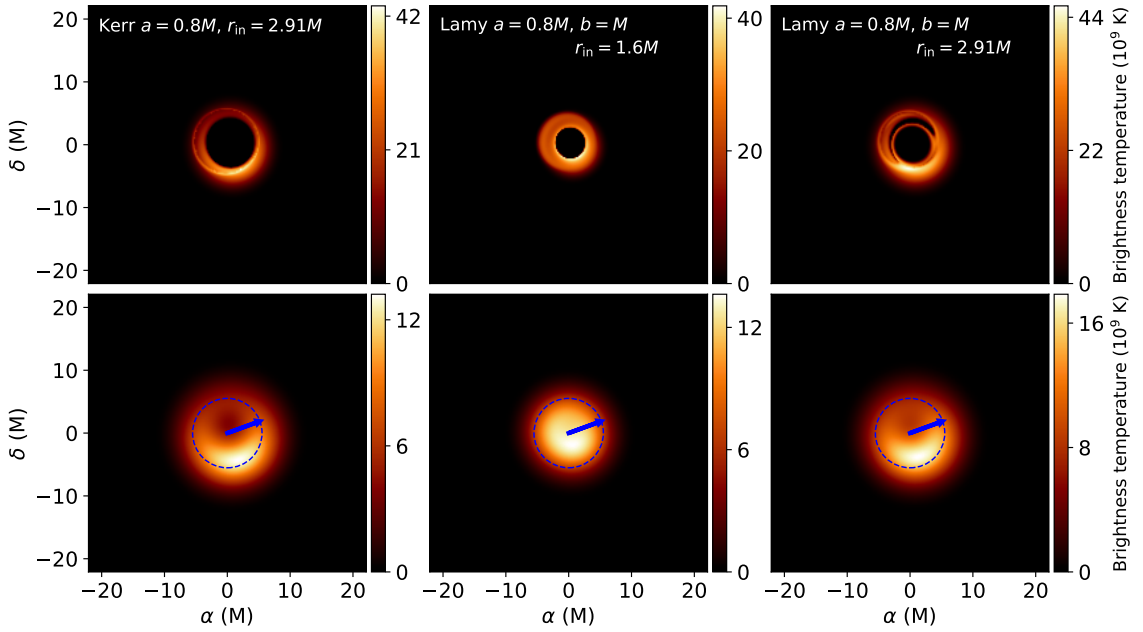

Figure 4.3: Images of a geometrically thick accretion disk with inner radius r_{in} in a Kerr spacetime with spin $a = 0.8M$ (left column), or in a rotating wormhole spacetime (so-called Lamy spacetime) with spin $a = 0.8M$ and charge $b = M$ (the charge is the non-Kerrness parameter of the wormhole spacetime). The inner disk radius changes between the middle and right panels. The bottom row corresponds to the top row images blurred to the EHT resolution of 20 μas; the dashed blue circle has a diameter of 40 μas (size of the ring feature reported by the EHT) and the blue arrow shows the projected direction of the approaching jet of M87. The bottom-left and bottom-right panels are extremely similar.

main finding was that the EHT-like image is extremely similar for the whole class of objects considered. Our conclusion is twofolds: (i) the spacetime geometry *alone* is not able to make a clear observable difference between different spacetime, at the resolution of the EHT; (ii) it might still be possible to make a difference between compact objects when the accreted matter is evolved in all spacetimes. The fate of this accreted matter will of course differ and might lead to observable differences. This is outside of the scope of our time-independent model, but it shows that the observational difference between alternative spacetimes, if within reach at all, depends crucially on the astrophysical fate of matter evolving around different compact objects. Unfortunately, this physics is still rather weakly constrained, which makes the goal of unambiguously testing the nature of M87* very difficult.

This conclusion is a great motivation for constraining as much as possible the properties of the accretion/ejection flow surrounding M87*. This goal has an obvious astrophysical interest (for advancing our knowledge of the strong-field accretion/ejection astrophysics, which has important impacts on many fields, see section 1.1.2), but it is also necessary for testing the nature of compact objects, and hence the underlying theory of gravity. To put it simply, my current conviction is that there will never be a "pure-gravity probe", but that we will have to first constrain a lot the astrophysics of the source, to be then (and only then) capable of using it as a test body for strong gravity.

4.4 Photon ring detection

4.4.1 Photon rings and shadows

This section tries to introduce quite a few important notions that will be discussed in the following, mainly photon rings and black hole shadow. These notions are used a lot in the literature, but I have the feeling that a lot of confusion exists on the topic and that many times, people use the same word to mean different things. Let me define how I understand these notions.

Photon orbit A Kerr black hole is surrounded by a set of very particular orbits called *photon orbits*. These are unstable, spherical orbits (in the sense that they are characterized by a constant value of the Boyer-Lindquist[4] radius, so that photons following a photon orbit evolve on a sphere). In the special case of a non-rotating black hole (the Schwarzschild geometry), this set of spherical orbits becomes degenerate to one single sphere, located at $r = 3GM/c^2$ [5]. Figure 4.4 illustrates these photon orbits for the Schwarzschild geometry by the dashed black circle. These photon orbits are of absolutely crucial importance regarding strong-field observables. They are arguably *the key feature* of an extremely compact object spacetime, as far as observations are concerned, much more than the event horizon[6].

Critical curve Let us imagine that the photon orbit (and it only) be painted with emitting material. The image on sky of this bright photon orbit is called the *critical curve*.

[4] A very standard radial coordinate describing the Kerr geometry.

[5] In Schwarzschild coordinates, i.e. Boyer-Lindquist coordinates for zero spin. Let us remind that the natural length scale around a compact object of mass M is GM/c^2.

[6] This is why the name "Event Horizon Telescope" is in my opinion not very justified. We will see in section 4.4.4 that the future prospect of a "Photon Ring Telescope" is better justified, in terms of wording.

Note that this critical curve has zero thickness: photons that asymptotically approach the photon orbit must be shot with infinite precision at the appropriate impact parameter ($b_c = 3\sqrt{3}GM/c^2$ for the Schwarzschild geometry). It is thus crucial to keep in mind that *the critical curve is not observable*. It is merely a limit, a theoretical concept of great importance, but that can be safely ignored by the relativistic astronomer. The critical curve is a *pure-gravity* feature, it is independent from the accretion flow.

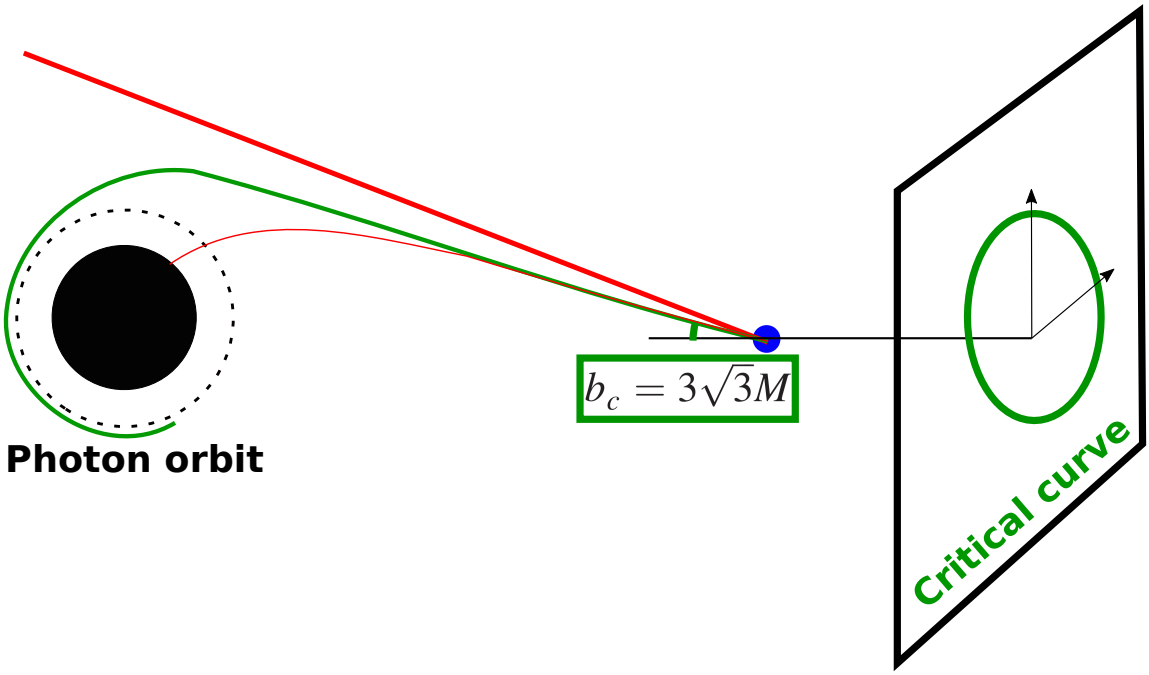

Figure 4.4: **Photon orbit and critical curve**. The black disk is the black hole's event horizon. Here the black hole is assumed to not rotate, so the horizon is located at $r = 2GM/c^2$ in Schwarzschild coordinates (this is the famous *Schwarzschild radius*). The unstable set of photon orbits is restricted to the sphere $r = 3GM/c^2$ in the Schwarzschild geometry. An observer is located at the blue dot. It shoots photons towards the black hole (red tracks). A photon shot at a sufficiently big impact parameter from the black hole is not deviated (red straight line). A photon precisely aimed to reach the unstable photon orbit (where is can orbit many times) must be shot with an impact parameter of $b_c = 3\sqrt{3}GM/c^2$ (green curve). The curve on sky corresponding to the incident directions of photons that asymptotically approach the photon orbit (i.e. the image on sky of the photon orbit, transported to the observer's screen by geodesics like the green one) is represented on the sky plane at the right of the sketch. It is called the *critical curve*, and is not observable.

Lensing bands Photons that asymptotically approach the photon orbit when shot backwards from the observer towards the black hole are part of the critical curve. Let us now consider a photon shot a bit off from the critical curve. It will approach close to the photon orbit, without reaching it, and will then either escape to infinity, or approach the horizon (remember that the photon orbit is unstable). Such a photon will then make a certain number of half turns around the black hole, close to the photon orbit, before leaving. Let us define the n-th *lensing band* on sky by the set of angular positions on sky, close to, but separated from the critical curve, that correspond to photons that make n half turns around the black hole before escaping. The $n = 1$ and $n = 2$ lensing bands are illustrated in Fig. 4.5. Lensing bands are again theoretical features, they form a mathematical locus on sky, are *not observable*, and are *pure-gravity* features (they are completely independent from the accretion flow).

Photon rings Of vital importance for the relativistic astronomer are the photon rings. There is a lot of confusion in the literature regarding photon rings, so let us try to introduce this notion simply and clearly. Let us consider the nth lensing band which is, as said earlier, a purely mathematical locus, not observable. A subset of this locus might contain observable radiation, if there is emitting matter around the black hole. This subset is called the nth *photon ring*, see the illustration in Fig. 4.6. Note, and this is a crucial point, that to answer the question "which subset of the lensing band will contain detectable radiation?", we must know the details of the astrophysics of the accretion flow. Different accretion flows will lead to different photon rings. *Photon rings are thus observable features, that are not pure-gravity, but rather strongly depend on the astrophysics assumption.* It can be shown [see e.g. Johnson et al., 2020] that (i) the photon rings exponentially converge towards the critical curve with increasing n, and (ii) the width of the photon rings exponentially decreases with n. It is thus very clear that only the very few first photon rings might be within reach of observation. As of now, no clear detection of even the $n = 1$ photon ring is at hand[7]. Future instruments should detect the $n = 1$, and likely the $n = 2$ photon ring (see the perspective in section 4.4.4).

To recap let us insist on a few points: (i) there is no "photon ring", there is an infinite set of photon rings, labeled by the number n of half turns around the black hole, that asymptotically converge to the critical curve[8]; (ii) the photon rings *are observable features*, contrary to the critical curve which is not. As such, photon rings *depend on the astrophysical assumption about the emitting matter surrounding the black hole, these are not pure-gravity features*. These definitions make it immediately very clear that it is far from obvious that photon rings can be efficient probes of strong-field GR. It will all depend on whether they

[7] In particular, the recent EHT results do not demonstrate the existence of these rings.

[8] It is still legitimate to call "photon ring" the full infinite sequence of photon rings for $n \geq 1$, but this simplification must be conscious!

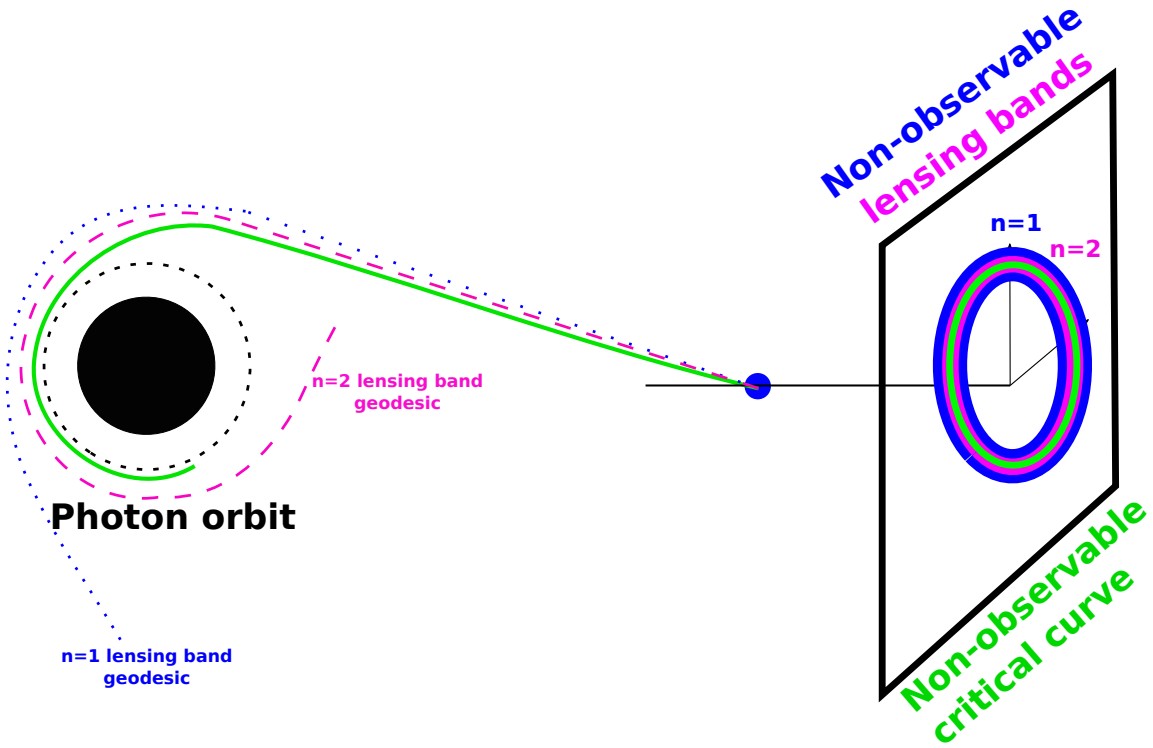

Figure 4.5: **Lensing bands**. Photons shot backwards from the observer towards the black hole that asymptotically reach the photon orbit correspond to the critical curve (green geodesic and green circle on sky). Photons shot a bit off from the critical curve will come close to the photon orbit without reaching it, and will make a number n of half turns around the black hole before escaping (blue dotted geodesic, for $n = 1$, and magenta dashed geodesic, for $n = 2$). The nth lensing band is the set of directions on sky corresponding to photons that make n half turns around the black hole. The figure illustrates the $n = 1$ (blue) and $n = 2$ (magenta) lensing bands (not at all to scale, this is simply for illustration purpose). Lensing bands are not observable.

are "enough dominated by GR, and not too polluted by (unconstrained) astrophysics". The next sections focus precisely on this crucial point. Before turning to this discussion, we still need to introduce the notion of black hole shadow.

The notions presented above regarding the photon rings are discussed much more in-depth in the following key papers: Johnson et al. [2020], Gralla and Lupsasca [2020a], Gralla and Lupsasca [2020b]. They are presented in a very detailed and pedagogical way[9] in the introduction of Paugnat et al. (2022, in prep., discussed below).

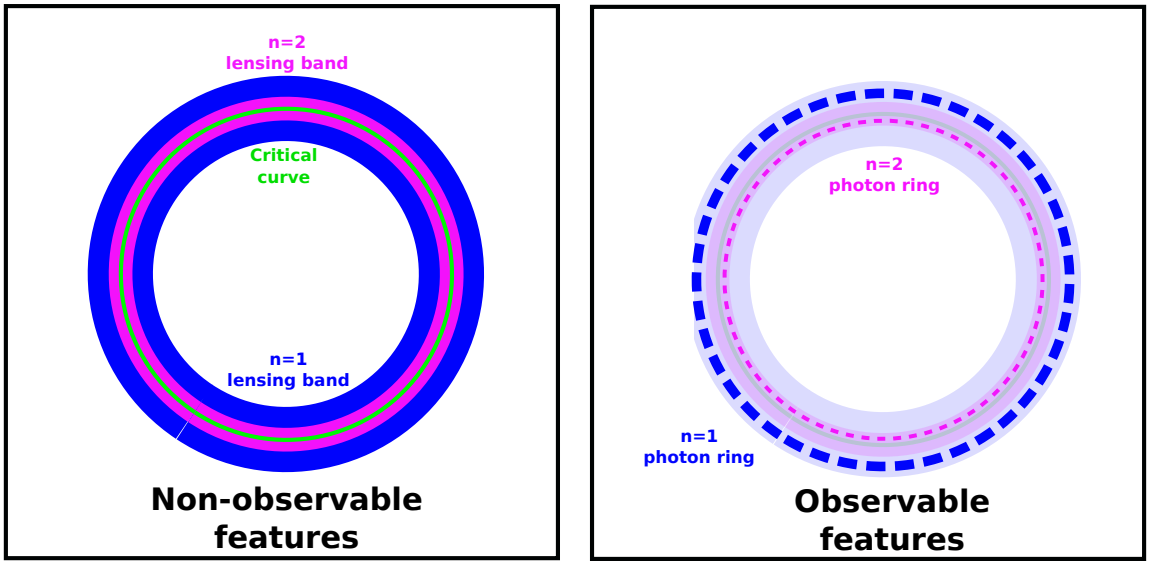

Figure 4.6: **Photon rings**. **Left:** the $n = 1$ and $n = 2$ lensing bands, and the critical curve, as depicted in Fig. 4.5. **Right:** the non-observable lensing bands and critical curve are represented in pale color, while the observable $n = 1$ and $n = 2$ photon rings are represented in dashed line. Each photon ring is located within the corresponding lensing band. The $n = 2$ photon ring is narrower and closer to the critical curve. Here we assume that some particular model of emitting matter is located around the black hole, and is responsible for the flux comprised within the photon rings. A different emission model would lead to different photon rings (still within the lensing bands of course).

Shadow The image of a black hole surrounded by optically thin material leads to a flux-depleted central region, which is often referred to as the *black hole shadow*. There is also a lot of confusion about this notion, so let us again try to introduce it clearly. The aim of this paragraph is to convince the reader that the notion of shadow is (i) not pure-gravity, (ii) actually even very astrophysics-dependent, (iii) can be in some cases strongly related

[9] I can say so, I didn't write it!

to special-relativistic effects. These three points make it clear that this notion is of very little use for testing strong-field gravity.

Let us consider a sphere of isotropically emitting material "at infinity", surrounding a black hole, and an observer inside the emitting sphere, far from the black hole. Photons shot backwards from the observer, with an impact parameter smaller than that of the critical curve, will asymptotically approach the event horizon and never reach the emitting sphere at infinity. As a consequence, the inside of the critical curve is dark, while the outside is bright. This is the classical, textbook black hole shadow (see Fig. 4.7). This setup is of course completely irrelevant for a realistic emission model around an astrophysical black hole. How is the shadow concept evolving with the emission model?

Let us now consider a scenario which is likely a reasonable approximation for M87*: most of the emission is concentrated in the equatorial plane of the black hole and extends down to the horizon (see Fig. 4.8). In this case, photons shot with impact parameters smaller than that of the critical curve will of course still asymptotically approach the horizon, but they will meet emitting matter along the way. So there will be radiation inside the critical curve. Actually, the black hole shadow will be restricted to the image on sky of the equatorial event horizon (see illustration in Fig. 4.8), which is *much* smaller than the textbook shadow discussed above (by a factor of ≈ 2 in the simulations discussed below).

Let us finally consider a spherically-symmetric distribution of optically-thin emitting matter in radial fall around the black hole (see Fig. 4.9). In this case, the shadow is the same as the textbook shadow. Why is that? Because of the special-relativistic strong Doppler shift experienced by the radiaion. Indeed, it can be shown that photons corresponding to angular directions located inside the critical curve never reach any radial turning point, i.e. they constantly flee from the black hole with increasing radial coordinate. So the photon is escaping while the emitter is falling towards the horizon: the consequence is a very strong redshift of the radiation located inside the critical curve, which is responsible for the black hole shadow. It is important to stress that if the outer boundary of the shadow is dictated by GR (the critical curve), the reason why there is a drop of flux in the central region of the image is a pure special-relativistic (redshift) effect.

The conclusion from these three simple scenarios is that the black hole shadow is a very astrophysics-dependent notion, which is not at all pure-gravity (it can be strongly related to special relativity effects). Let us also stress that the notion of shadow is not directly linked to the presence of an event horizon. Indeed, if we consider a compact star with a photosphere just above the event horizon, gravitational redshift effects will diverge on the photosphere and lead to an apparent shadow, exactly similarly as for a black hole [see Vincent et al., 2021]. On the contrary, photon rings are directly related to the existence of photon orbits, so they unambiguously constrain the spacetime properties. All this shows

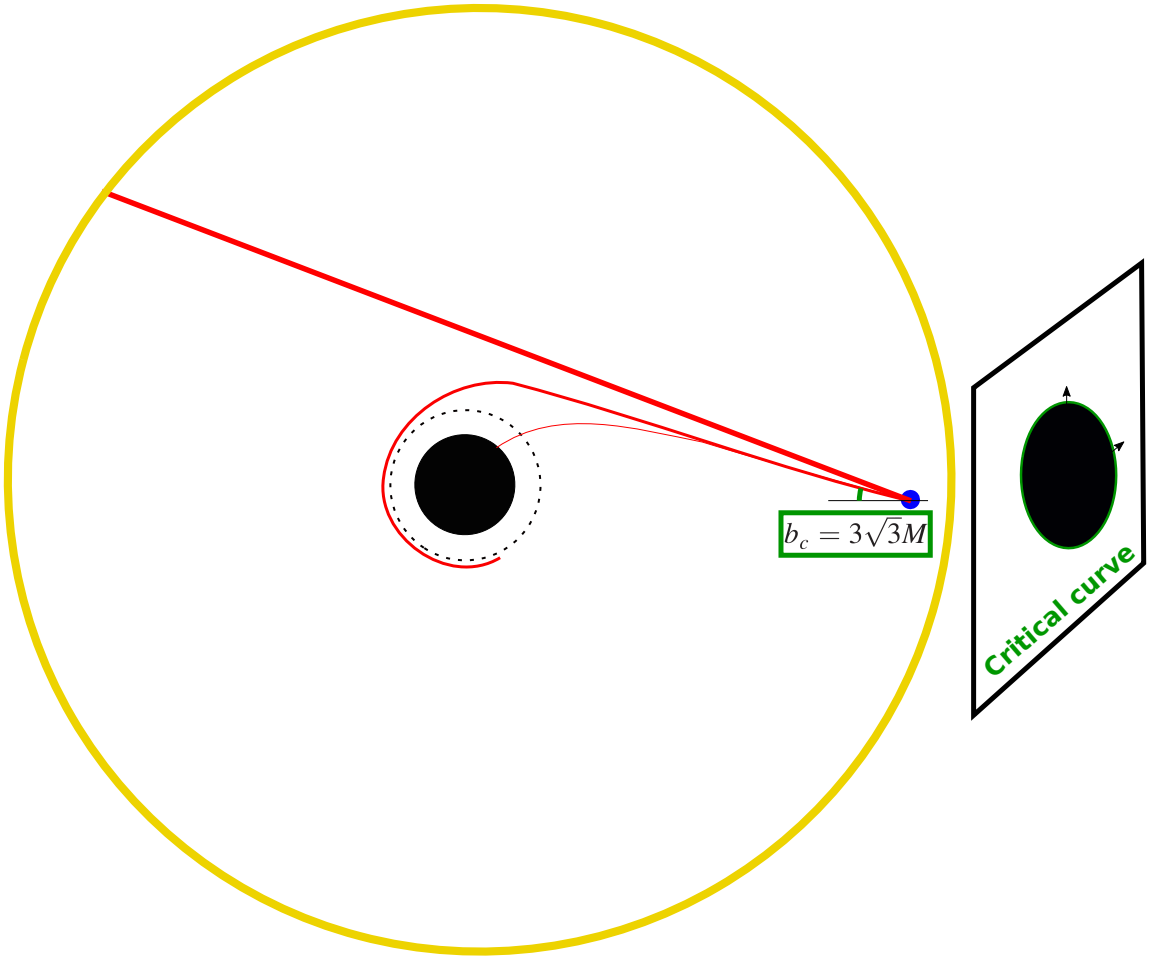

Figure 4.7: **Textbook shadow**. The black hole shadow cast by a sphere at infinity, emitting isotropically. The shadow is located exactly inside the critical curve. See text for details.

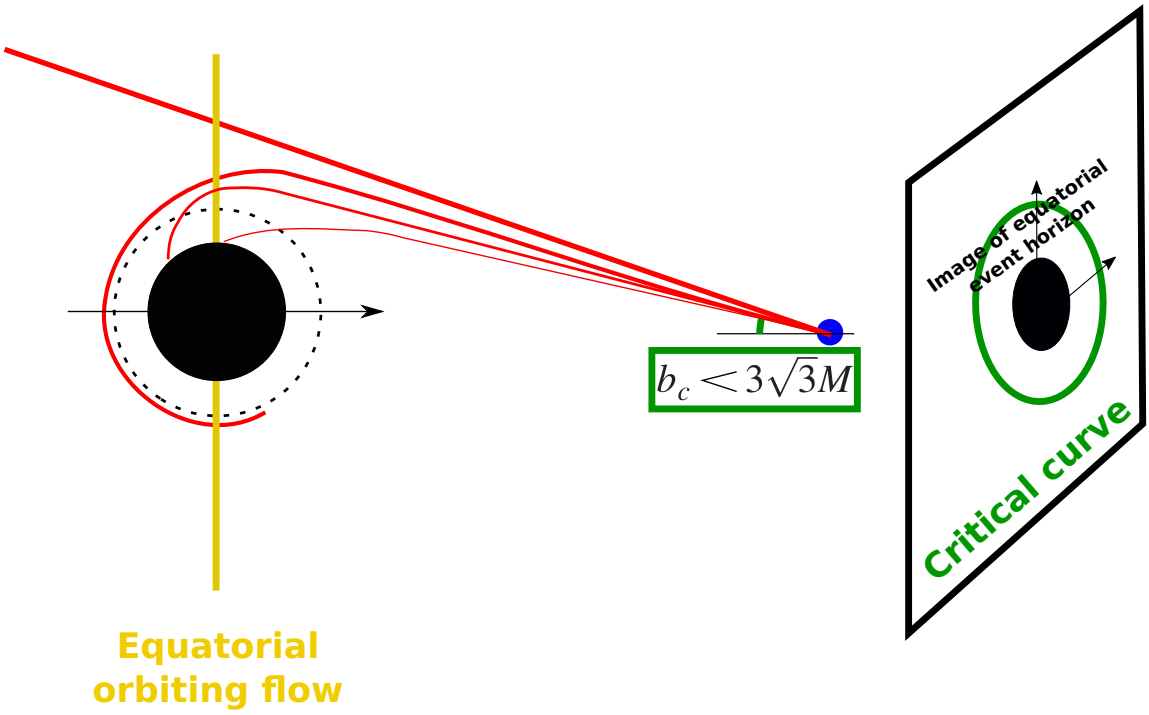

Figure 4.8: **Disk shadow**. The black hole shadow cast by an equatorial disk extending down to the horizon. A lot of radiation (actually, depending on the model, it is typically the large majority of the radiation) is emitted within the critical curve. The shadow is much smaller than the textbook shadow of Fig. 4.7.

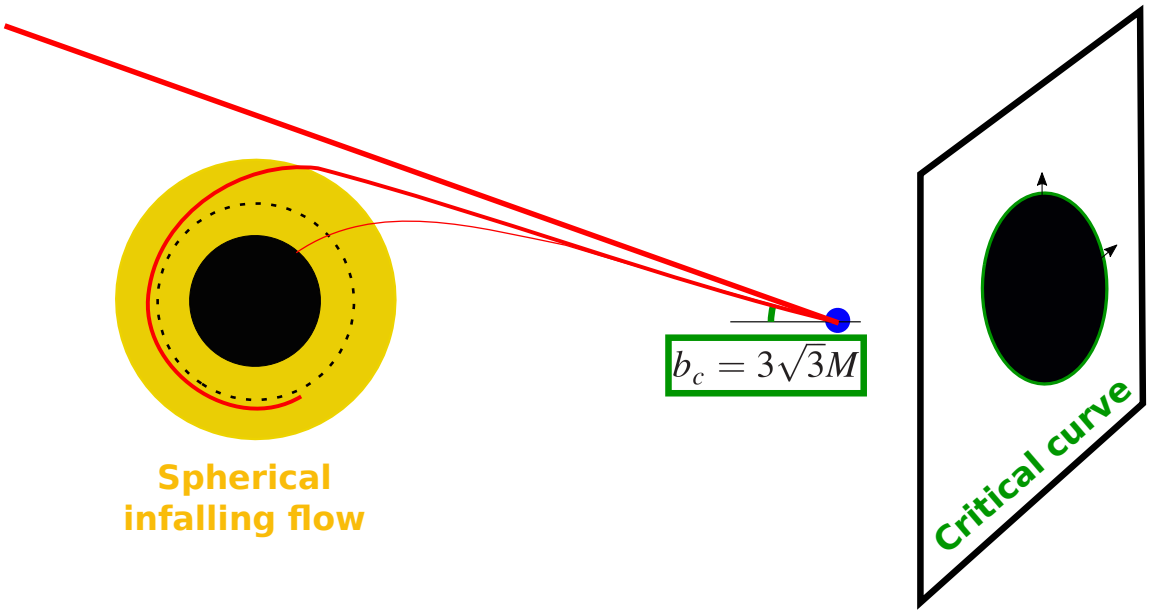

Figure 4.9: **Spherical shadow**. The black hole shadow cast by a spherically-symmetric distribution of optically-thin matter in radial fall onto the horizon. The shadow is the same as the tetextbook shadow of Fig. 4.7. See text for details.

that the shadow is thus not very promising for studying strong-field gravity. However, it is still a very interesting probe of the accretion flow properties. As we just saw, if an unambiguous, precise detection of the shadow outer boundary is obtained, it has direct implications for the inner accretion flow properties [see e.g. Chael et al., 2021].

How does all that look in real life? Figure 4.10 shows an illustration of M87* images corresponding to the two reasonable models above (equatorial disk or spherical infall). It shows that indeed things look like what is simply described above.

So what really matters? The photon rings. After this rather lengthy academic discussion (which was hopefully useful to clarify the basic notions), what to conclude? The photon rings are definitely the most promising features in the prospect of probing strong-field GR. They are of course astrophysics-dependent (but all observables will likely be so, at a sufficient level of precision!) but they are a very robust feature of accretion flows surrounding black holes, and are related to strong-field lensing effects in the vicinity of the key feature of extremely compact objects, the photon orbits. As a consequence, the following sections will focus only on photon rings, and will not discuss the shadow at all.

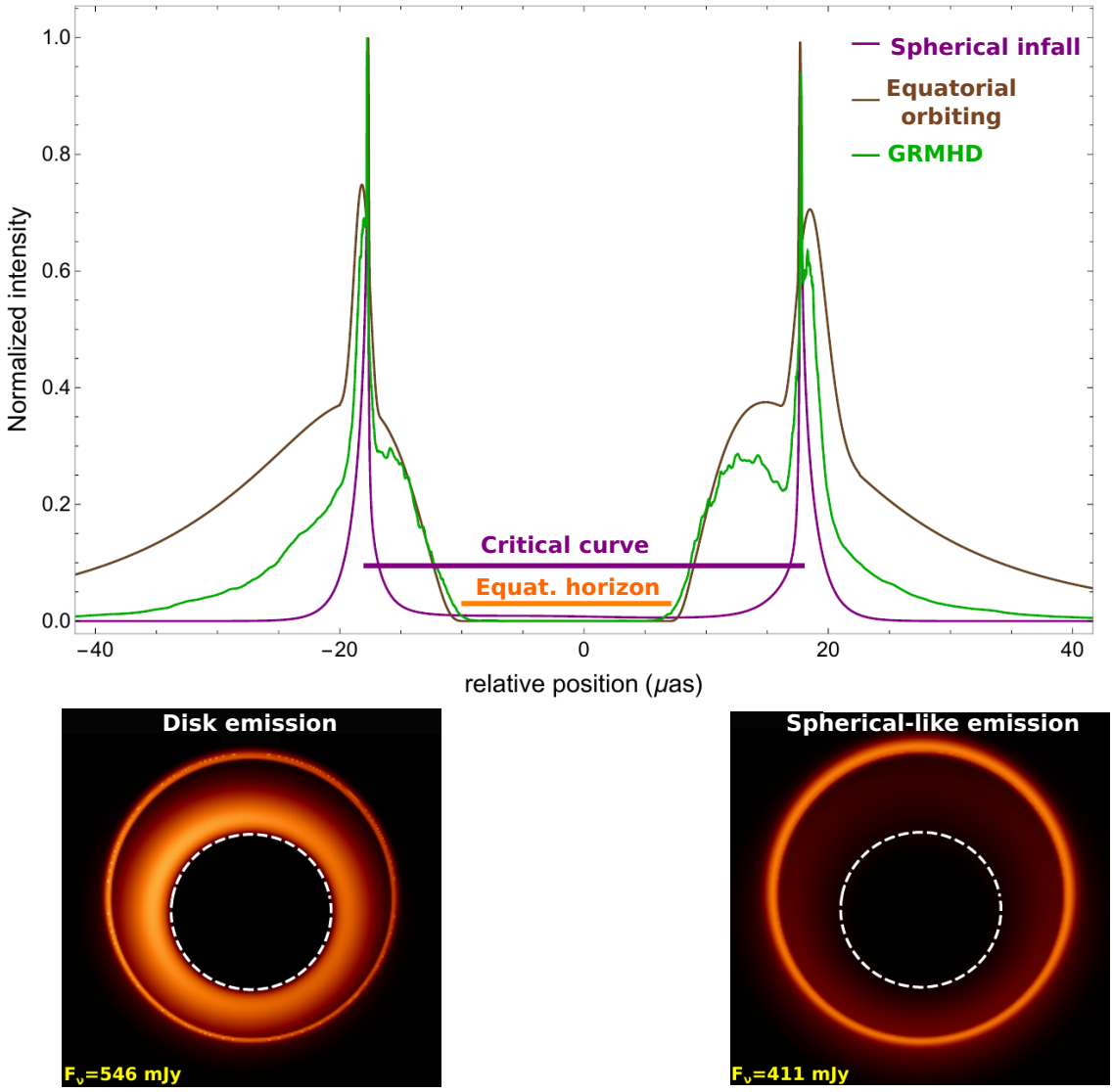

Figure 4.10: **Bottom panels:** two simulated images corresponding to a disk-like or a spherical-like accretion flow surrounding M87*. The dashed white line corresponds to the image of the equatorial event horizon. The shadow behaves as discussed in the text. The photon rings are always very clear. **Upper panel:** a cut parallel to the spin axis in the 2D images shown below, together with a GRMHD disk-like model [Johnson et al., 2020], to stress again the differing behavior of the shadow, depending on the model. Figures from Vincent et al. (2022, in prep.).

4.4.2 A photon-ring Kerr consistency test

Recently, Gralla et al. [2020] has proposed a Kerr consistency test that boils down to measuring the shape of the $n = 2$ photon ring of M87*. These authors have shown that the critical curve of a Kerr black hole should be very well approximated by a simple geometric curve known as a circlipse. The idea of the proposal is to fit the $n = 2$ photon ring to a circlipse[10], considering that this photon ring should already be very similar to the critical curve, given that photon rings exponentially converge towards the critical curve, as presented in section 4.4.1. Gralla et al. [2020] have demonstrated that the $n = 2$ ring indeed is well approximated by a circlipse, and thus allows for a powerful consistency test of the Kerr metric, for a few simple emission profiles restricted to the equatorial plane of the black hole (razor-thin disks).

In March 2021, Hadrien Paugnat has started his Master 2 internship with me in Meudon on the topic. The idea was first to find the same result as Gralla et al. [2020] independently, and then generalize it to a broader class of model in order to check the robustness of this very promising test of the Kerr paradigm in the strong-field region. We soon collaborated directly with Sam Gralla and Alex Lupsasca [the two first authors of Gralla et al., 2020], together with Maciek Wielgus with whom I have been collaborating since many years on the topic of tests of strong-field gravity.

This collaborative work has lead to a paper with Hadrien as first author, A. Lupsasca as second author, and myself as third author. Hadrien has been extremely efficient in mastering this very complex topic and has obtained within few months very interesting results at the level of a publication. The publication has been delayed quite a lot due to the limited availability of all the players, but will be submitted before the summer. The main result of the paper is to demonstrate that the Gralla et al. [2020] test of the Kerr spacetime is indeed robust and survives to considering a much more diverse set of emission profiles, provided that the inclination remains sufficiently low ($i \lesssim 45°$), which is a condition likely fulfilled by M87* (although it is not sure, because the spin axis might be tilted with respect to the jet axis). At higher inclination, the photon ring width becomes larger and starts to more strongly depend on the orientation of the baseline, which can break the test. The paper also discusses the prospect of constraining the spin parameter of the black hole and the inclination angle from $n = 2$ ring detection.

[10] Remember that the critical curve is not observable, so it cannot be fitted by anything in real life.

4.4.3 How "dirty astrophysics" makes it more difficult, but still feasible

Still motivated by the results of Gralla et al. [2020], I have been very interested in studying the impact of realistic astrophysical conditions on the $n = 2$ photon ring observable. To do so, I have used the accretion model presented in section 4.2 and computed images and visibility amplitude profiles corresponding to two directions on sky, parallel and perpendicular to the black hole spin direction, so essentially the same as what Hadrien was doing in his thin-disk model, but considering a much more astrophysically realistic model, i.e. a thick disk emitting thermal synchrotron radiation, with the full radiative transfer being self-consistently taken into account, and considering the observation frequency of the EHT, i.e. 230 GHz.

The main result of this study is the fact that self-absorption of the synchrotron radiation can destroy the $n = 2$ ring signature, which is obviously a very bad news for the Kerr consistency test advocated in the previous section. The good news however is that the $n = 2$ ring signature survives when going to a slightly higher frequency of 345 GHz (which is a target frequency for the future development of the EHT). This effect is natural because the medium becomes more and more optically thin with increasing frequency. More work is needed to understand the detail of the impact of self-absorption on the observables and determine the exact degree of astrophysical robustness of the Gralla et al. [2020] Kerr consistency test.

This study has lead to a paper with me as first author, to be submitted very soon[11] to A&A.

4.4.4 Towards a Photon Ring Telescope?

The sections above consider that a detection of the $n = 2$ photon ring might be possible in the close future. As discussed by Johnson et al. [2020] and Gralla et al. [2020], this means resorting to space-based very-long baseline interferometry, which in my view is the necessary next step to go clearly further than the EHT. Without giving more details on the prospect of such a "Photon Ring Telescope" mission (which is actively discussed both in the US and in Europe), let me explain the basic idea why such a detection might be possible.

Detecting a thin ring on sky, the width of which is of the order of one microarcsecond, might sound like science fiction. However this is not so, because as discussed above, a "black hole image" is essentially a blurry primary radiation plus a sequence of thin rings. In Fourier space, the blurry primary radiation, which is rather extended, will die fast with

[11] Essentially, when I finish this HDR dissertation!

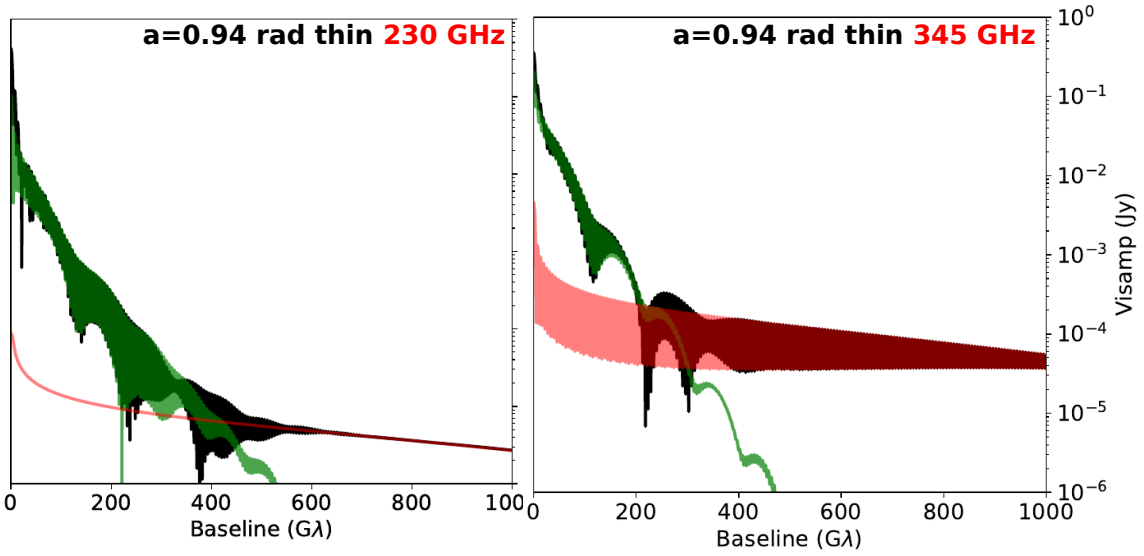

Figure 4.11: Visibility amplitude of a small-opening thick disk, in radial fall towards the black hole, at 230 GHz (left) and 345 GHz (right), at high spin. The full signal is in black, and the $n = 1$ and $n = 2$ contributions are in green and red, respectively. The material being more optically thin at 345 GHz, self-absorption is weaker and the Fourier oscillation corresponding to the $n = 2$ photon ring becomes much more pronounced at long baseline, allowing to perform the Gralla et al. [2020] Kerr consistency test. Figure from Vincent et al. (2022, in prep.).

Fourier frequency. At long baseline, only the thin features will survive. Actually, there is a sequence of baseline windows dominated first by the primary radiation, then by the $n = 1$ photon ring, then by the $n = 2$ photon ring (see Fig. 4.12)... Provided that sufficiently long baseline can be probed (hence, space mission) with sufficient sensitivity, the detection is feasible [see more details in Johnson et al., 2020; Gralla et al., 2020, and Paugnat et al., 2022, in prep.].

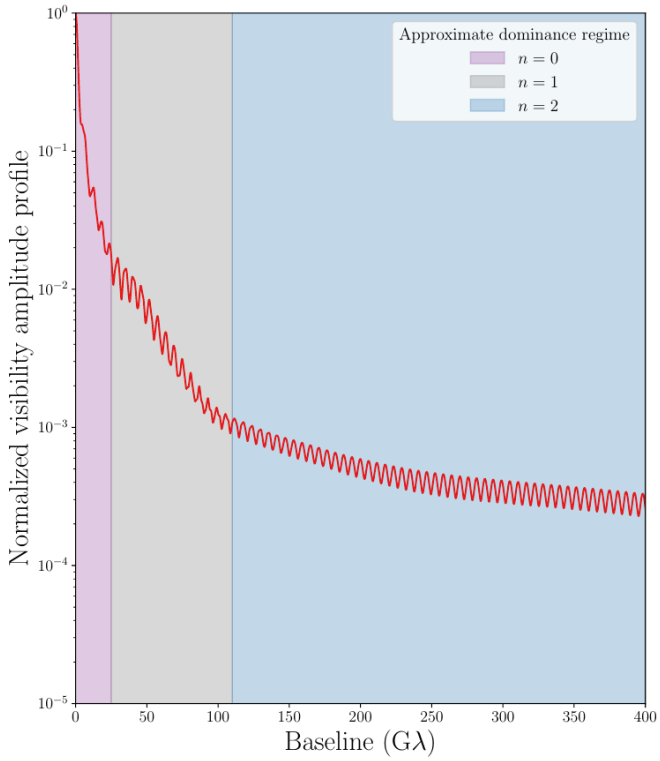

Figure 4.12: Visibility amplitude along a baseline orthogonal to the black hole spin for a thin-disk model of M87*. The primary image ($n = 0$), and photon rings contributions ($n = 1$, $n = 2$) are highlighted in color. Provided that a baseline higher than 150 Gλ is at hand, the $n = 2$ signal can be probed. Note that this threshold baseline depends a lot on the astrophysics (see Paugnat et al., 2022, in prep., for details). The current highest baseline within reach of the EHT is at ≈ 10 Gλ, before the $n = 1$ photon ring transition. Figure from Paugnat et al. (2022, in prep.).

5

Science field 3: X-ray binary spectra: oscillations & bursts

Contents

During my years of postdoc, I developed research activity on a new topic, namely the strong-gravitational field physics of X-ray binaries. These sources are much smaller on sky than their supermassive counterparts at the center of galaxies. As such, they offer fewer observables (spectroscopy, polarimetry and photometry, but no longer orbitography and imaging as is available for Sgr A* and M87*). Consequently, I never focused my attention on trying to use these sources for performing tests of strong-field gravity, but I was rather interested in the properties of matter and radiation in these extreme environments. In this perspective, I became mostly interested in two phenomena. I first focused on high-frequency quasi-periodic oscillations of black-hole binaries, that might share their physics with the flares of Sgr A*. More recently, I became interested in the X-ray bursts of neutron-star binaries, in the prospect of constraining the dense matter at the core of neutron stars. These topics will be the focus of the following two sub-sections. Note that in the last few years I have stopped this X-ray binary activity (because of lack of time, certainly not because of lack of interest), so the following is a description of past research only.

5.1 Quasi-periodic oscillations of black-hole binaries

High-frequency[1] quasi-periodic oscillations (HFQPO) appear as small narrow peaks in the power spectrum of some black-hole binaries, around few tens to few hundreds of Hz, that translate in a few-percent modulation of the X-ray flux. These features are particularly interesting because the innermost stable circular orbit (ISCO) frequency of a $10\,M_\odot$ black hole is of 220 Hz, so it is tempting to interpret these oscillations as related to orbital motion in the strong-field zone near the black hole, so something that might be similar to the hotspots of Sgr A*, which is one of the reason of my interest in these phenomena. I focused on two models of HFQPO.

5.1.1 Rossby-wave instability

I was first interested in modeling these events by the onset of an instability, the Rossby-wave instability, which in a 2D hydrostatic context develops when the accretion disk shows an extremum of the quantity $\kappa^2/\Omega\Sigma$, where κ is the radial epicyclic frequency, Ω is the rotation frequency, and Σ is the surface density. This quantity naturally shows an extremum in an accretion disk surrounding a black hole, because κ has an extremum close to the ISCO. It can also be triggered by a local maximum in Σ if a blob of matter is accreted for instance. Once it is triggered, the Rossby-wave instability leads to large-scale spiral patterns as well as small-scale Rossby vortices, that are viable candidates for hotspots. Vincent et al. [2013] considered the simulation of a 3D Rossby wave in a hydrostatic disk, and performed relativistic ray tracing on this disk to generate a light curve, taking into account bremsstrahlung radiation. This study showed that a level of a few percent modulation in the light curve is obtained, in agreement with observable constraints on HFQPOs (see Fig. 5.1). The Rossby-wave simulations used in this analysis were carried out considering a very simplified "pseudo-Newtonian" potential [Paczyński and Wiita, 1980]. Only recently were these simulations carried out in full general relativity, giving rise to more precise comparison to observations [Varniere et al., 2019, 2020, to which I am respectively third and second author].

5.1.2 Oscillating tori

I was also interested in studying the ability of accretion tori surrounding the central black hole to create HFQPOs through their oscillations. This model was initially developped

[1] There are also low-frequency QPOs of black-hole binaries, with frequencies between 0.1 and few tens of Hz, that have different properties and a different origin.

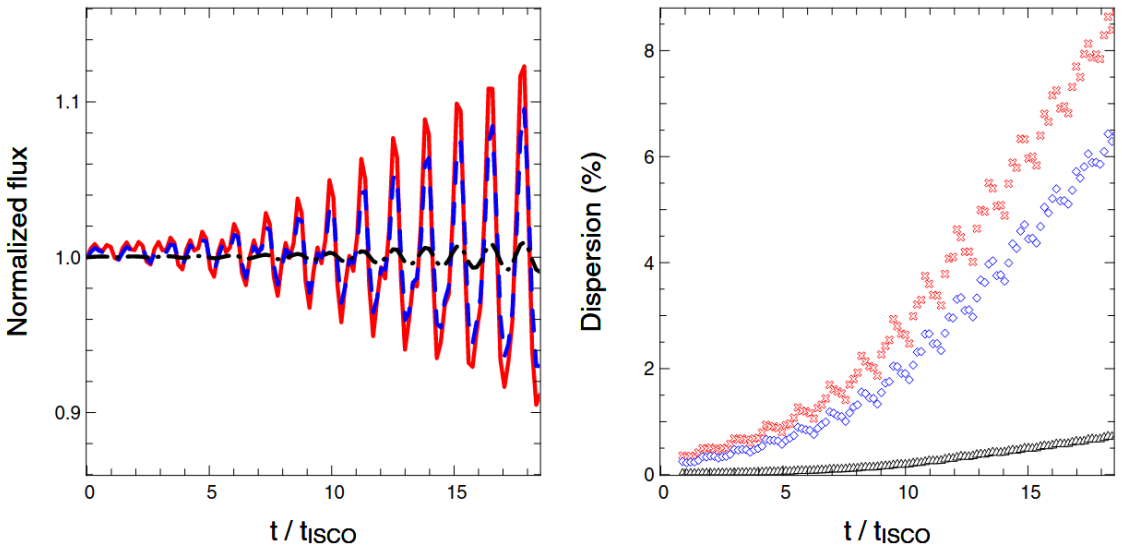

Figure 5.1: **Left:** light curves of a microquasar subject to the 3D RWI at 2 keV at an inclination of 5° (dash-dotted black), 45° (dashed blue), or 85° (solid red). **Right:** dispersion of the light curve points of the left panel. Each point is obtained by computing the dispersion of the light curve points over two orbital periods. Figure from Vincent et al. [2013].

by the pioneering works of Rezzolla et al. [2003]; Abramowicz et al. [2006]; Blaes et al. [2006]. Based on this, Vincent et al. [2014a] generated ray-tracing simulations of analytical models of oscillating slender tori, taking into account the tori oscillations modes derived by Blaes et al. [2006]. We consider the five lowest-order oscillation modes, i.e. the radial, vertical, plus, minus and X modes. These various modes and their interplay are interesting in particular because some sources have been shown to exhibit pairs of HFQPOs in a 3:2 frequency ratio, which lead Abramowicz and Kluźniak [2001] to suggest that this might be due to a resonance in a pair of natural oscillating frequencies of matter close to a black hole, which might be interesting in the perspective of constraining the spin parameter (the frequencies being affected by the black hole spin). Vincent et al. [2014a] discuss the radiated power associated to the various modes and show the importance of taking ray tracing into account to properly interpret the observables. Mishra et al. [2017, to which I am second author behind a PhD student, but I was not the main adviser of the first author] undertook a much more refined analysis, developing hydrodynamical simulations of a slender torus in a GRMHD context.

5.2 Spectra of neutron-star binaries X-ray bursts

Neutron stars (NS) are the most compact objects of the universe that are formed of matter. Only black holes are more compact, but are purely geometric objects. NS harbor extremely dense states of matter (higher than the density of atomic nuclei) that cannot be probed in laboratories on Earth. Consequently, neutron stars can be seen not only as extreme astronomical objects, but also as dedicated laboratories for the study of matter in its densest states. The very complex nuclear physics properties of matter inside a neutron star is encapsulated inside the equation of state (EoS), that is to say the relation between pressure and energy density that allows to close the system of equations describing the star's equilibrium. Let us consider a NS with a mass M. A given EoS will impose a particular value for the star's radius, R. This means that constraining both the mass and radius of a NS leads to constraining the star's EoS. Spectral monitoring of NS can allow to constrain M and R, thus linking astronomy to nuclear physics.

Measuring the mass of a neutron star is relatively easy when it lives in a binary system. Kepler's laws are applied and allow to determine the M parameter. However, the radius is very difficult to measure. A particular population of NS, living in a binary system with a normal low-mass star (known as a low-mass X-ray binary), can lead to episodic explosive events called X-ray bursts. These events are due to the matter accreted by the NS from its companion star, that can suddenly ignite in a thermonuclear runaway, the whole surface of the NS being burnt within seconds and shining as a modified blackbody. A considerable amount of attention has been given to the most extreme such bursts, for which the Eddington luminosity is reached, leading to the expansion of the photosphere. Fitting the spectroscopic data observed in such photospheric-radius-expansion (PRE) bursts can lead to constraining the mass and radius of the NS. Most of the effort dedicated to analyzing PRE bursts in the aim of constraining the EoS has been developed along two directions. The first avenue consists in fitting the X-ray spectra with a simple modified blackbody profile, incorporating some approximate general-relativistic effects [see Özel et al., 2016; Bauböck et al., 2015, and references therein]. The second avenue consists in developing sophisticated atmosphere models for the neutron star, in order to predict in a much more realistic way the outgoing radiation, but with no general-relativistic effects taken into account [see Madej et al., 2004; Suleimanov et al., 2012, and references therein].

In this context, Vincent et al. [2018] have developed a method allowing to benefit from the advantages of both avenues presented in the previous paragraph: it takes into account sophisticated atmospheric models for the computation of the emitted radiation, and evolves this radiation in a fully general-relativistic context. This is done following the steps below:

- the exact metric of the neutron star is computed by means of the open-source Lorene

library developed at Paris Observatory, considering some specific EoS.

- the ATM24 code of Madej et al. [2004] is then used to accurately compute the emitted spectrum at each point of the surface of the NS, taking into account the exact value of the local gravity as computed by Lorene in the previous step;
- the GYOTO ray-tracing code is then used to trace these outgoing photons in the exact NS metric, as computed by Lorene, towards a distant observer, thus creating an accurate observation simulation of a bursting NS spectrum.

These various steps are illustrated in Fig. 5.2. The study of Vincent et al. [2018] first presents this pipeline, but most importantly compares the resulting observed spectrum to that obtained using an atmospheric model, but without using ray tracing, which means that the emitted spectrum has to be averaged over the direction. The difference is of the order of 20 to 50%, due to the fact that the local spectrum at the surface of the NS depends a lot on the direction, an information which must be averaged over when neglecting ray tracing. Our study shows that this averaging of the directionality of the local spectrum is an important source of inaccuracy, which is certainly above the level needed to be able to constrain the EoS at a reasonable level.

Unfortunately, this study did not give rise to any follow-up work on my side. I tried two times to obtain grant money in order to build a small team around this topic, but I was not sucessful. Without this support, I had to drop the topic, which is one of my big regret, because I think that our point was important and could have lead to interesting observable constraints if we had been able to go as far as comparing to real data (which was one of the goal of the proposals of course).

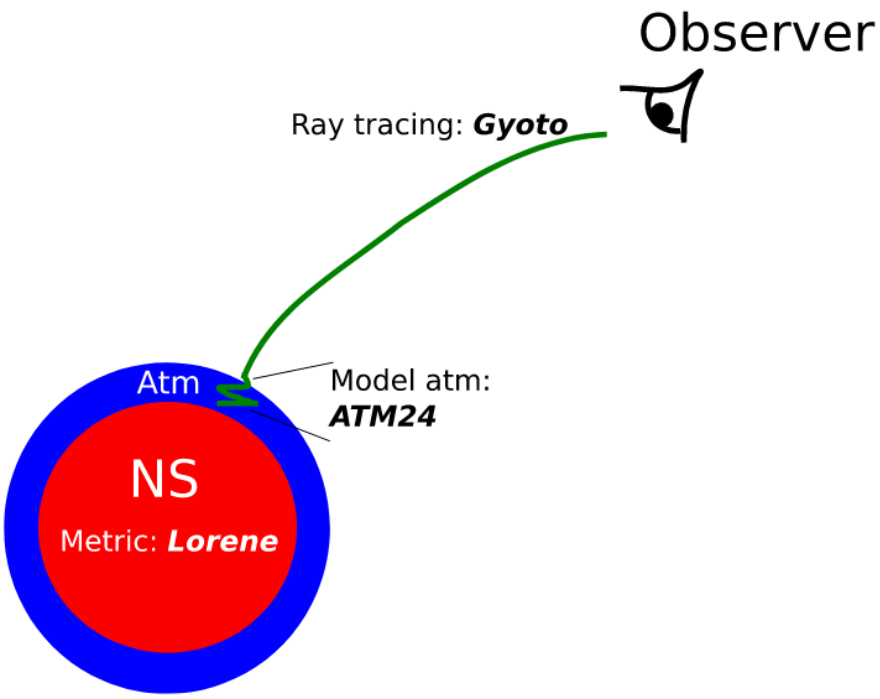

Figure 5.2: Sketch of the methods used to compute images and spectra of neutron stars. The neutron star is depicted in red; its structure and spacetime metric are computed with the LORENE/NROTSTAR code. Its atmosphere is represented in blue, but not to scale: the atmosphere is extremely thin, compared to the star's radius, typically 10s of cm vs. 10 km. The radiative transfer equation is solved there, together with hydrostatic equilibrium, via the ATM24 code. Finally, the emitted photons are ray-traced to a distant observer using the GYOTO code, which incorporates the neutron star's metric computed by LORENE/NROTSTAR. Figure from Vincent et al. [2018].

6

Science field 4: Dynamical spacetimes and gravitational waves

Contents

This last part of my dissertation is a perspective more than a report. This direction is one that I would very much like to be able to strongly push in the next 5 years, so I wanted to devote a specific (very short) chapter to it although at the present time it is far from the degree of maturity of the rest of my topics.

6.1 Dynamical spacetimes

The Gyoto code was developed since its very first steps with the aim of making it able to use not only standard analytic spacetime metrics (the Kerr metric of rotating black holes being the obvious first example), but also numerical metrics of other, less standard and more complicated sources. We massively used later this ability of Gyoto, which was unique at the time of the first publication of the code, and has become more standard by now. In particular, this property was at the basis of our ability to study boson-star spacetime images, using numerical metrics of rotating boson stars (see section 3.5.1). However, all these studies still consider stationary spacetimes.

The first illustration of the capability of Gyoto to handle numerical non-stationary

(dynamical) spacetimes was advertised in Vincent et al. [2012], which first presents a practical formulation of the geodesic equation (i.e. the basic equation for GYOTO) in a general "3+1" framework of general relativity. This paper then gives an example of ray tracing in a numerical time-evolving spacetime, by providing few successive images of a neutron star star that collapses to form a black hole (see Fig. 6.1).

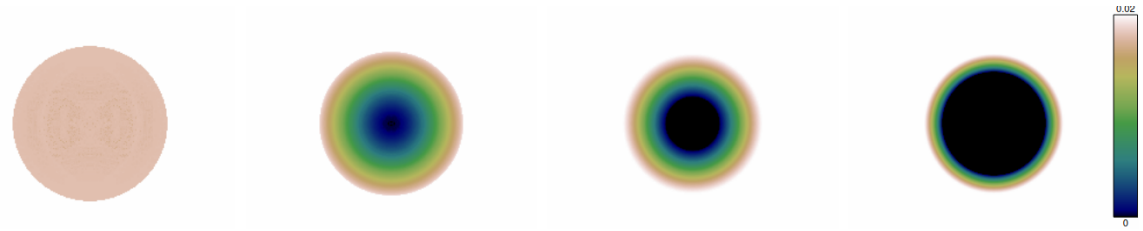

Figure 6.1: Images of a non-rotating collapsing neutron star, with an optically thick surface emitting blackbody radiation at 106 K. The color bar is common to the four panels and is given in SI units. The frequency of the photons in the observer's frame is chosen to be 1017 Hz, close to the maximum of the Planck function at 106 K. The growing central black area is due to the appearance of the event horizon while the star collapses to form a black hole. The difference in specific intensity in the non-dark region is due to the Doppler shift of the collapsing surface. Figure from Vincent et al. [2012].

However, between 2012 and the very recent past, the topic of imaging dynamical spacetimes was not continued. I would like to cite here two ongoing projects that aim at changing this conclusion in the close future. First, our APC colleagues (P. Varniere, R. Mignon-Risse, F. Casse and colleagues) are currently developing GYOTO, mainly independently from us in Meudon, to progress towards a multi-messenger simulation allowing to compute the electromagnetic counterpart to a black hole merger. Second, I am collaborating since mid 2020 with Daniel Heinesen, who was then a Master student and will hopefully start a PhD in the next fall. Daniel worked under the supervision of D. F. Mota and V. Cardoso on the topic of using GYOTO to compute images of black hole binary mergers generated by the public Einstein Toolkit library. I was involved in the supervision of the Master thesis to provide guidance on the use of GYOTO and critically discuss the results obtained. Daniel has made important progress during his Master thesis, and I hope that his PhD will allow to produce soon interesting GYOTO images of dynamical spacetimes.

6.2 Gravitational waves

I would like to briefly mention two other projects, that are not related with dynamical spacetimes, but are still dedicated to studying gravitational waves.

Gourgoulhon et al. [2019] (with me as third author) have analyzed the ability of the future LISA to detect orbiting bodies in close orbits around the supermassive black hole Sgr A*, motivated by the fact that the peak sensitivity of LISA happens to coincide (by chance of course) with the innermost stable circular orbit frequency around that black hole, at high spin. This paper discusses the ability of LISA to detect various astrophysical sources, focusing on stellar remnants and low-mass stars. Based on this study and on the past work on boson-star spacetimes, a collaboration between SYRTE, LESIA and LUTH is just starting to evaluate whether LISA could make an observable difference between a star orbiting around a supermassive black hole and a supermassive boson star. This study is the general context of the M2 internship of Samy Aoulad-Lafkih who has started to work under the supervision of Aurélien Hees (SYRTE, 70%) and myself (30%).

A last project that I took part in, related to gravitational waves, is the study of the SAGE project [Lacour et al., 2019, with me as second author], lead by Sylvestre Lacour at LESIA, a proposed gravitational-wave cubesat detector in the deciHz regime (in between LISA and the ground-based detectors). As far as I know this project has not been supported by the community and will probably not go beyond this initial paper unfortunately!

But, again, all this is more a perspective than a report. It is thus time to reach the conclusion and perspectives of this document.

7

Conclusion and perspectives

We are living in exciting times regarding the topic of strong-field gravity observationnal tests. The recent opening of the gravitational-wave astronomy era, together with the groundbreaking results of GRAVITY and the EHT, are allowing to completely renew the field.

In this exciting context, my work is mainly focused around two objects: the supermassive objects at center of the Milky Way and M87. These black hole candidates are key objects, because they are so big on sky, and allow direct electromagnetic probing of their close surroundings, giving direct access to the vicinity of the event horizon, the innermost accretion flow, and the putative jet-launching region. My main science objectives are

- to develop simple analytical models that allow investigating what physical features are key to account for the observables;
- from this, to help constrain the kind of accretion/ejection flow that surrounds Sgr A* and M87* (disk-dominated vs. jet-dominated, strongly vs. weakly magnetized...);
- to study relativistic effects in strong-field observables, discriminate between astrophysics-related and gravity-dominated features, and pave the way towards Kerr paradigm consistency tests;
- to investigate the constraints that can be put on the nature of supermassive compact objects at the core of galaxies, and consider the ultimate goal of constraining the gravity theory in the vicinity of black holes.

In the future, I will of course continue this research, which will be as always driven by the observational perspective. In the short term

- GRAVITY+[1], the upgrade of GRAVITY, will become fully operational in 2025. With its sensitivity going down to an impressive $m_K = 22$, this instrument might give access to one of the two holy grails[2] of Galactic center strong-gravity physics: a faint star, not detected so far, with a tight orbit around Sgr A*, which would be a perfect probe for constraining the black hole spin, and maybe go as far as constraining the no-hair theorems[3];
- the next-generation EHT [ngEHT, Doeleman et al., 2019] will allow observing at 230 and 345 GHz, with more ground-based stations, allowing a better coverage of the u-v plane. This upgrade should allow to constrain much more the properties of the accretion/ejection flow around M87*;
- the perspective of having a Photon Ring Telescope flying in the reasonably close future is of course particularly exciting.

Polarized radiative transfer in strong gravity is another direction of future work. My PhD student Nicolas Aimar is already working on implementing polarization in Gyoto, and I plan to also devote time to scrutinizing in what way can polarized strong-field electromagnetic observables help constrain the nature of accretion/ejection flows, and allow probing other aspects of strong-field gravity. Polarized information are delivered by both GRAVITY, the EHT, and their upgrades. Moreover, the recent launch of the IXPE mission [Weisskopf et al., 2016] for studying the polarization of black hole environments is a promising perspective of application.

In addition to all this, which boils down to going further in the directions that I am already exploring, I wish to devote much more time and energy to imaging dynamical spacetimes, with the obvious science case of binary merger in mind. It is of course a very fascinating perspective to develop tools that might be able to play a role in the multi-messenger, electromagnetic-gravitational astronomy that has risen in 2016 and will be a major field of the XXIst century relativistic astrophysics.

[1] See https://www.mpe.mpg.de/7480772/GRAVITYplus_WhitePaper.pdf.
[2] The second one would be the detection of a pulsar orbiting close to Sgr A*.
[3] Which states that the black hole should be completely described by its mass (which is well constrained already) and its spin (which is unknown).

8 CV and management tasks

Contents

A short CV and a list of publications are attached at the end of this document. This section goes a bit more in the details of my supervision, teaching, and administrative activities.

8.1 Supervision

I have participated at various levels in the supervision of 12 people listed in Tab. 8.1. I consider supervision as one of the most important tasks of a researcher, which is one of the main reasons why I am applying for this habilitation. I would consider that, as of now, I spend $\approx 15\%$ of my FTE time doing supervision.

I have also listed in Tab. 8.1 a few young researchers with whom I closely collaborated (in a "co-supervisor" mode) although they are mainly supervised by colleagues outside from the Meudon group. This is an important activity for me, which allows to strengthen the links with other groups.

In the future, I plan to continue collaborating with students, PhDs and postdocs, as

People	Level	Period	Involvement
Nicolas Aimar	PhD	2020-2023	85%
Gustavo Rodriguez-Coira	PhD	2017-2020	30%
Marion Grould	PhD (non-official)	2015-2016	30%
Gernot Heissel	Postdoc	2020-2022	30%
Karim Abd El Dayem	M2	2022	70%
Samy Aoulad-Lafkih	M2	2022	30%
Hadrien Paugnat	M2	2021	80%
Nicolas Aimar	M2	2020	80%
Weizmann Kiendrebeogo	M2	2019	50%
Rémi Danain	L3	2019	50%
Joao Rosa	Postdoc	2020-2022	10%
Daniel Heinesen	M2	2020-2021	10%
Alejandro Cardenas	M2	2019	10%

Table 8.1: **Supervision**. The bottom group of people separated from the rest by a double line corresponds to small, but significant, participation to the supervision of people mostly supervised by colleagues from outside of my LESIA group. The percentage in the last column is the percentage of the total amount of supervision time, not the percentage of my FTE.

much as possible, while keeping a reasonable amount of people under my supervision at a given time in order to have enough time to ensure a supervision of good quality. I am also very concerned by the future of the people I supervise, with the obvious goal, for those interested to make a carreer in science, to build a long-term strategy to maximize the probability for a permanent position hiring. In this perspecive, I am trying to propose topics that do not overlap too much (of course, they are always close from the perspective of astrophysics in general!) when students are separated by a small time (i.e. $\lesssim 3$ years), such that the young researchers from our team do not compete with each other on the job market.

8.2 Teaching

I consider teaching as a fundamental activity, also for CNRS staff like me who do not have to teach. This is at the same time a way to transfer knowledge to the younger generations,

which goes together with the supervising activities, and it is also very beneficial in order to progress towards the finest levels of mastering of a given topic. My motto would be "you know what you can teach"! I would consider that, averaged over the last few years, I spend $\lesssim 10\%$ of my FTE time for teaching.

Period	Level/topic	University	Hours/year
2021-	M1/relativity	Paris Obs.	15h (lecture)
2019-2021	L1/mecanics	Univ. Paris	36h (exercise)
2011-2012	L3/mecanics/QM	Univ. Paris	89h (exercise)
2008-2011	L1/mecanics	UPMC	64h (exercise)

Table 8.2: **Teaching**. The table gives an overwiew of my teaching activities since my PhD. There is a big gap between 2012 and 2019, corresponding to my postdocs (2012-2016) and the first few years of my permanent job in Meudon (I did not manage to obtain teaching hours immediately after getting my position).

Table 8.2 gives an overview of my teaching activity since 2008. I would like to stress that after getting my CNRS position, my goal was to teach at the lowest level of the university, ie L1, in order not only to interact with extremely selected people like those at the M2 level in astrophysics. In 2019-2021 I thus tought in L1 at the University of Paris (mecanics). I got the opportunity in 2020 to start teaching lectures in relativity at the M1 level, which I was of course very interested in. I did not manage to deal at the same time with teaching at M1 and L1 level, plus my administrative tasks detailed below, so I decided to stop my L1 teaching in 2021, hopefully to be restarted later.

8.3 Administration

Since 2019, I have started to have a few roles of science administration. I would like to insist on my two main such tasks that together take probably of the order of $\approx 25\%$ of my FTE time.

The first and most time-consuming such task is my participation as an elected member to the CNRS Section 17. CNRS, the French NSF, is divided in many sections devoted to various research topics. Section 17 focuses on the *Science of the Universe*. It is devoted to taking care of the carreer evaluation of CNRS staff, plus few other topics, and mostly to take care of the yearly competition for CNRS permanent positions. This means quite a lot of meetings, plus quite a lot of time reading application files[1].

[1] Typically very interesting and well-written ones, fortunately!

The second such task is my role as president of the IT commission of Paris Observatory since 2020. This commission has recently taken the charge of piloting the numerical strategy of the observatory. In this perspective, the IT commission has been in charge of writing the "Strategic scheme" for all numerical activities of the observatory, a 20-page document that I have been mostly in charge of writing. More recently, as Paris Observatory wants to rethink its definition at all levels, I am in charge of leading a working group on the "IT strategy" of the observatory to help frame the main future objectives.

These are my two main actions. Besides this, I am part of quite a few councils and boards, but not at a leading level, so it is much less intensive in terms of involvement. Table 8.3 summarizes my adminisrative tasks.

Period	Task	Role	Involvement (FTE)
2021-	CNRS Section 17	Elected member	15%
2020-	IT commission Paris Obs.	President	10%
2022-	IMCCE Council	Nominated member	
2019-	LUTH Council	Nominated member	
2019-	APC Project Cell	Nominated member	
2022-	GW/compact objects OP Action	Board member	
2019-2021	PhyFOG OP Action	Board member	
2018-	Team coordination	Coordination of LESIA/CGS team	

Table 8.3: **Administration**. The table gives an overwiew of my administrative activities. See text for details on the two main actions (at the top). When a percentage is not given, it means that the activity takes a negligible fraction of my FTE (typically few meetings a year). IMCCE and LUTH are two laboratories from Paris Observatory. APC Project Cell is a working group in charge of discussing the big projects of the laboratory AstroParticle and Cosmology in Paris. The "GW/compact objects" and "PhyFOG" actions are programs of Paris Observatory (OP) that aim at supporting research in the gravitation area. My team coordination duty is a very limited one, it consists in ensuring the transmission between the people in the team (≈ 10 people) and the rest of the "High Angular Resolution" pole that I am part of in LESIA, as well as representing the team for the yearly meeting of the pole.

To conclude this chapter, I would like to confess that I consider non-trivial to manage the transition between the postdoc time where I devoted $\approx 100\%$ FTE to my own research, to the permanent staff time where this number has rather suddenly decreased to $\approx 50\%$...

Bibliography

M. A. Abramowicz and W. Kluźniak. A precise determination of black hole spin in GRO J1655-40. A&A, 374:L19–L20, August 2001. doi: 10.1051/0004-6361:20010791.

Marek A. Abramowicz, Omer M. Blaes, Jíri Horák, Wlodek Kluzniak, and Paola Rebusco. Epicyclic oscillations of fluid bodies: II. Strong gravity. *Classical and Quantum Gravity*, 23(5):1689–1696, March 2006. doi: 10.1088/0264-9381/23/5/014.

Cosimo Bambi. Testing black hole candidates with electromagnetic radiation. *Reviews of Modern Physics*, 89(2):025001, April 2017. doi: 10.1103/RevModPhys.89.025001.

Michi Bauböck, Feryal Özel, Dimitrios Psaltis, and Sharon M. Morsink. Rotational Corrections to Neutron-star Radius Measurements from Thermal Spectra. ApJ, 799(1):22, January 2015. doi: 10.1088/0004-637X/799/1/22.

O. M. Blaes, P. Arras, and P. C. Fragile. Oscillation modes of relativistic slender tori. MNRAS, 369(3):1235–1252, July 2006. doi: 10.1111/j.1365-2966.2006.10370.x.

V. Bozza and L. Mancini. Observing Gravitational Lensing Effects by Sgr A* with GRAVITY. ApJ, 753(1):56, July 2012. doi: 10.1088/0004-637X/753/1/56.

Avery E. Broderick, Vincent L. Fish, Michael D. Johnson, Katherine Rosenfeld, Carlos Wang, Sheperd S. Doeleman, Kazunori Akiyama, Tim Johannsen, and Alan L. Roy. Modeling Seven Years of Event Horizon Telescope Observations with Radiatively Inefficient Accretion Flow Models. ApJ, 820(2):137, April 2016. doi: 10.3847/0004-637X/820/2/137.

Andrew Chael, Michael D. Johnson, and Alexandru Lupsasca. Observing the Inner Shadow

of a Black Hole: A Direct View of the Event Horizon. ApJ, 918(1):6, September 2021. doi: 10.3847/1538-4357/ac09ee.

Chi-kwan Chan, Dimitrios Psaltis, and Feryal Özel. GRay: A Massively Parallel GPU-based Code for Ray Tracing in Relativistic Spacetimes. ApJ, 777(1):13, November 2013. doi: 10.1088/0004-637X/777/1/13.

K. Chatterjee, Z. Younsi, M. Liska, A. Tchekhovskoy, S. B. Markoff, D. Yoon, D. van Eijnatten, C. Hesp, A. Ingram, and M. B. M. van der Klis. Observational signatures of disc and jet misalignment in images of accreting black holes. MNRAS, 499(1):362–378, November 2020. doi: 10.1093/mnras/staa2718.

Benjamin Crinquand, Benoît Cerutti, Guillaume Dubus, Kyle Parfrey, and Alexander A. Philippov. Images of magnetospheric reconnection-powered radiation around supermassive black holes. *arXiv e-prints*, art. arXiv:2202.04472, February 2022.

Pedro V. P. Cunha, Carlos A. R. Herdeiro, Eugen Radu, and Helgi F. Rúnarsson. Shadows of Kerr Black Holes with Scalar Hair. Phys. Rev. Lett., 115(21):211102, November 2015. doi: 10.1103/PhysRevLett.115.211102.

H. D. Curtis. Descriptions of 762 Nebulae and Clusters Photographed with the Crossley Reflector. *Publications of Lick Observatory*, 13:9–42, Jan 1918.

J. Davelaar, M. Mościbrodzka, T. Bronzwaer, and H. Falcke. General relativistic magnetohydrodynamical κ-jet models for Sagittarius A*. A&A, 612:A34, April 2018. doi: 10.1051/0004-6361/201732025.

Jordy Davelaar, Hector Olivares, Oliver Porth, Thomas Bronzwaer, Michael Janssen, Freek Roelofs, Yosuke Mizuno, Christian M. Fromm, Heino Falcke, and Luciano Rezzolla. Modeling non-thermal emission from the jet-launching region of M 87 with adaptive mesh refinement. A&A, 632:A2, December 2019. doi: 10.1051/0004-6361/201936150.

J. Dexter, A. Jiménez-Rosales, S. M. Ressler, A. Tchekhovskoy, M. Bauböck, P. T. de Zeeuw, F. Eisenhauer, S. von Fellenberg, F. Gao, R. Genzel, S. Gillessen, M. Habibi, T. Ott, J. Stadler, O. Straub, and F. Widmann. A parameter survey of Sgr A* radiative models from GRMHD simulations with self-consistent electron heating. MNRAS, 494(3): 4168–4186, May 2020. doi: 10.1093/mnras/staa922.

Jason Dexter and Eric Agol. A Fast New Public Code for Computing Photon Orbits in a Kerr Spacetime. ApJ, 696(2):1616–1629, May 2009. doi: 10.1088/0004-637X/696/2/1616.

A. Dmytriiev, H. Sol, and A. Zech. Connecting steady emission and very high energy flaring states in blazars: the case of Mrk 421. MNRAS, 505(2):2712–2730, August 2021. doi: 10.1093/mnras/stab1445.

Sheperd Doeleman, Lindy Blackburn, Jason Dexter, Jose L. Gomez, Michael D. Johnson, Daniel C. Palumbo, Jonathan Weintroub, Joseph R. Farah, Vincent Fish, Laurent Loinard, Colin Lonsdale, Gopal Narayanan, Nimesh A. Patel, Dominic W. Pesce, Alexander Raymond, Remo Tilanus, Maciek Wielgus, Kazunori Akiyama, Geoffrey Bower, Avery Broderick, Roger Deane, Christian Michael Fromm, Charles Gammie, Roman Gold, Michael Janssen, Tomohisa Kawashima, Thomas Krichbaum, Daniel P. Marrone, Lynn D. Matthews, Yosuke Mizuno, Luciano Rezzolla, Freek Roelofs, Eduardo Ros, Tuomas K. Savolainen, Feng Yuan, Guangyao Zhao, Lindy Blackburn, Sheperd Doeleman, Jason Dexter, Jose L. Gomez, Michael D. Johnson, Daniel C. Palumbo, Jonathan Weintroub, Joseph R. Farah, Vincent Fish, Laurent Loinard, Colin Lonsdale, Gopal Narayanan, Nimesh A. Patel, Dominic W. Pesce, Alexander Raymond, Remo Tilanus, Maciek Wielgus, Kazunori Akiyama, Geoffrey Bower, Avery Broderick, Roger Deane, Christian Michael Fromm, Charles Gammie, Roman Gold, Michael Janssen, Tomohisa Kawashima, Thomas Krichbaum, Daniel P. Marrone, Lynn D. Matthews, Yosuke Mizuno, Luciano Rezzolla, Freek Roelofs, Eduardo Ros, Tuomas K. Savolainen, Feng Yuan, and Guangyao Zhao. Studying Black Holes on Horizon Scales with VLBI Ground Arrays. In *Bulletin of the American Astronomical Society*, volume 51, page 256, September 2019.

I. El Mellah, B. Cerutti, B. Crinquand, and K. Parfrey. Spinning black holes magnetically connected to a Keplerian disk – Magnetosphere, reconnection sheet, particle acceleration and coronal heating. *arXiv e-prints*, art. arXiv:2112.03933, December 2021.

Event Horizon Telescope Collaboration, Kazunori Akiyama, Antxon Alberdi, Walter Alef, Keiichi Asada, Rebecca Azulay, Anne-Kathrin Baczko, David Ball, Mislav Baloković, John Barrett, Dan Bintley, Lindy Blackburn, Wilfred Boland, Katherine L. Bouman, Geoffrey C. Bower, Michael Bremer, Christiaan D. Brinkerink, Roger Brissenden, Silke Britzen, Avery E. Broderick, Dominique Broguiere, Thomas Bronzwaer, Do-Young Byun, John E. Carlstrom, Andrew Chael, Chi-kwan Chan, Shami Chatterjee, Koushik Chatterjee, Ming-Tang Chen, Yongjun Chen, Ilje Cho, Pierre Christian, John E. Conway, James M. Cordes, Geoffrey B. Crew, Yuzhu Cui, Jordy Davelaar, Mariafelicia De Laurentis, Roger Deane, Jessica Dempsey, Gregory Desvignes, Jason Dexter, Sheperd S. Doeleman, Ralph P. Eatough, Heino Falcke, Vincent L. Fish, Ed Fomalont, Raquel Fraga-Encinas, William T. Freeman, Per Friberg, Christian M. Fromm, José L. Gómez, Peter Galison, Charles F. Gammie, Roberto García, Olivier Gentaz, Boris Georgiev, Ciriaco Goddi, Roman Gold, Minfeng Gu, Mark Gurwell, Kazuhiro Hada, Michael H. Hecht, Ronald Hesper, Luis C. Ho, Paul Ho, Mareki Honma, Chih-Wei L. Huang, Lei Huang, David H. Hughes, Shiro Ikeda, Makoto Inoue, Sara Issaoun, David J. James, Buell T. Jannuzi, Michael Janssen, Britton Jeter, Wu Jiang, Michael D. Johnson, Svetlana Jorstad, Taehyun Jung, Mansour Karami, Ramesh Karuppusamy, Tomohisa Kawashima, Garrett K. Keating, Mark Kettenis, Jae-Young Kim, Junhan Kim, Jongsoo Kim, Motoki Kino, Jun Yi Koay, Patrick M. Koch, Shoko Koyama, Michael Kramer, Carsten Kramer, Thomas P. Krichbaum, Cheng-Yu Kuo, Tod R. Lauer, Sang-Sung Lee, Yan-Rong Li,

Zhiyuan Li, Michael Lindqvist, Kuo Liu, Elisabetta Liuzzo, Wen-Ping Lo, Andrei P. Lobanov, Laurent Loinard, Colin Lonsdale, Ru-Sen Lu, Nicholas R. MacDonald, Jirong Mao, Sera Markoff, Daniel P. Marrone, Alan P. Marscher, Iván Martí-Vidal, Satoki Matsushita, Lynn D. Matthews, Lia Medeiros, Karl M. Menten, Yosuke Mizuno, Izumi Mizuno, James M. Moran, Kotaro Moriyama, Monika Moscibrodzka, Cornelia Müller, Hiroshi Nagai, Neil M. Nagar, Masanori Nakamura, Ramesh Narayan, Gopal Narayanan, Iniyan Natarajan, Roberto Neri, Chunchong Ni, Aristeidis Noutsos, Hiroki Okino, Héctor Olivares, Gisela N. Ortiz-León, Tomoaki Oyama, Feryal Özel, Daniel C. M. Palumbo, Nimesh Patel, Ue-Li Pen, Dominic W. Pesce, Vincent Piétu, Richard Plambeck, Aleksandar PopStefanija, Oliver Porth, Ben Prather, Jorge A. Preciado-López, Dimitrios Psaltis, Hung-Yi Pu, Venkatessh Ramakrishnan, Ramprasad Rao, Mark G. Rawlings, Alexander W. Raymond, Luciano Rezzolla, Bart Ripperda, Freek Roelofs, Alan Rogers, Eduardo Ros, Mel Rose, Arash Roshanineshat, Helge Rottmann, Alan L. Roy, Chet Ruszczyk, Benjamin R. Ryan, Kazi L. J. Rygl, Salvador Sánchez, David Sánchez-Arguelles, Mahito Sasada, Tuomas Savolainen, F. Peter Schloerb, Karl-Friedrich Schuster, Lijing Shao, Zhiqiang Shen, Des Small, Bong Won Sohn, Jason SooHoo, Fumie Tazaki, Paul Tiede, Remo P. J. Tilanus, Michael Titus, Kenji Toma, Pablo Torne, Tyler Trent, Sascha Trippe, Shuichiro Tsuda, Ilse van Bemmel, Huib Jan van Langevelde, Daniel R. van Rossum, Jan Wagner, John Wardle, Jonathan Weintroub, Norbert Wex, Robert Wharton, Maciek Wielgus, George N. Wong, Qingwen Wu, Ken Young, André Young, Ziri Younsi, Feng Yuan, Ye-Fei Yuan, J. Anton Zensus, Guangyao Zhao, Shan-Shan Zhao, Ziyan Zhu, Juan-Carlos Algaba, Alexander Allardi, Rodrigo Amestica, Jadyn Anczarski, Uwe Bach, Frederick K. Baganoff, Christopher Beaudoin, Bradford A. Benson, Ryan Berthold, Jay M. Blanchard, Ray Blundell, Sandra Bustamente, Roger Cappallo, Edgar Castillo-Domínguez, Chih-Cheng Chang, Shu-Hao Chang, Song-Chu Chang, Chung-Chen Chen, Ryan Chilson, Tim C. Chuter, Rodrigo Córdova Rosado, Iain M. Coulson, Thomas M. Crawford, Joseph Crowley, John David, Mark Derome, Matthew Dexter, Sven Dornbusch, Kevin A. Dudevoir, Sergio A. Dzib, Andreas Eckart, Chris Eckert, Neal R. Erickson, Wendeline B. Everett, Aaron Faber, Joseph R. Farah, Vernon Fath, Thomas W. Folkers, David C. Forbes, Robert Freund, Arturo I. Gómez-Ruiz, David M. Gale, Feng Gao, Gertie Geertsema, David A. Graham, Christopher H. Greer, Ronald Grosslein, Frédéric Gueth, Daryl Haggard, Nils W. Halverson, Chih-Chiang Han, Kuo-Chang Han, Jinchi Hao, Yutaka Hasegawa, Jason W. Henning, Antonio Hernández-Gómez, Rubén Herrero-Illana, Stefan Heyminck, Akihiko Hirota, James Hoge, Yau-De Huang, C. M. Violette Impellizzeri, Homin Jiang, Atish Kamble, Ryan Keisler, Kimihiro Kimura, Yusuke Kono, Derek Kubo, John Kuroda, Richard Lacasse, Robert A. Laing, Erik M. Leitch, Chao-Te Li, Lupin C. C. Lin, Ching-Tang Liu, Kuan-Yu Liu, Li-Ming Lu, Ralph G. Marson, Pierre L. Martin-Cocher, Kyle D. Massingill, Callie Matulonis, Martin P. McColl, Stephen R. McWhirter, Hugo Messias, Zheng Meyer-Zhao, Daniel Michalik, Alfredo Montaña, William Montgomerie, Matias Mora-Klein, Dirk Muders, Andrew Nadolski, Santiago Navarro, Joseph Neilsen, Chi H. Nguyen, Hiroaki Nishioka, Timothy Norton,

Michael A. Nowak, George Nystrom, Hideo Ogawa, Peter Oshiro, Tomoaki Oyama, Harriet Parsons, Scott N. Paine, Juan Peñalver, Neil M. Phillips, Michael Poirier, Nicolas Pradel, Rurik A. Primiani, Philippe A. Raffin, Alexandra S. Rahlin, George Reiland, Christopher Risacher, Ignacio Ruiz, Alejandro F. Sáez-Madaín, Remi Sassella, Pim Schellart, Paul Shaw, Kevin M. Silva, Hotaka Shiokawa, David R. Smith, William Snow, Kamal Souccar, Don Sousa, T. K. Sridharan, Ranjani Srinivasan, William Stahm, Anthony A. Stark, Kyle Story, Sjoerd T. Timmer, Laura Vertatschitsch, Craig Walther, Ta-Shun Wei, Nathan Whitehorn, Alan R. Whitney, David P. Woody, Jan G. A. Wouterloot, Melvin Wright, Paul Yamaguchi, Chen-Yu Yu, Milagros Zeballos, Shuo Zhang, and Lucy Ziurys. First M87 Event Horizon Telescope Results. I. The Shadow of the Supermassive Black Hole. ApJ, 875(1):L1, April 2019. doi: 10.3847/2041-8213/ab0ec7.

A. C. Fabian. Observational Evidence of Active Galactic Nuclei Feedback. ARA&A, 50: 455–489, September 2012. doi: 10.1146/annurev-astro-081811-125521.

Karl Gebhardt, Joshua Adams, Douglas Richstone, Tod R. Lauer, S. M. Faber, Kayhan Gültekin, Jeremy Murphy, and Scott Tremaine. The Black Hole Mass in M87 from Gemini/NIFS Adaptive Optics Observations. ApJ, 729(2):119, Mar 2011. doi: 10.1088/0004-637X/729/2/119.

Reinhard Genzel, Frank Eisenhauer, and Stefan Gillessen. The Galactic Center massive black hole and nuclear star cluster. *Reviews of Modern Physics*, 82(4):3121–3195, October 2010. doi: 10.1103/RevModPhys.82.3121.

Anastasia A. Golubtsova, Eric Gourgoulhon, and Marina K. Usova. Heavy quarks in rotating plasma via holography. *arXiv e-prints*, art. arXiv:2107.11672, July 2021.

E. Gourgoulhon, A. Le Tiec, F. H. Vincent, and N. Warburton. Gravitational waves from bodies orbiting the Galactic center black hole and their detectability by LISA. A&A, 627:A92, July 2019. doi: 10.1051/0004-6361/201935406.

Samuel E. Gralla and Alexandru Lupsasca. Null geodesics of the Kerr exterior. Phys. Rev. D, 101(4):044032, February 2020a. doi: 10.1103/PhysRevD.101.044032.

Samuel E. Gralla and Alexandru Lupsasca. Lensing by Kerr black holes. Phys. Rev. D, 101(4):044031, February 2020b. doi: 10.1103/PhysRevD.101.044031.

Samuel E. Gralla, Alexandru Lupsasca, and Daniel P. Marrone. The shape of the black hole photon ring: A precise test of strong-field general relativity. Phys. Rev. D, 102(12): 124004, December 2020. doi: 10.1103/PhysRevD.102.124004.

Philippe Grandclément, Claire Somé, and Eric Gourgoulhon. Models of rotating boson stars and geodesics around them: New type of orbits. Phys. Rev. D, 90(2):024068, July 2014. doi: 10.1103/PhysRevD.90.024068.

Gravity Collaboration, R. Abuter, M. Accardo, A. Amorim, N. Anugu, G. Ávila, N. Azouaoui, M. Benisty, J. P. Berger, N. Blind, H. Bonnet, P. Bourget, W. Brandner, R. Brast, A. Buron, L. Burtscher, F. Cassaing, F. Chapron, É. Choquet, Y. Clénet, C. Collin, V. Coudé Du Foresto, W. de Wit, P. T. de Zeeuw, C. Deen, F. Delplancke-Ströbele, R. Dembet, F. Derie, J. Dexter, G. Duvert, M. Ebert, A. Eckart, F. Eisenhauer, M. Esselborn, P. Fédou, G. Finger, P. Garcia, C. E. Garcia Dabo, R. Garcia Lopez, E. Gendron, R. Genzel, S. Gillessen, F. Gonte, P. Gordo, M. Grould, U. Grözinger, S. Guieu, P. Haguenauer, O. Hans, X. Haubois, M. Haug, F. Haussmann, Th. Henning, S. Hippler, M. Horrobin, A. Huber, Z. Hubert, N. Hubin, C. A. Hummel, G. Jakob, A. Janssen, L. Jochum, L. Jocou, A. Kaufer, S. Kellner, S. Kendrew, L. Kern, P. Kervella, M. Kiekebusch, R. Klein, Y. Kok, J. Kolb, M. Kulas, S. Lacour, V. Lapeyrère, B. Lazareff, J. B. Le Bouquin, P. Lèna, R. Lenzen, S. Lévêque, M. Lippa, Y. Magnard, L. Mehrgan, M. Mellein, A. Mérand, J. Moreno-Ventas, T. Moulin, E. Müller, F. Müller, U. Neumann, S. Oberti, T. Ott, L. Pallanca, J. Panduro, L. Pasquini, T. Paumard, I. Percheron, K. Perraut, G. Perrin, A. Pflüger, O. Pfuhl, T. Phan Duc, P. M. Plewa, D. Popovic, S. Rabien, A. Ramírez, J. Ramos, C. Rau, M. Riquelme, R. R. Rohloff, G. Rousset, J. Sanchez-Bermudez, S. Scheithauer, M. Schöller, N. Schuhler, J. Spyromilio, C. Straubmeier, E. Sturm, M. Suarez, K. R. W. Tristram, N. Ventura, F. Vincent, I. Waisberg, I. Wank, J. Weber, E. Wieprecht, M. Wiest, E. Wiezorrek, M. Wittkowski, J. Woillez, B. Wolff, S. Yazici, D. Ziegler, and G. Zins. First light for GRAVITY: Phase referencing optical interferometry for the Very Large Telescope Interferometer. A&A, 602:A94, June 2017. doi: 10.1051/0004-6361/201730838.

Gravity Collaboration, R. Abuter, A. Amorim, M. Bauböck, J. P. Berger, H. Bonnet, W. Brandner, Y. Clénet, V. Coudé Du Foresto, P. T. de Zeeuw, C. Deen, J. Dexter, G. Duvert, A. Eckart, F. Eisenhauer, N. M. Förster Schreiber, P. Garcia, F. Gao, E. Gendron, R. Genzel, S. Gillessen, P. Guajardo, M. Habibi, X. Haubois, Th. Henning, S. Hippler, M. Horrobin, A. Huber, A. Jiménez-Rosales, L. Jocou, P. Kervella, S. Lacour, V. Lapeyrère, B. Lazareff, J. B. Le Bouquin, P. Léna, M. Lippa, T. Ott, J. Panduro, T. Paumard, K. Perraut, G. Perrin, O. Pfuhl, P. M. Plewa, S. Rabien, G. Rodríguez-Coira, G. Rousset, A. Sternberg, O. Straub, C. Straubmeier, E. Sturm, L. J. Tacconi, F. Vincent, S. von Fellenberg, I. Waisberg, F. Widmann, E. Wieprecht, E. Wiezorrek, J. Woillez, and S. Yazici. Detection of orbital motions near the last stable circular orbit of the massive black hole SgrA*. A&A, 618:L10, October 2018. doi: 10.1051/0004-6361/201834294.

Gravity Collaboration, R. Abuter, A. Amorim, M. Bauböck, J. P. Berger, H. Bonnet, W. Brandner, V. Cardoso, Y. Clénet, P. T. de Zeeuw, J. Dexter, A. Eckart, F. Eisenhauer, N. M. Förster Schreiber, P. Garcia, F. Gao, E. Gendron, R. Genzel, S. Gillessen, M. Habibi, X. Haubois, T. Henning, S. Hippler, M. Horrobin, A. Jiménez-Rosales, L. Jochum, L. Jocou, A. Kaufer, P. Kervella, S. Lacour, V. Lapeyrère, J. B. Le Bouquin, P. Léna, M. Nowak, T. Ott, T. Paumard, K. Perraut, G. Perrin, O. Pfuhl, G. Rodríguez-

Coira, J. Shangguan, S. Scheithauer, J. Stadler, O. Straub, C. Straubmeier, E. Sturm, L. J. Tacconi, F. Vincent, S. von Fellenberg, I. Waisberg, F. Widmann, E. Wieprecht, E. Wiezorrek, J. Woillez, S. Yazici, and G. Zins. Detection of the Schwarzschild precession in the orbit of the star S2 near the Galactic centre massive black hole. A&A, 636: L5, April 2020. doi: 10.1051/0004-6361/202037813.

M. Grould, Z. Meliani, F. H. Vincent, P. Grandclément, and E. Gourgoulhon. Comparing timelike geodesics around a Kerr black hole and a boson star. *Classical and Quantum Gravity*, 34(21):215007, November 2017a. doi: 10.1088/1361-6382/aa8d39.

M. Grould, F. H. Vincent, T. Paumard, and G. Perrin. General relativistic effects on the orbit of the S2 star with GRAVITY. A&A, 608:A60, December 2017b. doi: 10.1051/0004-6361/201731148.

Gernot Heißel, Thibaut Paumard, Guy Perrin, and Frédéric Vincent. The dark mass signature in the orbit of S2. *arXiv e-prints*, art. arXiv:2112.07778, December 2021.

Carlos A. R. Herdeiro and Eugen Radu. Kerr Black Holes with Scalar Hair. Phys. Rev. Lett., 112(22):221101, June 2014. doi: 10.1103/PhysRevLett.112.221101.

Michael D. Johnson, Alexandru Lupsasca, Andrew Strominger, George N. Wong, Shahar Hadar, Daniel Kapec, Ramesh Narayan, Andrew Chael, Charles F. Gammie, Peter Galison, Daniel C. M. Palumbo, Sheperd S. Doeleman, Lindy Blackburn, Maciek Wielgus, Dominic W. Pesce, Joseph R. Farah, and James M. Moran. Universal interferometric signatures of a black hole's photon ring. *Science Advances*, 6(12):eaaz1310, March 2020. doi: 10.1126/sciadv.aaz1310.

Etienne Klein and Marc Lachieze-Rey. *The Quest for Unity.* Oxford University Press, New York, 1999.

Michael Kramer. Pulsars as probes of gravity and fundamental physics. *International Journal of Modern Physics D*, 25(14):1630029-61, July 2016. doi: 10.1142/S0218271816300299.

S. Lacour, F. H. Vincent, M. Nowak, A. Le Tiec, V. Lapeyrere, L. David, P. Bourget, A. Kellerer, K. Jani, J. Martino, J. Y. Vinet, O. Godet, O. Straub, and J. Woillez. SAGE: finding IMBH in the black hole desert. *Classical and Quantum Gravity*, 36(19): 195005, October 2019. doi: 10.1088/1361-6382/ab3583.

F. Lamy, E. Gourgoulhon, T. Paumard, and F. H. Vincent. Imaging a non-singular rotating black hole at the center of the Galaxy. *Classical and Quantum Gravity*, 35(11):115009, June 2018. doi: 10.1088/1361-6382/aabd97.

J. Madej, P. C. Joss, and A. Różańska. Model Atmospheres and X-Ray Spectra of Bursting Neutron Stars: Hydrogen-Helium Comptonized Spectra. ApJ, 602(2):904–912, February 2004. doi: 10.1086/379761.

S. Markoff, H. Falcke, F. Yuan, and P. L. Biermann. The Nature of the 10 kilosecond X-ray flare in Sgr A*. A&A, 379:L13–L16, November 2001. doi: 10.1051/0004-6361:20011346.

B. Mishra, F. H. Vincent, A. Manousakis, P. C. Fragile, T. Paumard, and W. Kluźniak. Quasi-periodic oscillations from relativistic ray-traced hydrodynamical tori. MNRAS, 467(4):4036–4049, June 2017. doi: 10.1093/mnras/stx299.

M. Mościbrodzka and C. F. Gammie. IPOLE - semi-analytic scheme for relativistic polarized radiative transport. MNRAS, 475(1):43–54, March 2018. doi: 10.1093/mnras/stx3162.

Enmanuelle Mossoux, Nicolas Grosso, Frédéric H. Vincent, and Delphine Porquet. Study of the X-ray activity of <ASTROBJ>Sagittarius A*</ASTROBJ> during the 2011 XMM-Newton campaign. A&A, 573:A46, January 2015. doi: 10.1051/0004-6361/201424682.

Hector Olivares, Ziri Younsi, Christian M. Fromm, Mariafelicia De Laurentis, Oliver Porth, Yosuke Mizuno, Heino Falcke, Michael Kramer, and Luciano Rezzolla. How to tell an accreting boson star from a black hole. MNRAS, 497(1):521–535, September 2020. doi: 10.1093/mnras/staa1878.

Feryal Özel, Dimitrios Psaltis, and Ramesh Narayan. Hybrid Thermal-Nonthermal Synchrotron Emission from Hot Accretion Flows. ApJ, 541(1):234–249, September 2000. doi: 10.1086/309396.

Feryal Özel, Dimitrios Psaltis, Tolga Güver, Gordon Baym, Craig Heinke, and Sebastien Guillot. The Dense Matter Equation of State from Neutron Star Radius and Mass Measurements. ApJ, 820(1):28, March 2016. doi: 10.3847/0004-637X/820/1/28.

B. Paczyński and P. J. Wiita. Thick accretion disks and supercritical luminosities. A&A, 500:203–211, August 1980.

Kyle Parfrey, Alexander Philippov, and Benoît Cerutti. First-Principles Plasma Simulations of Black-Hole Jet Launching. Phys. Rev. Lett., 122(3):035101, January 2019. doi: 10.1103/PhysRevLett.122.035101.

Oliver Porth, Koushik Chatterjee, Ramesh Narayan, Charles F. Gammie, Yosuke Mizuno, Peter Anninos, John G. Baker, Matteo Bugli, Chi-kwan Chan, Jordy Davelaar, Luca Del Zanna, Zachariah B. Etienne, P. Chris Fragile, Bernard J. Kelly, Matthew Liska, Sera Markoff, Jonathan C. McKinney, Bhupendra Mishra, Scott C. Noble, Héctor Olivares, Ben Prather, Luciano Rezzolla, Benjamin R. Ryan, James M. Stone, Niccolò Tomei, Christopher J. White, Ziri Younsi, Kazunori Akiyama, Antxon Alberdi, Walter Alef,

Keiichi Asada, Rebecca Azulay, Anne-Kathrin Baczko, David Ball, Mislav Baloković, John Barrett, Dan Bintley, Lindy Blackburn, Wilfred Boland, Katherine L. Bouman, Geoffrey C. Bower, Michael Bremer, Christiaan D. Brinkerink, Roger Brissenden, Silke Britzen, Avery E. Broderick, Dominique Broguiere, Thomas Bronzwaer, Do-Young Byun, John E. Carlstrom, Andrew Chael, Shami Chatterjee, Ming-Tang Chen, Yongjun Chen, Ilje Cho, Pierre Christian, John E. Conway, James M. Cordes, Geoffrey, B. Crew, Yuzhu Cui, Mariafelicia De Laurentis, Roger Deane, Jessica Dempsey, Gregory Desvignes, Sheperd S. Doeleman, Ralph P. Eatough, Heino Falcke, Vincent L. Fish, Ed Fomalont, Raquel Fraga-Encinas, Bill Freeman, Per Friberg, Christian M. Fromm, José L. Gómez, Peter Galison, Roberto García, Olivier Gentaz, Boris Georgiev, Ciriaco Goddi, Roman Gold, Minfeng Gu, Mark Gurwell, Kazuhiro Hada, Michael H. Hecht, Ronald Hesper, Luis C. Ho, Paul Ho, Mareki Honma, Chih-Wei L. Huang, Lei Huang, David H. Hughes, Shiro Ikeda, Makoto Inoue, Sara Issaoun, David J. James, Buell T. Jannuzi, Michael Janssen, Britton Jeter, Wu Jiang, Michael D. Johnson, Svetlana Jorstad, Taehyun Jung, Mansour Karami, Ramesh Karuppusamy, Tomohisa Kawashima, Garrett K. Keating, Mark Kettenis, Jae-Young Kim, Junhan Kim, Jongsoo Kim, Motoki Kino, Jun Yi Koay, Patrick, M. Koch, Shoko Koyama, Michael Kramer, Carsten Kramer, Thomas P. Krichbaum, Cheng-Yu Kuo, Tod R. Lauer, Sang-Sung Lee, Yan-Rong Li, Zhiyuan Li, Michael Lindqvist, Kuo Liu, Elisabetta Liuzzo, Wen-Ping Lo, Andrei P. Lobanov, Laurent Loinard, Colin Lonsdale, Ru-Sen Lu, Nicholas R. MacDonald, Jirong Mao, Daniel P. Marrone, Alan P. Marscher, Iván Martí-Vidal, Satoki Matsushita, Lynn D. Matthews, Lia Medeiros, Karl M. Menten, Izumi Mizuno, James M. Moran, Kotaro Moriyama, Monika Moscibrodzka, Cornelia Müller, Hiroshi Nagai, Neil M. Nagar, Masanori Nakamura, Gopal Narayanan, Iniyan Natarajan, Roberto Neri, Chunchong Ni, Aristeidis Noutsos, Hiroki Okino, Tomoaki Oyama, Feryal Özel, Daniel C. M. Palumbo, Nimesh Patel, Ue-Li Pen, Dominic W. Pesce, Vincent Piétu, Richard Plambeck, Aleksandar PopStefanija, Jorge A. Preciado-López, Dimitrios Psaltis, Hung-Yi Pu, Venkatessh Ramakrishnan, Ramprasad Rao, Mark G. Rawlings, Alexander W. Raymond, Bart Ripperda, Freek Roelofs, Alan Rogers, Eduardo Ros, Mel Rose, Arash Roshanineshat, Helge Rottmann, Alan L. Roy, Chet Ruszczyk, Kazi L. J. Rygl, Salvador Sánchez, David Sánchez-Arguelles, Mahito Sasada, Tuomas Savolainen, F. Peter Schloerb, Karl-Friedrich Schuster, Lijing Shao, Zhiqiang Shen, Des Small, Bong Won Sohn, Jason SooHoo, Fumie Tazaki, Paul Tiede, Remo P. J. Tilanus, Michael Titus, Kenji Toma, Pablo Torne, Tyler Trent, Sascha Trippe, Shuichiro Tsuda, Ilse van Bemmel, Huib Jan van Langevelde, Daniel R. van Rossum, Jan Wagner, John Wardle, Jonathan Weintroub, Norbert Wex, Robert Wharton, Maciek Wielgus, George N. Wong, Qingwen Wu, Ken Young, André Young, Feng Yuan, Ye-Fei Yuan, J. Anton Zensus, Guangyao Zhao, Shan-Shan Zhao, Ziyan Zhu, and Event Horizon Telescope Collaboration. The Event Horizon General Relativistic Magnetohydrodynamic Code Comparison Project. ApJS, 243(2):26, August 2019. doi: 10.3847/1538-4365/ab29fd.

S. M. Ressler, E. Quataert, and J. M. Stone. Hydrodynamic simulations of the inner accretion flow of Sagittarius A* fuelled by stellar winds. MNRAS, 478(3):3544–3563, August 2018. doi: 10.1093/mnras/sty1146.

Sean M. Ressler, Christopher J. White, Eliot Quataert, and James M. Stone. Ab Initio Horizon-scale Simulations of Magnetically Arrested Accretion in Sagittarius A* Fed by Stellar Winds. ApJ, 896(1):L6, June 2020. doi: 10.3847/2041-8213/ab9532.

L. Rezzolla, S'i. Yoshida, T. J. Maccarone, and O. Zanotti. A new simple model for high-frequency quasi-periodic oscillations in black hole candidates. MNRAS, 344(3):L37–L41, September 2003. doi: 10.1046/j.1365-8711.2003.07018.x.

B. Ripperda, M. Liska, K. Chatterjee, G. Musoke, A. A. Philippov, S. B. Markoff, A. Tchekhovskoy, and Z. Younsi. Black Hole Flares: Ejection of Accreted Magnetic Flux through 3D Plasmoid-mediated Reconnection. ApJ, 924(2):L32, January 2022. doi: 10.3847/2041-8213/ac46a1.

G. F. Rubilar and A. Eckart. Periastron shifts of stellar orbits near the Galactic Center. A&A, 374:95–104, July 2001. doi: 10.1051/0004-6361:20010640.

Nicolas Scepi, Jason Dexter, and Mitchell C. Begelman. Sgr A* X-ray flares from non-thermal particle acceleration in a magnetically arrested disc. MNRAS, 511(3):3536–3547, April 2022. doi: 10.1093/mnras/stac337.

N. I. Shakura and R. A. Sunyaev. Black holes in binary systems. Observational appearance. A&A, 24:337–355, January 1973.

O. Straub, F. H. Vincent, M. A. Abramowicz, E. Gourgoulhon, and T. Paumard. Modelling the black hole silhouette in Sagittarius A* with ion tori. A&A, 543:A83, July 2012. doi: 10.1051/0004-6361/201219209.

V. Suleimanov, J. Poutanen, and K. Werner. X-ray bursting neutron star atmosphere models using an exact relativistic kinetic equation for Compton scattering. A&A, 545: A120, September 2012. doi: 10.1051/0004-6361/201219480.

K. Van Aelst, E. Gourgoulhon, and F. H. Vincent. Equatorial orbits and imaging of hairy cubic Galileon black holes. Phys. Rev. D, 104(12):124034, December 2021. doi: 10.1103/PhysRevD.104.124034.

P. Varniere, F. Casse, and F. H. Vincent. Rossby wave instability and high-frequency quasi-periodic oscillations in accretion discs orbiting around black holes. A&A, 625:A116, May 2019. doi: 10.1051/0004-6361/201935208.

P. Varniere, F. H. Vincent, and F. Casse. Living on the edge: Rossby wave instability and HFQPOs in black hole binaries. A&A, 638:A33, June 2020. doi: 10.1051/0004-6361/202037816.

F. H. Vincent, T. Paumard, E. Gourgoulhon, and G. Perrin. GYOTO: a new general relativistic ray-tracing code. *Classical and Quantum Gravity*, 28(22):225011, November 2011. doi: 10.1088/0264-9381/28/22/225011.

F. H. Vincent, E. Gourgoulhon, and J. Novak. 3+1 geodesic equation and images in numerical spacetimes. *Classical and Quantum Gravity*, 29(24):245005, December 2012. doi: 10.1088/0264-9381/29/24/245005.

F. H. Vincent, H. Meheut, P. Varniere, and T. Paumard. Flux modulation from the Rossby wave instability in microquasars' accretion disks: toward a HFQPO model. A&A, 551: A54, March 2013. doi: 10.1051/0004-6361/201220695.

F. H. Vincent, G. P. Mazur, O. Straub, M. A. Abramowicz, W. Kluźniak, G. Török, and P. Bakala. Spectral signature of oscillating slender tori surrounding Kerr black holes. A&A, 563:A109, March 2014a. doi: 10.1051/0004-6361/201323103.

F. H. Vincent, T. Paumard, G. Perrin, P. Varniere, F. Casse, F. Eisenhauer, S. Gillessen, and P. J. Armitage. Distinguishing an ejected blob from alternative flare models at the Galactic Centre with GRAVITY. MNRAS, 441(4):3477–3487, July 2014b. doi: 10.1093/mnras/stu812.

F. H. Vincent, W. Yan, O. Straub, A. A. Zdziarski, and M. A. Abramowicz. A magnetized torus for modeling Sagittarius A* millimeter images and spectra. A&A, 574:A48, January 2015. doi: 10.1051/0004-6361/201424306.

F. H. Vincent, E. Gourgoulhon, C. Herdeiro, and E. Radu. Astrophysical imaging of Kerr black holes with scalar hair. Phys. Rev. D, 94(8):084045, October 2016a. doi: 10.1103/PhysRevD.94.084045.

F. H. Vincent, Z. Meliani, P. Grandclément, E. Gourgoulhon, and O. Straub. Imaging a boson star at the Galactic center. *Classical and Quantum Gravity*, 33(10):105015, May 2016b. doi: 10.1088/0264-9381/33/10/105015.

F. H. Vincent, M. A. Abramowicz, A. A. Zdziarski, M. Wielgus, T. Paumard, G. Perrin, and O. Straub. Multi-wavelength torus-jet model for Sagittarius A*. A&A, 624:A52, April 2019. doi: 10.1051/0004-6361/201834946.

F. H. Vincent, M. Wielgus, M. A. Abramowicz, E. Gourgoulhon, J. P. Lasota, T. Paumard, and G. Perrin. Geometric modeling of M87* as a Kerr black hole or a non-Kerr compact object. A&A, 646:A37, February 2021. doi: 10.1051/0004-6361/202037787.

Frederic H. Vincent, Michał Bejger, Agata Różańska, Odele Straub, Thibaut Paumard, Morgane Fortin, Jerzy Madej, Agnieszka Majczyna, Eric Gourgoulhon, Paweł Haensel, Leszek Zdunik, and Bartosz Beldycki. Accurate Ray-tracing of Realistic Neutron Star

Atmospheres for Constraining Their Parameters. ApJ, 855(2):116, March 2018. doi: 10.3847/1538-4357/aab0a3.

Marta Volonteri, Mélanie Habouzit, and Monica Colpi. The origins of massive black holes. *Nature Reviews Physics*, 3(11):732–743, September 2021. doi: 10.1038/s42254-021-00364-9.

Idel Waisberg, Jason Dexter, Stefan Gillessen, Oliver Pfuhl, Frank Eisenhauer, Phillip M. Plewa, Michi Bauböck, Alejandra Jimenez-Rosales, Maryam Habibi, Thomas Ott, Sebastiano von Fellenberg, Feng Gao, Felix Widmann, and Reinhard Genzel. What stellar orbit is needed to measure the spin of the Galactic centre black hole from astrometric data? MNRAS, 476(3):3600–3610, May 2018. doi: 10.1093/mnras/sty476.

Jonelle L. Walsh, Aaron J. Barth, Luis C. Ho, and Marc Sarzi. The M87 Black Hole Mass from Gas-dynamical Models of Space Telescope Imaging Spectrograph Observations. ApJ, 770(2):86, Jun 2013. doi: 10.1088/0004-637X/770/2/86.

Martin C. Weisskopf, Brian Ramsey, Stephen O'Dell, Allyn Tennant, Ronald Elsner, Paolo Soffitta, Ronaldo Bellazzini, Enrico Costa, Jeffrey Kolodziejczak, Victoria Kaspi, Fabio Muleri, Herman Marshall, Giorgio Matt, and Roger Romani. The Imaging X-ray Polarimetry Explorer (IXPE). In Jan-Willem A. den Herder, Tadayuki Takahashi, and Marshall Bautz, editors, *Space Telescopes and Instrumentation 2016: Ultraviolet to Gamma Ray*, volume 9905 of *Society of Photo-Optical Instrumentation Engineers (SPIE) Conference Series*, page 990517, July 2016. doi: 10.1117/12.2235240.

Philippe Z. Yao, Jason Dexter, Alexander Y. Chen, Benjamin R. Ryan, and George N. Wong. Radiation GRMHD simulations of M87: funnel properties and prospects for gap acceleration. MNRAS, 507(4):4864–4878, November 2021. doi: 10.1093/mnras/stab2462.

D. Yoon, K. Chatterjee, S. B. Markoff, D. van Eijnatten, Z. Younsi, M. Liska, and A. Tchekhovskoy. Spectral and imaging properties of Sgr A* from high-resolution 3D GRMHD simulations with radiative cooling. MNRAS, 499(3):3178–3192, December 2020. doi: 10.1093/mnras/staa3031.

Qingjuan Yu, Fupeng Zhang, and Youjun Lu. Prospects for Constraining the Spin of the Massive Black Hole at the Galactic Center via the Relativistic Motion of a Surrounding Star. ApJ, 827(2):114, August 2016. doi: 10.3847/0004-637X/827/2/114.

Feng Yuan and Ramesh Narayan. Hot Accretion Flows Around Black Holes. ARA&A, 52: 529–588, August 2014. doi: 10.1146/annurev-astro-082812-141003.